

**NASA TECHNICAL  
MEMORANDUM**



**NASA TM X-3560**

**NASA TM X-3560**

**FLOW-FIELD SURVEYS ON  
THE WINDWARD SIDE OF THE NASA  
040A SPACE SHUTTLE ORBITER AT 31°  
ANGLE OF ATTACK AND MACH 20 IN HELIUM**

*George C. Ashby, Jr., and Vernon T. Helms III*

*Langley Research Center*

*Hampton, Va. 23665*

1. Report No. NASA TM X-3560		2. Government Accession No.		3. Recipient's Catalog No.	
4. Title and Subtitle FLOW-FIELD SURVEYS ON THE WINDWARD SIDE OF THE NASA 040A SPACE SHUTTLE ORBITER AT 31° ANGLE OF ATTACK AND MACH 20 IN HELIUM				5. Report Date October 1977	
				6. Performing Organization Code	
7. Author(s) George C. Ashby, Jr., and Vernon T. Helms III				8. Performing Organization Report No. L-11600	
				10. Work Unit No. 506-26-30-04	
9. Performing Organization Name and Address NASA Langley Research Center Hampton, VA 23665				11. Contract or Grant No.	
				13. Type of Report and Period Covered Technical Memorandum	
12. Sponsoring Agency Name and Address National Aeronautics and Space Administration Washington, DC 20546				14. Sponsoring Agency Code	
15. Supplementary Notes					
16. Abstract <p>Pitot-pressure and flow-angle distributions in the windward flow field of the NASA 040A space shuttle orbiter configuration and surface pressures have been measured in the 22-inch aerodynamics leg of the Langley hypersonic helium tunnel facility at a Mach number of 20 and an angle of attack of 31°. The free-stream Reynolds number, based on model length, was <math>5.39 \times 10^6</math>.</p> <p>The results show that cores of high pitot pressure, which are related to the body-shock—wing-shock intersections, occur on the windward plane of symmetry in the vicinity of the wing-body junction and near midspan on the wing. Theoretical estimates of the flow-field pitot pressures show that conical-flow values for the windward plane of symmetry surface are representative of the average level over the entire lower surface.</p>					
17. Key Words (Suggested by Author(s)) Hypersonic Flow fields Helium			18. Distribution Statement Unclassified - Unlimited  Subject Category 15		
19. Security Classif. (of this report) Unclassified	20. Security Classif. (of this page) Unclassified	21. No. of Pages 60	22. Price* \$4.50		

# FLOW-FIELD SURVEYS ON THE WINDWARD SIDE OF THE NASA 040A SPACE SHUTTLE

## ORBITER AT 31° ANGLE OF ATTACK AND MACH 20 IN HELIUM

George C. Ashby, Jr., and Vernon T. Helms III  
Langley Research Center

### SUMMARY

Pitot-pressure and flow-angle distributions in the windward flow field of the NASA 040A space shuttle orbiter configuration and surface pressures have been measured in the 22-inch aerodynamics leg of the Langley hypersonic helium tunnel facility at a Mach number of 20 and an angle of attack of 31°. The free-stream Reynolds number, based on model length, was  $5.39 \times 10^6$ .

The results show that cores of high pitot pressure, which are related to the body-shock—wing-shock intersections, occur on the windward plane of symmetry in the vicinity of the wing-body junction and near midspan on the wing. Theoretical estimates of the flow-field pitot pressures show that conical-flow values for the windward plane of symmetry surface are representative of the average level over the entire lower surface.

### INTRODUCTION

The National Aeronautics and Space Administration is actively engaged in the development of three-dimensional inviscid and viscous flow-field computer programs. (See, for example, ref. 1.) These programs are part of a developing capability to assess the aerodynamics, heating, real-gas chemistry effects, and so forth on hypersonic configurations, such as the space shuttle. Very few experimental data for flow fields are available for evaluating the calculation methods as they evolve.

The present study was conducted to provide a set of data which can be used to aid in the development and verification of computer codes at high Mach numbers. Pitot-pressure surveys and surface-pressure measurements were made at 14 orifice locations on the windward surface of a delta-wing orbiter at an angle of attack of 31° (nominal entry angle of attack for the shuttle at time of study) and a Mach number of 20.3 in helium. In addition, flow-direction surveys were made at selected locations. The use of helium as a test medium provides data in a flow field involving viscous and dynamic effects without additional effects arising from internal excitation of the gas molecules (ref. 2). This ideal characteristic of helium with regard to fluid-mechanics research at high Mach numbers has been established by previous studies (ref. 3). Although complete simultaneous simulation of all flow conditions about a model will probably be rare, it seems

possible to obtain sufficient simulation for many types of aerodynamic as well as fluid-dynamic studies and to interpret most helium results in terms of air results (ref. 4).

This paper presents the flow-field surveys from the windward surface of the configuration through the bow shock into the free stream at each orifice location. Theoretical approximations from several techniques are used to help in the analysis of the data.

#### SYMBOLS

A	aspect ratio
b	wing span, mm
l	model length, mm (see fig. 1)
M	Mach number
$P_s$	local static pressure, $N/m^2$
$P_{t,B}$	pressure, bottom tube of five-tube probe, $N/m^2$
$P_{t,C}$	pressure, center tube of five-tube probe, $N/m^2$
$P_{t,L}$	pressure, left tube of five-tube probe, $N/m^2$
$P_{t,R}$	pressure, right tube of five-tube probe, $N/m^2$
$P_{t,T}$	pressure, top tube of five-tube probe, $N/m^2$
$P_{t,\infty}$	free-stream total pressure, $N/m^2$
$P_{t,3}$	pitot pressure behind body shock, $N/m^2$
$r_n$	nose radius of model, mm
S	planform area, $mm^2$
$x_m$	axial distance from model reference origin, mm (see fig. 2)
$y_m$	spanwise distance from model reference axis, mm
$z_m$	vertical distance from model reference axis, mm
$z_\infty$	distance from model surface normal to free stream, mm
$\alpha$	angle of attack, deg

## APPARATUS AND TESTS

### Tunnel

The tests were conducted in the 22-inch aerodynamics leg of the Langley hypersonic helium tunnel facility at a Mach number of 20.3 and a Reynolds number, based on model length, of  $5.39 \times 10^6$ . Average stagnation temperature and pressure were 300 K and  $7.0 \times 10^6$  N/m<sup>2</sup>, respectively. Operational characteristics of the facility and details of the contoured nozzle flow characteristics are available in reference 5.

### Model and Instrumentation

A 0.0075-scale model of the NASA 040A space shuttle orbiter with orifices located as shown in figure 1 was used in the investigation. The measured model cross sections and profiles and their respective coordinates are presented in figure 2 and tables I and II. The body asymmetries noted in the tables result from the mode of model construction. The body was cast, the wing was machined, and the two were assembled after the pressure tubes were installed. Cast bodies are generally limited to accuracies of  $\pm 0.25$  mm. Multiple-range electrical pressure transducers were used to sense the model surface and flow-field pressures, and the outputs were recorded on magnetic tape. The static-pressure-orifice size is given in figure 1, and the survey probe designs are shown in figure 3.

### Test and Methods

The pitot-pressure and flow-angle surveys were conducted from the model surface through the shock to the undisturbed flow. All probe traverses were made normal to the free-stream flow direction with the probe center line approximately parallel to the model surface. A fouling light indicated probe departure from the surface, and a calibrated slide-wire potentiometer measured the survey distances. Data acquisition was started by a relay in the fouling light circuit when the probe departed from the model surface. Therefore, the initial probe position was a half diameter off of the surface and this was used as a reference value to compute the remainder of the survey positions. Data were sampled 20 times per second, and the rate of probe travel was adjusted to be compatible with the observed pressure-lag rate within the boundary-layer and shock-layer regions. The data sample rate and the probe travel rate resulted in a maximum spacing between survey points of 0.050 mm. Figure 4 shows the shock pattern and flow field illuminated by an electron beam during a pitot-pressure survey.

The top and bottom tubes of the flow-direction probe were 1 mm above and below the center (pitot-pressure) tube, respectively, so that the individual frames of data for each tube, when it was at the identical  $z_\infty$ -coordinate, were used to obtain the flow angle at that point and to eliminate the first-order effects of the pitot-pressure gradient. Because of the gradient and other effects, the angle measurements in the boundary layer are not considered to be so accurate as those in the shock layer. This pressure gradient correction was not made in the horizontal plane because the distance between the survey planes was too great and because the spanwise pitot-pressure gradient was small. The

vertical flow angle was referenced to the local body slope in a plane parallel to the model symmetry plane, and the spanwise flow angle was referenced to the model symmetry plane.

### Measuring Accuracy

Based on static calibrations of the pressure transducers, the error in the measured pressures normalized by the free-stream total pressure is less than  $0.048 \times 10^{-3}$ . The agreement of the pitot-pressure measurements outside of the bow shock in the free stream (probe at  $30^\circ$  to  $35^\circ$  to the flow) with the theoretical free-stream value indicates the relative insensitivity of the probe readings to vertical flow angularity. Also, repeated surveys with the pitot probe aligned with the free stream and yawed  $15^\circ$  show good agreement between the two profiles and, thereby, insensitivity to spanwise angle as well as vertical angle (fig. 5). The five-tube flow-direction probe was calibrated in uniform flow at combination vertical and spanwise angles up to  $26^\circ$  and at a Mach number of 20.3 in helium. The calibration was checked in the Langley 20-inch Mach 6 tunnel (air) over similar angle-of-attack and sideslip-angle ranges. Several probes were used during the test program; a typical calibration is shown in figure 6.

## RESULTS AND DISCUSSION

The measured surface pressures and pitot-pressure profiles from the model surface through the bow shock at the 14 orifice locations are listed in table III. The surface pressures are plotted in figure 7; the pitot-pressure profiles are plotted in figures 8 to 12; and the longitudinal and spanwise pitot-pressure contours are plotted in figure 13. Figure 14 presents the flow-angle profiles.

### Surface Pressures

All measured surface pressures and theoretical estimates along the model plane of symmetry are presented in figure 7. The theoretical pressure distributions along the plane of symmetry of the orbiter at angle of attack were obtained by calculating the distributions on axisymmetric shapes at an angle of attack of  $0^\circ$  to approximate the model contour in the windward symmetry plane. An overexpansion of the flow is indicated by the measured pressures along the plane of symmetry in the vicinity of orifice 2. This overexpansion is shown by tangent-cone theory to be related somewhat to the variation in the actual model surface slopes (measured slopes along the plane of symmetry were used in the calculations) as well as flow conditions. The combination blunt-body program and method-of-characteristics calculations (using codes of refs. 6 and 7) give good average estimates of the pressure distribution along the windward plane of symmetry, but the flow overexpansion at orifice 2 is not predicted. However, a second calculation (using the program of ref. 8), wherein a blunter nose than the actual body nose was combined with a  $33.75^\circ$  cone frustum to represent the configuration shape in the symmetry plane, indicates an overexpansion near orifice 2 which is close to the measured pressure distribution. These latter results suggest that the orbiter nose pressure distribution at angle of attack resembles that of a blunter configuration at an angle of attack of  $0^\circ$ . The difference between the origin of the

blunt nose and the true nose can be seen in figure 7 by the difference in the location of the stagnation points. The beginning of the cone frustum is noted in the plot. Pressures at the outboard orifices are also presented in the figure and generally increase in the outboard direction.

### Pitot-Pressure Profiles

Pitot-pressure surveys were made from each orifice on the model surface through the shock layer into the free-stream flow, and these pressures have been nondimensionalized by the free-stream total pressure (figs. 8 to 12). The static pressure at the model surface, which is also the pitot pressure (surface velocity zero), provides an end point at the wall for the measured profile. The distortion in the measured profile near the body surface is attributed to probe-wall interference and is usually confined to the region within 0.5 mm of the surface. In the region outside the bow shock, the calculated free-stream pitot pressure is identified in each plot for comparison with the probe reading. Although the probe axis in this region is at an angle of  $30^\circ$  to  $35^\circ$  to the free stream, the measured pitot pressure approaches the calculated value at an angle of  $0^\circ$ .

An attempt was made to calculate the flow field and body surface pressures for the conditions of these tests by using the computer program developed in references 9 and 10. The calculations failed because the axial velocity of the flow along the leading edge of the forebody at these flow conditions always dropped below sonic velocity. Because of this calculation failure, some established theories were used on bodies of revolution that represented the windward plane of symmetry profile in the data analysis. The initial calculations were made by using tangent-cone theory because previously published pitot-pressure surveys in the windward symmetry plane of previous space-shuttle configurations (ref. 11) showed that flow-field properties at the edge of the boundary layer can be reasonably predicted by tangent-cone theory. Pitot-pressure values for a  $33.75^\circ$  sharp cone, which is representative of the aft 82 percent of the lower surface along the windward symmetry plane, were computed and are compared with the measured pitot-pressure profiles at stations along the windward symmetry plane in figure 8(a). Except at the most forward orifices where nose bluntness and viscous effects are strong, the pitot-pressure profiles, based on tangent-cone approximation, are a reasonably good average of the measured profiles. A comparison of the calculated tangent-cone profiles for the windward symmetry plane with the measured profiles off the symmetry plane (figs. 8(b) and 8(c)) also shows them to be a reasonably good average at all stations, except for orifice 10, which is in the vicinity of the bow-shock—wing-shock intersection.

The previous calculation was for a  $9^\circ$  sharp nose. To account for the nose effects of the configuration, a power-law body of revolution at an angle of attack of  $0^\circ$  was fitted to the lower surface plane of symmetry contour at an angle of attack of  $31^\circ$ , and the method of characteristics with a  $45^\circ$  sharp starting cone was used to calculate the flow field. The computed profiles (fig. 8(a)) are somewhat low at the forward orifices and near the body surface at all orifices, but they are a good representation of the measured pitot-pressure level and the trends in the outer regions of the flow field at the rear orifices. The difference between the calculated and measured profiles in the flow field near the body is probably caused largely by nose bluntness and/or viscous effects. Further insight

into the nose effect was sought by using an ellipsoid nose on the power-law body representation of the lower surface plane of symmetry instead of the  $45^\circ$  cone and by using the blunt-body and method-of-characteristics programs (refs. 6 and 7) to compute the flow field. The actual body was less blunt than the minimum bluntness body for which the program would run and could contribute to the calculated pitot level being much lower than the measured values. However, the shapes of the computed profiles near the surface are more representative of the measured ones than the calculation for a conical nose.

To investigate the viscous effects on the pitot-pressure profile, the values in the boundary layer along the windward plane of symmetry were calculated by using the computer code of reference 12 and by assuming that the flow along the plane of symmetry at an angle of attack of  $31^\circ$  can be represented by flow along a body of revolution at an angle of attack of  $0^\circ$ . These data are shown in figure 9 along with the measured profiles and the calculated inviscid profiles for the power-law body with an ellipsoid nose. The surface pressures and shock coordinates used as inputs to the boundary-layer program were obtained from experimental data.

The pitot-pressure level is only about half the measured values, and the calculated boundary-layer thickness is generally greater than that indicated by the definite change of the slope of the measured profile shown by the intersecting straight lines. The calculated boundary-layer thicknesses are greater than the measured values partly because of crossflow effects in the experimental data. A comparison of the calculated boundary-layer pitot-profile shape with the calculated inviscid pitot-profile shape in the boundary-layer region indicates that forward of orifice 4 (22.71 nose radii downstream) viscous effects predominate in altering the pitot-profile shape near the body. Aft of orifice 4 the calculated pitot-pressure profiles near the body for inviscid flow and a blunt nose are similar in shape to the measured profile; therefore, nose bluntness has a more significant effect on the profile shape in the aft region of the body than viscous effects.

Cross plots of the measured pitot-pressure profiles along lines located at stations through several orifice axes are compared in figures 10 to 12. Examination of these plots reveals some notable trends. The peak does not occur at the same location in the shock layer. Along the plane of symmetry (fig. 10(a)), the peak pitot-pressure level progressively increases from orifices 1 to 4, remains nearly constant between orifices 4 and 6, and then decreases from orifices 6 to 11. At the two outboard stations (figs. 10(b) and 10(c)), the profiles at the orifices along each longitudinal line are similar in shape.

In the spanwise direction, a comparison of adjacent profiles (fig. 11) shows very little change in pitot-pressure level or general shape of the profile for axial locations forward of orifice 8. Some shifting of the profiles for the two adjacent locations occurs because the distance between the shock and the body changes. At the axial stations of orifices 8 and 11, the peak pitot pressure increases significantly at the more outboard locations (figs. 11(d) and 11(e)). The largest increase occurs at approximately midspan on the wing near orifice 10 (figs. 11(d) and 12) where the profile has the highest level and has a distinct



double peak. The profiles at orifices 12 and 13 also have a tendency toward a double peak, but they are not so pronounced as those for orifice 10. The anomalies associated with the central portion of the wing, especially in the vicinity of orifice 10, are attributed to the bow-shock—wing-shock interaction which occurs in that area.

Contours of measured pitot pressures (normalized by  $p_{t,\infty}$ ) between various groups of orifices are presented in figure 13. The contour plot along the body plane of symmetry (fig. 13(a)) also shows the shock location, which was assumed to be at the sharp drop in pitot pressure in the flow field, and the projections of the pressure contours to the appropriate portion of the shock. In these contour plots of the pitot pressure, the high value within a core along the plane of symmetry in the vicinity of orifices 4 and 6 is noted to be located near the junction of the wing leading edge and body and just behind the shock inflection point. This high-pressure core is observed to extend outboard of the plane of symmetry to at least orifices 5 and 7. (Note that the pitot-pressure contours are parallel between orifices 4 and 5 and between orifices 6 and 7 in figs. 13(f) and 13(g), respectively.) The high pressure within a core in the region of orifice 10 is also observed by comparing its contour levels with those at orifice 13 in figure 13(c), with those of orifices 7 and 14 in figure 13(d), and with those of orifices 8 and 9 in figure 13(h). At stations behind orifice 6, the maximum pitot pressure increases in the spanwise direction. The pitot-pressure levels at all orifices except 10 and 14 are consistent from orifice to orifice with the flow direction between them. (See following section entitled "Flow-Direction Surveys.")

### Flow-Direction Surveys

Flow-direction profiles in the flow field (fig. 14) at all but the first three forward orifices were measured by using a five-tube pressure probe (fig. 3). As discussed in the section entitled "Test and Methods," the vertical flow angles were corrected for the first-order pitot-pressure-gradient effects, but the spanwise flow angles are uncorrected.

In general, the flow direction and distributions were as expected. For example, the flow near the body for all the orifices is deflected away from the surface by the boundary layer and gradually changes to a direction toward the body as the flow field is traversed out to the shock. Also, the spanwise flow direction is nearly zero on the plane of symmetry and becomes increasingly more outboard at successive stations in the spanwise direction.

As mentioned in the section entitled "Pitot-Pressure Profiles," the pitot-pressure levels are consistent from orifice to orifice with the flow direction between them. For example, the spanwise flow angle of approximately  $8^\circ$  at orifice 7 directs its flow toward orifice 13, which has an average flow angle of  $10^\circ$ . The average pitot-pressure level for the two are approximately the same. However, the spanwise flow direction from orifice 10 is an average of  $22^\circ$  and flows toward orifice 14, but its pitot level is less than that of orifice 10.

## SYMMARY OF RESULTS

Pitot-pressure and flow-angle distributions in the flow field on the windward side of the NASA 040A space shuttle orbiter configuration and surface pressures have been measured in the 22-inch aerodynamics leg of the Langley hypersonic helium tunnel facility at a Mach number of 20 and an angle of attack of  $31^\circ$ . From an analysis of the measurements the following summary of results is made:

1. The pitot-pressure profiles indicate that cores of high pitot pressure occur in the vicinity of the wing-body junction and at about midspan of the wing. The two high pitot-pressure regions are attributed to body-shock—wing-shock interactions.

2. The average value of pitot pressure in the shock layer does not vary much in the spanwise direction, and tangent-cone-theory estimates of the pitot pressure in the flow field about a cone at an angle of attack of  $0^\circ$ , representing the contour in the plane of symmetry of the configuration, are reasonably close to this average value.

3. Calculations of the inviscid and viscous pitot-pressure profiles along the body windward plane of symmetry show that the nose bluntness and viscous effects appear to have a large influence on the pitot-profile shapes.

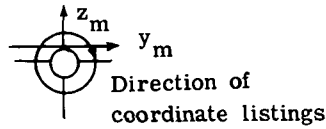
4. An overexpansion of the flow is indicated by the measured surface pressures along the windward plane of symmetry. The average surface pressure and the flow overexpansion are estimated very well by tangent-cone theory and by a combination of blunt-body and method-of-characteristics programs, wherein the model contour in the plane of symmetry is represented by axisymmetric shapes at an angle of attack of  $0^\circ$ .

Langley Research Center  
National Aeronautics and Space Administration  
Hampton, VA 23665  
August 9, 1977

## REFERENCES

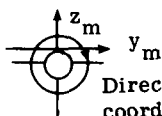
1. Aerodynamic Analyses Requiring Advanced Computers, Parts I and II. NASA SP-347, 1975.
2. Johnson, Robert H.: A Hypersonic Helium Tunnel for Mach Numbers Above Twenty. Rep. No. 58-RL-2089, Gen. Elec. Res. Lab., Sept. 1958.
3. Henderson, Arthur, Jr.: Experimental Investigation of the Air-Helium Simulation Problem on Various General and Specific Configurations at Hypersonic Speeds. Presented at The Second Nat. Symposium on Hypervelocity Techniques (Univ. of Denver), Mar. 1962.
4. Love, Eugene S.; Henderson, Arthur, Jr.; and Bertram, Mitchel H.: Some Aspects of Air-Helium Simulation and Hypersonic Approximations. NASA TN D-49, 1959.
5. Arrington, James P.; Joiner, Roy C., Jr.; and Henderson, Arthur, Jr.: Longitudinal Characteristics of Several Configurations at Hypersonic Mach Numbers in Conical and Contoured Nozzles. NASA TN D-2489, 1964.
6. Lomax, Harvard; and Inouye, Mamoru: Numerical Analysis of Flow Properties About Blunt Bodies Moving at Supersonic Speeds in an Equilibrium Gas. NASA TR R-204, 1964.
7. Inouye, Mamoru; and Lomax, Harvard: Comparison of Experimental and Numerical Results for the Flow of a Perfect Gas About Blunt-Nosed Bodies. NASA TN D-1426, 1962.
8. Zoby, Ernest V.; and Graves, Randolph A., Jr.: A Computer Program for Calculating the Perfect Gas Inviscid Flow Field About Blunt Axisymmetric Bodies at an Angle of Attack of  $0^\circ$ . NASA TM X-2843, 1973.
9. Marconi, Frank; Salas, Manuel; and Yaeger, Larry: Development of a Computer Code for Calculating the Steady Super/Hypersonic Inviscid Flow Around Real Configurations. Volume I - Computational Technique. NASA CR-2675, 1976.
10. Marconi, Frank; and Yaeger, Larry: Development of a Computer Code for Calculating the Steady Super/Hypersonic Inviscid Flow Around Real Configurations. Volume II - Code Description. NASA CR-2676, 1976.
11. Ashby, George C., Jr.: Experimental Boundary-Layer Edge Mach Numbers for Two Space Shuttle Orbiters at Hypersonic Speeds. NASA TN D-6574, 1972.
12. Price, Joseph M.; and Harris, Julius E.: Computer Program for Solving Compressible Nonsimilar-Boundary-Layer Equations for Laminar, Transitional, or Turbulent Flows of a Perfect Gas. NASA TM X-2458, 1972.

TABLE I.- COORDINATES FOR CROSS SECTIONS



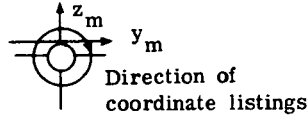
$x/l = 0.01$		$x/l = 0.025$		$x/l = 0.051$		$x/l = 0.051$		$x/l = 0.075$		$x/l = 0.075$	
y, mm	z, mm	y, mm	z, mm	y, mm	z, mm	y, mm	z, mm	y, mm	z, mm	y, mm	z, mm
3.5687	-6.5024	5.0927	-6.4084	7.0739	-6.1189	-0.2616	1.1709	8.8367	-5.7760	3.2537	2.7762
3.5001	-6.9266	5.0444	-6.7005	7.0434	-6.4110	.6140	1.1151	8.7960	-6.2840	4.5644	2.1031
3.3731	-7.4778	4.8768	-7.4270	6.9926	-6.8174	1.3691	.9881	8.7173	-6.9469	5.5474	1.3868
3.0607	-8.1686	4.5695	-8.2271	6.9621	-7.0206	2.7457	.5309	8.5674	-7.7953	6.2865	.7087
2.7915	-8.5573	4.2113	-8.9560	6.8605	-7.5057	3.7617	.0000	8.4303	-8.3668	7.0612	-.2591
2.4079	-9.0907	3.9141	-9.4336	6.7793	-7.8537	4.8209	-.8153	8.2296	-9.0881	7.6657	-1.2700
1.9507	-9.5809	3.6170	-9.8425	6.6065	-8.4582	5.5499	-1.6027	7.9578	-9.8679	8.2194	-2.6772
1.6434	-9.7993	3.1191	-10.4064	6.3271	-9.2050	6.0020	-2.3165	7.6784	-10.5689	8.5166	-3.6805
.9525	-10.1168	2.4562	-10.9855	6.1849	-9.5225	6.2941	-2.9185	7.2339	-11.4808	8.6893	-4.5060
.6325	-10.2337	1.9253	-11.3157	6.0274	-9.8730	6.6446	-3.8227	6.6904	-12.4054	8.8011	-5.3797
-.2515	-10.2997	1.1659	-11.6103	5.6312	-10.6020	6.8555	-4.5822	6.1671	-13.1420	8.8341	-5.7760
-1.0109	-10.3200	.3251	-11.8034	5.1460	-11.3233	6.9977	-5.3086	5.6159	-13.7643		
-1.7247	-10.2591	-.3124	-11.8516	4.6990	-11.9101	7.0739	-6.1189	4.6990	-14.4983		
-2.1615	-10.1346	-1.3106	-11.8491	4.1808	-12.4739			3.3299	-15.0089		
-2.7483	-9.8298	-2.1006	-11.7450	3.6500	-12.8626			2.1539	-15.1638		
-3.2664	-9.4005	-3.0683	-11.4351	3.0099	-13.2563			.9703	-15.2756		
-3.4417	-9.2050	-3.5611	-11.1862	2.3698	-13.5230			-.1880	-15.3518		
-3.9345	-8.5420	-4.1707	-10.7544	1.7348	-13.6119			-1.6180	-15.3899		
-4.1148	-8.1636	-4.7523	-10.1905	.8077	-13.6779			-3.0861	-15.3543		
-4.2850	-7.6937	-5.1841	-9.6520	-.1448	-13.7262			-4.1580	-15.2121		
-4.4221	-7.0866	-5.3772	-9.3548	-1.4275	-13.7770			-4.9225	-14.9479		
-4.4755	-6.5100	-5.5143	-9.0780	-2.3216	-13.7770			-5.6566	-14.5948		
-4.4755	-6.5075	-5.7277	-8.5192	-3.1521	-13.6779			-6.6700	-13.8532		
-4.3917	-5.8268	-5.7988	-8.2855	-4.6380	-13.0886			-7.4574	-12.9997		
-4.1605	-4.8311	-5.8953	-7.9197	-5.3391	-12.5705			-7.9146	-12.2631		
-3.7490	-4.1427	-5.9792	-7.4117	-5.7429	-12.2022			-8.4303	-11.1938		
-2.8169	-3.3884	-6.0173	-7.1298	-6.2306	-11.6434			-8.7960	-10.2311		
-1.8999	-2.9896	-6.0477	-6.8834	-6.5735	-11.1506			-9.1338	-9.1669		
-1.1176	-2.7889	-6.0528	-6.6396	-6.9037	-10.5258			-9.4158	-8.1382		
-.2565	-2.7432	-6.0528	-6.6396	-7.1171	-10.0457			-9.5860	-7.3914		
.5080	-2.8677	-5.9995	-5.8903	-7.4117	-9.2659			-9.7257	-6.5126		
1.2217	-3.1064	-5.6794	-4.4958	-7.6987	-8.3033			-9.7892	-5.7760		
1.7678	-3.4036	-5.3924	-3.8227	-7.8511	-7.6175			-9.7917	-5.7760		
2.0955	-3.6754	-4.9403	-3.1217	-7.9426	-7.1247			-9.7460	-5.1689		
2.7407	-4.3790	-4.3053	-2.4714	-8.0061	-6.6650			-9.6393	-4.2443		
3.0963	-5.0165	-3.4011	-1.7856	-8.0416	-6.1671			-9.5021	-3.5154		
3.4366	-5.9919	-2.3749	-1.3564	-8.0416	-6.1646			-9.2481	-2.7076		
3.5687	-6.5049	-1.0439	-1.1328	-7.9731	-5.4331			-8.9027	-1.8390		
		.4699	-1.1633	-7.8359	-4.7193			-8.4303	-.9855		
		1.2903	-1.3411	-7.6581	-4.0132			-8.0137	-.3607		
		1.9710	-1.6104	-7.3127	-3.0709			-7.4701	.4089		
		2.7813	-2.0422	-7.0561	-2.5933			-6.7158	1.1582		
		3.1826	-2.3571	-6.6700	-1.9228			-5.6794	1.9964		
		3.6347	-2.7534	-6.1341	-1.1913			-4.7219	2.5298		
		4.1580	-3.4138	-5.3975	-.5080			-3.5535	2.8854		
		4.4018	-3.8303	-4.7371	.0279			-2.4562	3.1801		
		4.6812	-4.4298	-3.8075	.5105			-1.6434	3.3401		
		4.8463	-4.8870	-2.7788	.8407			-.6756	3.4392		
		5.0013	-5.5143	-1.9355	1.0058			.5359	3.4290		
		5.0876	-6.4110	-1.0947	1.1405			1.8720	3.2283		

TABLE I.- Continued



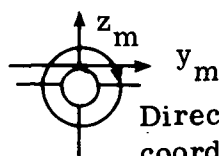
$x/l = 0.1017$		$x/l = 0.1017$		$x/l = 0.12$		$x/l = 0.12$		$x/l = 0.234$		$x/l = 0.234$	
y, mm	z, mm	y, mm	z, mm	y, mm	z, mm	y, mm	z, mm	y, mm	z, mm	y, mm	z, mm
10.4826	-5.2984	-8.0848	2.7356	11.6002	-4.7066	-2.3368	7.1349	17.5209	-0.9373	-17.7343	-0.9830
10.4292	-6.0046	-7.6657	3.0988	11.5748	-5.3035	-7.7468	7.3431	17.4854	-1.6180	-17.7190	-4.115
10.3657	-6.6523	-6.7412	3.8557	11.4910	-6.1747	.2032	7.3558	17.4371	-2.4384	-17.6454	1.0160
10.2133	-7.6098	-6.0198	4.2393	11.3716	-7.0333	1.8161	7.2492	17.3330	-3.5941	-17.5031	2.1387
10.1041	-8.1610	-5.0317	4.7473	11.2166	-7.9299	3.3045	6.9266	17.1450	-5.2451	-17.1933	3.7490
9.9898	-8.6970	-3.8303	5.1664	11.0287	-8.7859	4.8209	6.3500	17.0332	-6.0325	-16.7818	5.1308
9.7968	-9.3828	-2.8448	5.4000	10.8280	-9.5352	5.8369	5.7937	16.8986	-6.9164	-16.4059	6.0731
9.5428	-10.2108	-1.8288	5.5575	10.5918	-10.3988	6.8072	5.1638	16.6649	-8.1915	-15.8826	7.2619
9.3904	-10.6553	-.9982	5.6667	10.3048	-11.2370	7.6784	4.4679	16.4186	-9.3726	-15.2629	8.3541
9.0932	-11.4300	.4394	5.6947	9.9390	-12.2149	8.2855	3.8760	16.0934	-10.7315	-14.5872	9.4132
8.8443	-12.0752	1.6002	5.5982	9.6545	-12.8651	9.0957	2.9439	15.9106	-11.4427	-13.8963	10.3149
8.4734	-12.8118	2.8600	5.3238	9.2913	-13.6271	9.7028	2.1107	15.6413	-12.3774	-12.6213	11.6611
8.1229	-13.4214	4.1605	4.8311	8.8671	-14.3256	10.3175	.9550	15.3873	-13.1267	-11.7246	12.4714
7.6683	-14.1021	5.2781	4.2570	8.4201	-15.0393	10.9296	-.5969	15.0292	-14.1554	-10.7442	13.2994
7.1526	-14.7498	6.3576	3.5204	7.6149	-15.7963	11.3309	-2.0193	14.5618	-15.2527	-10.0889	13.7465
6.6319	-15.2425	7.1831	2.8118	6.7208	-16.3678	11.5265	-3.3249	13.9522	-16.3068	-9.7257	13.9852
5.9055	-15.7124	7.9273	2.0549	5.4864	-16.9774	11.5748	-4.3536	13.3198	-17.0612	-9.4666	15.2654
5.2934	-16.0376	8.5369	1.2090	4.7600	-17.1602	11.6027	-4.7066	12.6797	-17.5920	-9.0780	16.4236
4.3028	-16.3678	8.9332	.5817	3.4722	-17.3152			11.8542	-18.2321	-8.4328	18.1407
3.1775	-16.4846	9.4513	-.4572	2.2809	-17.3609			10.7747	-18.7960	-7.6022	19.6088
2.1234	-16.5583	9.6799	-1.0617	1.3665	-17.4219			9.8374	-19.1770	-6.6878	20.7823
1.1455	-16.6294	9.8958	-1.7120	-1.0744	-17.4828			8.6792	-19.5301	-5.4864	21.7856
.2667	-16.6726	10.0609	-2.3241	-2.6010	-17.4777			8.2956	-19.6240	-4.2723	22.4942
-4.4140	-16.6802	10.2641	-3.3376	-4.0310	-17.4219			6.7462	-19.8780	-2.8778	22.9819
-1.4021	-16.6853	10.3657	-4.0107	-4.8971	-17.2847			5.4966	-20.0025	-1.4580	23.1953
-2.3190	-16.6827	10.4115	-4.7371	-5.7480	-17.0536			4.2647	-20.0914	-.3226	23.3553
-3.3706	-16.6599	10.4800	-5.2984	-6.6294	-16.7615			2.5908	-20.1625	1.9431	23.2105
-4.6634	-16.5100			-7.6505	-16.2636			.8509	-20.1930	3.1217	22.9006
-5.6312	-16.2281			-8.5547	-15.5931			-.8560	-20.1930	4.3485	22.2910
-6.8224	-15.6845			-9.4107	-14.7295			-2.3749	-20.1752	5.5601	21.4401
-7.5311	-15.1740			-10.1346	-13.7262			-3.8760	-20.1168	6.3348	20.7315
-8.3464	-14.4399			-10.5105	-13.0023			-5.2908	-20.0406	7.0002	20.0025
-8.7935	-13.8659			-10.8001	-12.3292			-7.5260	-19.8755	8.0239	18.5725
-9.2608	-13.0988			-11.2624	-11.0693			-8.9535	-19.6825	8.5750	17.4396
-9.6571	-12.3038			-11.6103	-9.9085			-10.4369	-19.2938	8.8925	16.6040
-10.1270	-11.1227			-11.9939	-8.5192			-11.3157	-18.9459	9.2354	15.5778
-10.4978	-9.9873			-12.1920	-7.6835			-12.2682	-18.4048	9.5936	14.3027
-10.6959	-9.3015			-12.5019	-5.7480			-13.2309	-17.6911	10.1676	13.5230
-11.0033	-8.1610			-12.5628	-4.9124			-13.9624	-16.9901	11.2090	12.6390
-11.2065	-7.2669			-12.5959	-4.3536			-14.6253	-16.1773	12.0371	11.7983
-11.3208	-6.5380			-12.5959	-4.3596			-15.2552	-15.1130	12.8575	10.9474
-11.4071	-5.7226			-12.5476	-3.5814			-15.5981	-14.3891	13.5280	10.1498
-11.4402	-5.3061			-12.4079	-2.5400			-16.1671	-12.8092	14.4551	8.8697
-11.4452	-4.7396			-12.2326	-1.7018			-16.5329	-11.3462	15.2730	7.5463
-11.4427	-4.7396			-11.8720	-.5563			-16.8021	-9.9822	15.8775	6.2408
-11.4198	-4.3028			-11.4224	.5283			-17.0688	-8.3109	16.4084	4.9276
-11.3335	-3.5027			-10.7163	1.7678			-17.2390	-7.1323	16.7411	3.9700
-11.1633	-2.6822			-10.1244	2.5959			-17.4396	-5.5753	17.0231	3.0124
-10.9957	-2.0498			-9.0426	3.9014			-17.5438	-4.4755	17.2491	1.9837
-10.6324	-1.0490			-8.1280	4.7600			-17.6708	-2.9489	17.3507	1.3614
-10.1829	-.1499			-6.6319	5.7201			-17.7165	-2.0295	17.4219	.6756
-9.5199	.9627			-5.1079	6.4567			-17.7343	-1.2598	17.4828	-.1473
-8.8621	1.8593			-3.7668	6.8834			-17.7343	-.9830	17.5158	-.9373

TABLE I.- Continued



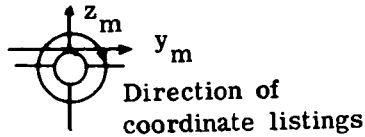
$x/l = 0.386$		$x/l = 0.386$		$x/l = 0.386$		$x/l = 0.543$		$x/l = 0.543$		$x/l = 0.543$	
y, mm	z, mm	y, mm	z, mm	y, mm	z, mm	y, mm	z, mm	y, mm	z, mm	y, mm	z, mm
19.5097	-17.2974	-18.8671	-0.5004	19.1922	8.8925	32.9946	-17.5641	-25.2908	-14.8869	19.1618	0.3404
19.4767	-17.8664	-18.8366	.2616	19.2024	9.8527	32.8295	-18.2626	-24.0538	-14.7726	19.2329	-1.3589
19.2964	-18.7833	-18.7782	1.3691	19.2024	11.0515	32.1539	-18.9992	-22.8244	-14.6634	19.2456	-3.7770
18.9306	-19.6418	-18.6893	2.3012	19.2049	12.2047	31.1201	-19.7104	-21.6408	-14.4678	19.2557	-5.2603
18.4175	-20.2413	-18.4480	3.7313	19.2354	13.2664	30.1269	-20.2819	-20.4775	-14.1097	19.2634	-6.7640
17.9959	-20.5359	-18.2499	4.5568	19.2227	14.2392	29.1008	-20.8026	-19.9085	-13.8379	19.2735	-8.2956
17.2568	-20.8178	-17.6784	6.3475	19.2329	14.9809	28.0010	-21.3106	-19.5504	-13.4645	19.2786	-9.7053
16.4313	-21.0058	-17.0942	7.7191	19.2862	15.5778	26.8707	-21.7551	-19.3573	-13.1597	19.2786	-10.9626
15.0774	-21.3081	-16.5024	8.8468	19.4031	16.6243	25.5905	-22.2453	-19.2481	-12.8829	19.2761	-12.2911
14.0030	-21.4757	-16.0096	9.7511	19.5072	17.2999	24.5720	-22.6187	-19.1186	-12.5603	19.4462	-12.6187
13.0861	-21.5875	-14.9581	11.3411			23.3756	-23.0251	-19.0119	-11.2801	19.6723	-13.2105
11.4554	-21.7907	-14.1199	12.3546			22.1539	-23.4061	-19.0144	-10.1600	20.0228	-13.6169
9.9847	-21.9227	-13.3579	13.2055			20.4826	-24.0157	-19.0170	-8.3464	20.7213	-14.0005
8.7732	-21.9989	-12.3469	14.1707			18.8062	-24.1071	-19.0144	-5.5905	21.7119	-14.2646
7.2085	-22.1107	-11.5773	14.8057			16.8275	-24.1071	-19.0119	-4.1732	22.6568	-14.4551
6.0046	-22.1564	-10.0660	15.9131			14.8692	-24.1021	-18.9916	-1.2421	23.8887	-14.5847
4.7777	-22.1869	-8.7833	16.6573			12.7864	-24.1046	-18.9357	.7722	25.0673	-14.6863
3.6525	-22.1945	-7.5844	17.2568			9.9263	-24.1173	-18.8163	2.3927	26.4617	-14.8285
2.3952	-22.1996	-6.5862	17.6124			7.4397	-24.1173	-18.3693	4.7320	27.7698	-15.0038
1.4656	-22.2021	-4.7828	18.1331			4.8616	-24.1249	-17.9349	6.1570	29.1668	-15.2603
-.6756	-22.2098	-3.6703	18.3083			2.1463	-24.1300	-17.0612	8.1712	30.3149	-15.5575
-2.2301	-22.2098	-2.3901	18.4226			.9398	-24.1325	-16.0630	10.0178	31.3080	-15.8877
-3.4315	-22.1996	-1.1176	18.4607			-.8915	-24.1376	-14.6075	12.0345	31.7932	-16.1036
-4.8590	-22.1742	-.1854	18.4633			-3.6525	-24.1325	-13.4163	13.3071	31.8795	-16.2179
-5.9792	-22.1463	1.3437	18.4506			-6.5532	-24.1046	-12.1818	14.4348	32.2047	-16.4236
-7.4346	-22.0726	2.6924	18.4099			-9.6342	-24.1071	-10.6756	15.5372	32.6263	-16.8148
-8.7884	-21.9939	4.3510	18.2423			-12.6822	-24.1173	-8.9764	16.5710	32.9184	-17.2390
-9.9111	-21.9075	5.9411	17.9299			-15.4737	-24.1173	-7.5946	17.2466	32.9946	-17.5641
-11.3284	-21.7678	7.2669	17.5158			-17.8968	-24.1275	-6.2662	17.7546		
-13.0708	-21.5646	8.6716	16.9012			-19.4412	-24.1046	-4.6609	18.1838		
-14.4221	-21.3589	9.8298	16.2865			-21.1480	-23.7973	-3.2588	18.3871		
-15.3137	-21.2217	10.9855	15.5423			-22.7762	-23.1851	-1.1405	18.4887		
-16.1468	-21.0566	11.9431	14.8057			-24.0182	-22.7965	.3480	18.4887		
-17.1272	-20.7772	12.8575	14.0310			-25.3848	-22.3139	2.2733	18.4506		
-17.9476	-20.2387	13.8989	12.9769			-26.8351	-21.7678	4.6888	18.1915		
-18.5928	-19.3065	14.6736	12.1285			-28.0645	-21.2903	6.9926	17.5743		
-18.8519	-18.2118	15.5397	10.9550			-29.1948	-20.7899	8.3160	17.0536		
-18.9662	-17.4117	16.3246	9.7511			-29.9390	-20.4343	9.8781	16.2331		
-19.0297	-16.6599	17.1425	8.2448			-30.7289	-20.0279	11.0312	15.4686		
-19.0297	-16.6599	17.7292	6.9952			-31.4630	-19.5707	11.9583	14.7472		
-18.9535	-15.7404	18.1940	5.7125			-32.0523	-19.0221	12.9438	13.8582		
-18.9128	-14.1503	18.6436	4.1148			-32.3494	-18.3693	14.1935	12.5755		
-18.9027	-12.3723	18.9154	2.7915			-32.3952	-17.9324	14.8311	11.8135		
-18.9027	-10.8585	19.0906	1.4300			-32.3952	-17.9324	15.8115	10.5131		
-18.9052	-9.6977	19.1414	.2007			-32.2199	-17.3787	16.7691	8.9332		
-18.9078	-8.3261	19.1719	1.3360			-31.7195	-16.7640	17.5108	7.4524		
-18.9052	-7.4320	19.1694	2.8219			-30.8229	-16.1696	17.9756	6.3348		
-18.9128	-5.8547	19.1821	4.7650			-29.4615	-15.6616	18.4709	4.7346		
-18.9128	-4.7904	19.1897	6.5380			-28.2169	-15.3314	18.7782	3.3884		
-18.8849	-2.0472	19.1922	7.8257			-26.7081	-15.0774	19.0043	1.9533		

TABLE I.- Continued

Direction of  
coordinate listings

$x/l = 0.695$		$x/l = 0.695$		$x/l = 0.695$		$x/l = 0.695$	
y, mm	z, mm	y, mm	z, mm	y, mm	z, mm	y, mm	z, mm
54.9250	-15.7251	-21.7195	-25.3644	-22.8498	-14.5059	18.5674	4.2367
54.8564	-16.1620	-23.5814	-25.0063	-21.6205	-14.4450	18.9713	2.4105
54.6329	-16.5354	-25.3187	-24.6710	-20.8991	-14.2011	19.1618	.5309
54.2112	-16.8910	-27.1577	-24.3180	-20.2032	-13.9471	19.2202	-1.6205
53.4746	-17.3990	-29.0322	-23.9573	-19.6164	-13.4849	19.2329	-3.7744
52.2834	-18.0264	-30.8204	-23.6118	-19.2786	-12.9489	19.2456	-5.2476
51.2775	-18.4810	-32.5501	-23.2664	-19.1237	-12.4739	19.2532	-6.8224
50.2564	-18.8493	-34.3789	-22.9083	-19.0119	-9.4082	19.2659	-8.8697
48.5800	-19.4107	-36.3093	-22.4841	-19.0119	-6.5761	19.2684	-10.0686
46.4693	-20.0025	-38.1864	-22.0650	-19.0170	-3.9395	19.2659	-11.1125
44.6938	-20.4699	-40.3657	-21.5621	-18.9967	-.3759	19.2684	-12.2022
43.1013	-20.8788	-42.3901	-21.0820	-18.9687	1.0262	19.5224	-12.7737
42.1894	-21.1049	-44.2925	-20.6146	-18.6233	3.9980	19.8857	-13.5001
41.3537	-21.2852	-46.5252	-20.0254	-18.0848	5.9944	20.4978	-13.9573
39.6342	-21.7119	-48.4403	-19.4818	-17.4117	7.6200	20.9906	-14.2037
38.6486	-21.9405	-49.9821	-18.9916	-16.4313	9.4691	21.5417	-14.3053
36.8503	-22.3495	-51.8516	-18.2829	-15.6616	10.6553	22.3266	-14.4374
35.2730	-22.7000	-52.8980	-17.8054	-14.4653	12.1768	23.8912	-14.3916
33.3604	-23.1115	-53.5661	-17.4244	-13.1470	13.5077	25.2146	-14.3180
31.1328	-23.5712	-53.8759	-17.2110	-11.4198	14.9327	27.0535	-14.2138
28.5344	-24.0919	-54.1249	-16.9647	-10.2997	15.6820	28.4861	-14.1376
26.8630	-24.4069	-54.3865	-16.2306	-8.4760	16.7005	30.1600	-14.0843
24.9326	-24.7904	-54.3839	-16.2331	-6.7183	17.4117	32.4028	-13.9979
23.4290	-25.0673	-54.2798	-15.7734	-5.3010	17.8232	34.0487	-13.9421
21.8237	-25.3568	-53.9496	-15.3746	-3.5966	18.1991	35.3263	-13.9014
19.9669	-25.5397	-53.3070	-14.9708	-1.9812	18.3871	37.0256	-13.8557
18.6258	-25.5702	-52.4510	-14.6583	-.9271	18.4506	40.4012	-13.7820
16.3220	-25.5676	-51.1505	-14.3408	.5563	18.4607	41.6662	-13.7693
13.2410	-25.5753	-49.7383	-14.1630	2.8829	18.2347	43.3832	-13.7693
10.6578	-25.5778	-48.0924	-14.0437	5.2146	17.7571	45.1764	-13.7770
8.0899	-25.5905	-46.4490	-13.9700	6.8453	17.2695	46.9671	-13.8125
5.1867	-25.5930	-44.5389	-13.9167	8.2499	16.7005	48.4149	-13.8735
2.7788	-25.6057	-42.3621	-13.8963	9.7231	15.9487	50.1472	-13.9979
1.2294	-25.6159	-40.2590	-13.8989	11.0846	15.0774	51.0464	-14.0945
-1.1989	-25.6235	-38.2930	-13.9167	12.2784	14.1783	52.5628	-14.3307
-4.5314	-25.6261	-36.4363	-13.9471	13.6322	12.8981	53.7947	-14.6710
-8.2829	-25.6311	-34.0614	-14.0106	14.6507	11.7069	54.8894	-15.4915
-11.2598	-25.6388	-32.0751	-14.0716	15.6159	10.4115	54.9275	-15.7251
-13.6931	-25.6438	-29.9466	-14.1503	16.4973	8.9865		
-16.1569	-25.6489	-27.8663	-14.2392	17.1856	7.7064		
-18.0238	-25.6515	-25.9766	-14.3332	17.8714	6.1747		
-19.3929	-25.6438	-24.7345	-14.4094	18.3007	5.0749		

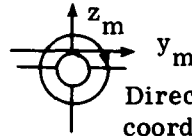
TABLE I.- Continued



$x/l = 0.848$		$x/l = 0.848$		$x/l = 0.848$		$x/l = 0.848$		$x/l = 0.848$	
y, mm	z, mm	y, mm	z, mm	y, mm	z, mm	y, mm	z, mm	y, mm	z, mm
76.5327	-14.0487	-3.0963	-25.0952	-62.8015	-13.3680	-1.4859	25.3721	59.4817	-13.4518
76.4718	-14.3764	-5.0571	-25.1028	-60.3352	-13.5001	-1.0592	26.6014	64.3890	-13.1674
76.2102	-14.7701	-7.3304	-25.1079	-57.6605	-13.6677	-.4851	27.3990	65.8114	-13.0962
75.8546	-15.0774	-9.6876	-25.1079	-54.8564	-13.8608	.2794	27.5438	67.6275	-13.0353
75.1434	-15.4559	-11.8313	-25.1079	-52.4612	-14.0437	.6985	27.4168	69.4792	-13.0150
74.1020	-15.8521	-13.7846	-25.1079	-49.3141	-14.3027	1.4376	26.1696	71.5086	-13.0073
72.7024	-16.2814	-15.7759	-25.0952	-46.1467	-14.5720	1.8517	24.6456	73.1139	-13.0353
71.4096	-16.6116	-18.0238	-25.0952	-43.3019	-14.8361	2.1133	23.1927	74.5134	-13.1216
69.7078	-17.0307	-19.9390	-25.0927	-40.7746	-15.0774	2.2606	21.8161	75.5421	-13.2715
68.9077	-17.2085	-22.2377	-24.8920	-37.5031	-15.3822	2.4790	20.9144	76.4413	-13.6144
67.3989	-17.5590	-24.1198	-24.6151	-35.3593	-15.5854	2.7889	20.2057	76.5327	-14.0487
65.9892	-17.8562	-26.9392	-24.1960	-33.1089	-15.8039	3.4163	19.4640		
64.8894	-18.0797	-29.2506	-23.8633	-30.6807	-16.0426	4.2291	18.8671		
64.0715	-18.2372	-31.3868	-23.5560	-28.2270	-16.2865	4.6380	18.6258		
62.4815	-18.5699	-33.2562	-23.2791	-25.9842	-16.4948	5.3442	18.4607		
61.1226	-18.8265	-35.0418	-23.0251	-23.8277	-16.6751	6.1570	18.3490		
59.4970	-19.1287	-36.8224	-22.7686	-22.6466	-16.7869	7.5006	18.0772		
57.7393	-19.4462	-38.5674	-22.5171	-21.3639	-16.7005	8.8519	17.6149		
55.9943	-19.7510	-40.5359	-22.2352	-20.8509	-16.4389	9.8247	17.1907		
54.5465	-20.0025	-42.7076	-21.9100	-20.4419	-16.2001	11.2751	16.3906		
52.5577	-20.3175	-44.3382	-21.6637	-19.8780	-15.7582	12.4612	15.6058		
50.7949	-20.6070	-45.5930	-21.4732	-19.3167	-15.0419	13.7084	14.6075		
48.8137	-20.9194	-47.2338	-21.2141	-19.1618	-14.3129	14.6406	13.6982		
46.6700	-21.2547	-48.6435	-20.9931	-19.1211	-13.6169	15.4686	12.7483		
45.1485	-21.4884	-50.2920	-20.7239	-19.1135	-12.6619	16.4668	11.3513		
43.3705	-21.7576	-52.1335	-20.4216	-19.0373	-12.0498	17.6555	9.1415		
41.7932	-21.9862	-54.0715	-20.1041	-19.0144	-9.6266	18.3109	7.5159		
39.8399	-22.2936	-56.6217	-19.6571	-19.0221	-6.0579	18.6868	6.1671		
38.7807	-22.4485	-58.4886	-19.3192	-19.0246	-3.7465	18.9865	4.6838		
36.8630	-22.7355	-60.5003	-18.9484	-19.0144	-1.1303	19.1414	2.7178		
34.9021	-23.0327	-62.7278	-18.5166	-18.9992	1.4351	19.1694	1.0008		
32.8422	-23.3350	-64.5617	-18.1483	-18.8519	4.7523	19.1745	-.3708		
30.9220	-23.6220	-65.9994	-17.8435	-18.4506	6.6523	19.1795	-1.9634		
29.1592	-23.8811	-67.7240	-17.4701	-17.6124	9.0780	19.1897	-3.9243		
27.0789	-24.1808	-69.0626	-17.1628	-16.8478	10.5410	19.1999	-6.0350		
25.0571	-24.4754	-70.7542	-16.7589	-15.8369	12.1183	19.1999	-7.7546		
23.1064	-24.7574	-71.9938	-16.4363	-14.9225	13.2258	19.2075	-9.5021		
21.2623	-24.9809	-73.2917	-16.0757	-13.6042	14.5263	19.2202	-11.8364		
19.8755	-25.0571	-74.5846	-15.6693	-12.4917	15.3899	19.3827	-13.0150		
18.3617	-25.0698	-75.4482	-15.3137	-11.4427	16.0249	19.4666	-14.4475		
16.4668	-25.0698	-76.0120	-14.9479	-10.4902	16.5405	19.6317	-15.1028		
14.6533	-25.0673	-76.2051	-14.4450	-8.8367	17.2517	19.0195	-16.1798		
12.4435	-25.0698	-76.2051	-14.4450	-7.3228	17.7521	32.9565	-15.8217		
10.1600	-25.0749	-75.8088	-13.8582	-5.6159	18.1712	34.5669	-15.6616		
7.8207	-25.0825	-74.8284	-13.4544	-4.6101	18.3439	39.7002	-15.1536		
5.2934	-25.0825	-73.2968	-13.2486	-4.4983	18.5115	45.2882	-14.6126		
3.2995	-25.0825	-71.5112	-13.1826	-3.8811	18.9687	47.8257	-14.3662		
1.4986	-25.0927	-69.8856	-13.1699	-2.7711	20.4445	50.7467	-14.1199		
.4928	-25.0901	-67.1576	-13.2105	-2.2885	22.0828	54.0106	-13.8557		
-1.3868	-25.0952	-64.8792	-13.2817	-2.0066	23.3680	57.0154	-13.6195		



TABLE I.- Concluded



Direction of  
coordinate listings

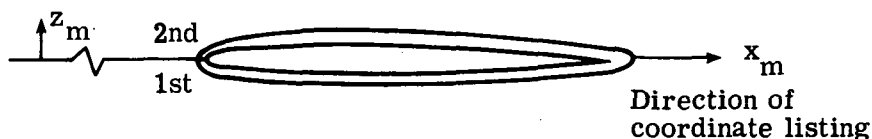
$x/l = 0.997$		$x/l = 0.997$		$x/l = 0.997$		$x/l = 0.997$		$x/l = 0.997$	
y, mm	z, mm	y, mm	z, mm	y, mm	z, mm	y, mm	z, mm	y, mm	z, mm
84.1223	-14.5415	-28.5902	-21.4249	-50.2818	-18.0340	4.3764	67.8282	48.3235	-18.2423
83.0301	-14.6812	-31.0845	-21.1074	-46.6547	-18.4836	1.6840	59.2176	51.9862	-17.7876
80.9219	-14.9454	-33.3350	-20.8255	-43.3451	-18.8951	1.8669	57.1271	56.7512	-17.2034
77.7367	-15.3416	-35.5371	-20.5486	-40.2387	-19.2888	2.0498	54.3839	59.7383	-16.8351
76.0781	-15.5397	-37.5717	-20.2946	-37.4701	-19.6266	2.1692	51.6814	62.8802	-16.4465
73.9470	-15.8115	-39.7535	-20.0228	-35.0139	-19.9187	2.2581	49.1922	65.2094	-16.1874
70.2412	-16.2687	-41.3588	-19.8171	-31.9557	-20.2844	2.3165	46.8782	68.7248	-15.7378
67.7266	-16.5633	-43.5254	-19.5453	-29.0474	-20.6375	2.3520	43.9801	71.2140	-15.4508
65.1586	-16.8859	-45.8902	-19.2456	-26.5684	-20.9347	2.3597	41.4934	73.8708	-15.1054
62.8447	-17.1628	-47.9323	-18.9890	-26.0325	-20.9753	2.3546	39.1465	73.8759	-12.4612
60.3885	-17.4727	-50.1193	-18.7096	-23.7795	-21.2674	2.3317	36.4287	73.7616	-11.2344
58.3514	-17.7089	-51.9887	-18.4683	-21.3589	-21.2674	2.2962	34.3484	74.1324	-10.4343
56.1391	-17.9959	-54.1350	-18.1991	-20.4394	-20.6604	2.2479	32.0192	74.8157	-9.6977
53.9471	-18.2702	-56.4794	-17.9045	-19.1440	-18.0137	2.2022	29.6774	75.7022	-9.3167
51.8719	-18.2702	-58.6410	-17.6276	-19.1338	-16.0579	2.1082	26.7310	77.8637	-9.2024
49.6214	-18.8011	-61.3994	-17.2822	-16.3982	14.6101	2.0447	24.5008	79.0575	-9.1288
47.2008	-19.0881	-63.8480	-16.9672	-14.9784	16.0071	2.1133	22.5146	80.9650	-9.0373
44.6964	-19.4132	-66.1060	-16.6776	-14.0183	16.6218	2.2352	21.1201	82.1284	-8.9916
42.6441	-19.6596	-68.6079	-16.3627	-13.1343	17.1831	2.3927	20.5537	83.2764	-9.3142
40.3327	-19.9517	-71.3410	-16.0122	-10.1752	18.2169	2.7229	19.8806	83.9267	-9.9771
37.9120	-20.2565	-73.5736	-15.7277	-8.7351	18.3921	3.3884	19.2303	84.2797	-10.9677
35.4203	-20.5740	-75.5777	-15.4686	-6.5684	18.5293	3.8075	18.9789	84.3255	-12.0294
33.1876	-20.8534	-78.0212	-15.1511	-5.0952	18.5547	4.3663	18.8036	84.3280	-12.8854
31.1455	-21.0947	-79.9465	-14.8971	-4.5314	18.6309	4.7498	18.6131	84.2848	-13.7236
28.3566	-21.4503	-81.4400	-14.6990	-4.2316	18.8519	5.8801	18.5979	84.3178	-14.5390
26.4389	-21.6941	-82.6872	-14.6431	-3.7363	19.0805	7.0942	18.6106		
24.2240	-21.9532	-83.5203	-14.6456	-3.1598	19.3929	8.2296	18.6030		
22.2606	-22.1894	-83.7971	-14.3256	-2.6467	19.8476	9.9695	18.5445		
20.6477	-22.3926	-83.7971	-14.3256	-2.1666	20.6832	10.8991	18.4074		
18.5903	-22.4460	-83.7387	-13.1699	-1.7755	22.5984	11.9990	18.1229		
16.5049	-22.4663	-83.6549	-11.5367	-1.8542	26.6548	13.1801	17.6327		
14.4221	-22.4917	-83.5609	-10.6426	-1.9380	30.3581	13.9192	17.2390		
12.6390	-22.5069	-82.9386	-9.5809	-2.0066	34.5364	14.7320	16.6929		
10.8534	-22.5196	-82.2833	-9.0170	-2.0320	39.3065	15.4813	16.0960		
8.2702	-22.5425	-80.1980	-9.0576	-2.0091	43.4391	15.8877	15.7150		
5.9411	-22.5450	-78.0263	-9.1694	-1.9253	48.3870	16.3373	15.2527		
3.3909	-22.5527	-75.9587	-9.2634	-1.7907	51.6433	19.5021	-18.8976		
1.1786	-22.5577	-75.0646	-9.3447	-1.6027	55.3060	20.2032	-20.0584		
-1.1074	-22.5679	-74.3026	-9.6164	-1.3589	58.2066	21.2420	-20.9499		
-3.7973	-22.5755	-73.5330	-10.4546	-4.1199	68.0339	24.3815	-21.1328		
-6.1087	-22.5781	-73.2409	-11.5976	-3.7109	69.1896	26.1671	-20.9728		
-8.0416	-22.5806	-73.2409	-12.8372	-2.8321	70.0608	27.6276	-20.7848		
-10.5334	-22.5831	-73.2409	-13.8709	-1.4529	70.3631	29.3268	-20.5791		
-13.1064	-22.5781	-73.2434	-15.1943	-0.7087	70.3656	30.8712	-20.3911		
-15.3111	-22.5654	-70.8762	-15.4788	.3175	70.3885	33.1597	-20.1244		
-17.5539	-22.5425	-67.7824	-15.8648	1.6231	70.3783	35.2400	-19.8730		
-19.3827	-22.5247	-64.6582	-16.2484	2.6772	70.2716	37.5564	-19.5910		
-20.6299	-22.5019	-60.0989	-16.8148	3.3782	69.9668	40.5435	-19.2227		
-22.9768	-22.1564	-56.9214	-17.2085	4.0132	69.3471	43.1571	-18.8925		
-26.2915	-21.7170	-53.4010	-17.6479	4.3307	68.5419	45.7225	-18.5699		

TABLE II.- COORDINATES FOR WING PROFILES



$y/(b/2) = 0.272$		$y/(b/2) = 0.272$		$y/(b/2) = 0.333$		$y/(b/2) = 0.333$	
$x, \text{ mm}$	$z, \text{ mm}$	$x, \text{ mm}$	$z, \text{ mm}$	$x, \text{ mm}$	$z, \text{ mm}$	$x, \text{ mm}$	$z, \text{ mm}$
113.63	-18.075	123.15	-15.639	126.69	-17.996	155.23	-14.232
114.17	-18.809	125.22	-15.349	127.42	-18.809	158.65	-14.191
115.40	-19.431	127.54	-15.133	128.72	-19.444	161.23	-14.168
117.20	-20.079	129.37	-14.983	130.80	-20.079	165.01	-14.155
119.03	-20.612	131.19	-14.869	132.54	-20.523	167.63	-14.155
121.42	-21.196	132.92	-14.783	134.14	-20.904	171.17	-14.194
124.79	-21.864	136.18	-14.658	135.99	-21.278	174.91	-14.254
128.15	-22.342	138.95	-14.547	138.40	-21.641	179.12	-14.348
131.53	-22.736	142.02	-14.455	141.52	-22.047	182.66	-14.453
133.75	-22.949	144.65	-14.397	145.08	-22.426	186.44	-14.602
137.03	-23.241	146.49	-14.359	148.24	-22.720	190.59	-14.790
141.11	-23.559	149.00	-14.321	152.40	-23.051	195.75	-15.070
146.15	-23.899	152.75	-14.280	157.08	-23.368	200.82	-15.400
149.20	-24.094	156.75	-14.267	163.59	-23.736	204.49	-15.644
153.33	-24.328	160.65	-14.277	170.04	-24.028	208.34	-15.946
157.93	-24.562	164.26	-14.308	176.31	-24.239	211.84	-16.251
162.63	-24.755	168.94	-14.379	181.39	-24.359	216.51	-16.698
167.77	-24.956	172.58	-14.458	185.70	-24.422	220.91	-17.160
173.86	-25.123	176.98	-14.567	191.34	-24.460	226.02	-17.727
179.56	-25.243	180.86	-14.694	196.59	-24.435	232.42	-18.485
184.40	-25.298	186.01	-14.907	204.07	-24.285	237.97	-19.197
190.18	-25.319	190.40	-15.133	210.90	-24.077	241.66	-19.705
194.97	-25.283	193.25	-15.286	217.99	-23.787	245.66	-20.271
200.89	-25.154	197.18	-15.532	224.13	-23.465	249.18	-20.805
206.03	-24.994	201.05	-15.822	229.90	-23.086	250.24	-20.996
212.05	-24.768	204.44	-16.071	234.36	-22.758	250.38	-21.128
218.05	-24.491	209.27	-16.492	240.09	-22.289		
224.82	-24.089	214.50	-16.967	246.94	-21.679		
229.64	-23.749	220.17	-17.549	249.17	-21.453		
234.03	-23.409	225.44	-18.161	249.46	-21.044		
238.22	-23.068	228.61	-18.539	128.06	-18.118		
242.40	-22.708	246.09	-20.970	128.94	-17.142		
246.37	-22.360	248.73	-21.379	130.09	-16.584		
248.67	-22.131	250.10	-21.587	132.15	-15.951		
249.29	-22.052	250.40	-21.839	133.30	-15.715		
249.46	-21.659			135.31	-15.362		
115.46	-18.494			137.91	-14.070		
115.92	-17.727			139.83	-14.879		
116.88	-17.188			142.58	-14.689		
118.25	-16.670			145.87	-14.506		
119.62	-16.317			149.39	-14.374		
121.43	-15.905			152.10	-14.298		

TABLE II.- Continued



$y/(b/2) = 0.454$		$y/(b/2) = 0.454$		$y/(b/2) = 0.482$		$y/(b/2) = 0.482$	
x, mm	z, mm	x, mm	z, mm	x, mm	z, mm	x, mm	z, mm
145.03	-17.186	156.35	-14.533	149.25	-16.886	160.52	-14.409
145.85	-18.062	157.91	-14.402	149.61	-17.577	162.11	-14.308
147.08	-18.580	159.79	-14.298	150.31	-18.021	163.99	-14.196
148.51	-19.037	161.61	-14.227	150.90	-18.255	165.97	-14.097
149.64	-19.327	163.11	-14.168	151.75	-18.542	168.10	-14.016
151.35	-19.731	165.35	-14.054	152.62	-18.809	169.99	-13.952
153.40	-20.135	167.11	-14.003	153.96	-19.152	171.82	-13.917
153.30	-20.434	169.35	-13.952	155.41	-19.472	173.56	-13.889
157.07	-20.673	171.60	-13.927	156.86	-19.761	175.84	-13.856
159.69	-20.968	173.84	-13.899	159.23	-20.147	178.05	-13.838
162.73	-21.250	176.26	-13.886	160.79	-20.358	179.30	-13.835
165.77	-21.491	178.82	-13.889	163.04	-20.612	181.62	-13.835
167.79	-21.641	181.07	-13.901	166.09	-20.892	183.15	-13.846
170.33	-21.808	184.25	-13.947	168.94	-21.120	185.55	-13.866
173.34	-21.994	187.51	-14.021	171.78	-21.328	187.55	-13.901
176.35	-22.159	190.07	-14.092	173.78	-21.448	190.63	-13.967
181.00	-22.367	193.99	-14.229	175.51	-21.565	192.75	-14.023
184.20	-22.489	197.75	-14.391	178.86	-21.753	195.33	-14.117
187.56	-22.586	200.45	-14.524	182.33	-21.920	198.00	-14.221
191.22	-22.657	203.84	-14.714	185.97	-22.060	199.88	-14.315
195.26	-22.708	207.86	-14.981	190.50	-22.200	202.18	-14.425
199.77	-22.720	210.90	-15.197	195.56	-22.289	205.20	-14.613
204.18	-22.680	213.55	-15.390	198.82	-22.314	207.51	-14.730
209.01	-22.601	216.26	-15.626	202.84	-22.304	210.24	-14.917
211.49	-22.548	218.87	-15.862	207.03	-22.263	213.48	-15.171
213.79	-22.487	221.82	-16.153	210.70	-22.200	215.88	-15.349
217.38	-22.365	225.35	-16.528	214.35	-22.111	218.48	-15.578
221.37	-22.212	228.45	-16.858	219.03	-21.958	221.43	-15.847
225.50	-22.017	231.12	-17.165	223.42	-21.788	223.70	-16.086
230.10	-21.755	234.66	-17.610	227.86	-21.565	225.71	-16.289
234.80	-21.435	237.36	-17.925	232.64	-21.278	228.89	-16.634
239.60	-21.054	240.58	-18.339	236.77	-20.978	231.33	-16.909
243.04	-20.765	243.54	-18.735	240.61	-20.673	233.64	-17.178
247.10	-20.393	246.12	-19.086	245.20	-20.269	236.09	-17.475
249.91	-20.091	248.48	-19.431	248.02	-20.003	237.87	-17.704
250.43	-20.028	249.99	-19.670	250.34	-19.736	240.43	-18.026
250.47	-19.926	250.45	-19.759	250.48	-19.675	243.06	-18.367
146.06	-17.254	250.45	-19.870	150.26	-17.257	245.29	-18.677
146.60	-16.840			150.49	-16.985	247.28	-18.959
147.48	-16.269			151.76	-16.035	249.38	-19.266
148.62	-15.781			152.61	-15.682	250.35	-19.451
149.52	-15.517			153.41	-15.451	250.46	-19.682
150.87	-15.197			154.50	-15.171		
152.29	-14.943			155.43	-14.973		
153.65	-14.765			156.58	-14.790		
154.88	-14.641			158.07	-14.613		

TABLE II.- Continued



$y/(b/2) = 0.605$		$y/(b/2) = 0.605$		$y/(b/2) = 0.756$		$y/(b/2) = 0.756$	
$x, \text{ mm}$	$z, \text{ mm}$	$x, \text{ mm}$	$z, \text{ mm}$	$x, \text{ mm}$	$z, \text{ mm}$	$x, \text{ mm}$	$z, \text{ mm}$
167.12	-16.152	182.86	-13.724	189.18	-15.100	208.28	-13.277
167.27	-16.548	184.72	-13.673	189.46	-15.558	210.53	-13.292
167.81	-16.916	186.97	-13.627	190.43	-16.088	213.59	-13.338
168.49	-17.236	193.09	-13.597	191.61	-16.424	219.93	-13.559
169.35	-17.539	195.91	-13.622	193.18	-16.777	223.80	-13.762
169.97	-17.717	199.47	-13.668	195.27	-17.130	226.91	-13.965
170.94	-17.983	201.97	-13.721	197.00	-17.361	230.11	-14.216
172.01	-18.238	204.47	-13.810	199.05	-17.567	233.49	-14.508
173.42	-18.517	207.42	-13.917	200.66	-17.704	236.45	-14.803
175.34	-18.809	211.39	-14.115	203.67	-17.920	238.85	-15.067
176.86	-18.997	214.44	-14.288	206.70	-18.098	241.26	-15.349
179.04	-19.238	217.76	-14.498	209.53	-18.232	243.81	-15.654
181.11	-19.426	220.48	-14.702	211.40	-18.308	246.04	-15.936
182.94	-19.578	223.99	-14.981	213.34	-18.374	248.58	-16.302
186.31	-19.820	227.83	-15.352	215.39	-18.415	250.07	-16.518
189.82	-20.041	232.23	-15.799	218.91	-18.461	250.54	-16.612
193.80	-20.244	236.20	-16.264	221.23	-18.466	250.53	-16.711
197.82	-20.404	240.32	-16.759	224.92	-18.428		
201.89	-20.518	244.24	-17.263	227.92	-18.364		
206.60	-20.587	246.70	-17.597	231.48	-18.252		
211.68	-20.577	248.72	-17.879	234.73	-18.118		
215.33	-20.536	249.73	-18.044	237.94	-17.945		
220.09	-20.439	250.45	-18.148	240.69	-17.755		
225.87	-20.257	250.55	-18.336	243.26	-17.562		
230.18	-20.066			245.99	-17.336		
233.97	-19.850			247.99	-17.158		
238.82	-19.520			249.50	-17.005		
243.13	-19.167			250.60	-16.863		
246.74	-18.844			250.66	-16.754		
249.43	-18.572			190.07	-15.415		
250.39	-18.458			190.49	-14.945		
250.63	-18.268			191.43	-14.448		
168.08	-16.264			192.44	-14.158		
168.41	-15.923			193.51	-13.947		
169.60	-15.237			194.73	-13.774		
170.65	-14.892			196.17	-13.625		
171.92	-14.618			197.85	-13.508		
173.36	-14.376			199.29	-13.442		
174.96	-14.194			200.98	-13.381		
177.24	-14.003			202.50	-13.343		
178.95	-13.891			204.01	-13.315		
181.06	-13.810			205.83	-13.292		

TABLE II.- Concluded



$y/(b/2) = 0.907$		$y/(b/2) = 0.907$	
$x, \text{ mm}$	$z, \text{ mm}$	$x, \text{ mm}$	$z, \text{ mm}$
211.71	-14.102	249.67	-9.304
211.82	-14.338	250.83	-9.464
212.38	-14.773	250.93	-14.940
213.11	-15.070		
214.04	-15.304		
214.88	-15.453		
216.68	-15.677		
218.65	-15.850		
220.04	-15.951		
221.85	-16.053		
227.18	-16.269		
229.31	-16.320		
231.64	-16.332		
233.66	-16.320		
239.46	-16.152		
242.55	-15.999		
245.71	-15.784		
248.12	-15.583		
249.83	-15.418		
250.91	-15.151		
212.35	-14.453		
212.61	-14.178		
213.35	-13.724		
214.12	-13.457		
214.88	-13.327		
215.46	-13.254		
216.51	-13.152		
217.53	-13.076		
218.57	-13.038		
219.43	-13.020		
219.68	-7.325		
221.02	-7.290		
223.33	-7.328		
225.61	-7.389		
228.55	-7.513		
231.91	-7.717		
235.13	-7.945		
238.15	-8.148		
240.42	-8.321		
243.12	-8.555		
245.54	-8.799		
247.39	-9.012		

TABLE III.- MEASURED PITOT PRESSURES

ORIFICE 1 $p_s/p_{t_\infty} = 0.001224$		ORIFICE 2 $p_s/p_{t_\infty} = 0.000718$		ORIFICE 3 $p_s/p_{t_\infty} = 0.000897$		ORIFICE 4 $p_s/p_{t_\infty} = 0.001066$	
$z_{\infty}$ mm	$p_{t,3}/p_{t_\infty}$	$z_{\infty}$ mm	$p_{t,3}/p_{t_\infty}$	$z_{\infty}$ mm	$p_{t,3}/p_{t_\infty}$	$z_{\infty}$ mm	$p_{t,3}/p_{t_\infty}$
3.17500E-01	3.93227E-03	3.17500E-01	3.11906E-03	3.17500E-01	4.03559E-03	3.17500E-01	2.88190E-03
4.25900E-01	4.15695E-03	4.25900E-01	3.39225E-03	3.82540E-01	4.07862E-03	4.04220E-01	2.93734E-03
6.42699E-01	4.51170E-03	6.42699E-01	3.94290E-03	4.47579E-01	4.17286E-03	5.12619E-01	3.17840E-03
8.37818E-01	4.74446E-03	8.16138E-01	4.47768E-03	5.55979E-01	4.32990E-03	6.21019E-01	3.56062E-03
9.89577E-01	4.90250E-03	1.01126E+00	4.85260E-03	5.99339E-01	4.55652E-03	7.07738E-01	3.99766E-03
1.18470E+00	5.06013E-03	1.18470E+00	5.06453E-03	7.07739E-01	4.80055E-03	7.94458E-01	4.43427E-03
1.40150E+00	5.16841E-03	1.33646E+00	5.19989E-03	7.51098E-01	4.99056E-03	8.81178E-01	4.83147E-03
1.55326E+00	5.26257E-03	1.50990E+00	5.28538E-03	8.59498E-01	5.11245E-03	1.01126E+00	5.16809E-03
1.79173E+00	5.33820E-03	1.85677E+00	5.42652E-03	9.46218E-01	5.18828E-03	1.27142E+00	5.74359E-03
2.05189E+00	5.41041E-03	2.09525E+00	5.51192E-03	9.89577E-01	5.25332E-03	1.57496E+00	6.03752E-03
2.39877E+00	5.47920E-03	2.33373E+00	5.59616E-03	1.05462E+00	5.29380E-03	1.87845E+00	6.31496E-03
2.70229E+00	5.54365E-03	2.61557E+00	5.69435E-03	1.16302E+00	5.29114E-03	2.20365E+00	6.56391E-03
3.02749E+00	5.60505E-03	2.96245E+00	5.81717E-03	1.22806E+00	5.36937E-03	2.50717E+00	6.79198E-03
3.35269E+00	5.66665E-03	3.43941E+00	5.99242E-03	1.37982E+00	5.40639E-03	2.91909E+00	7.03314E-03
3.65621E+00	5.73018E-03	3.91637E+00	6.18723E-03	1.59662E+00	5.48264E-03	3.39605E+00	7.26128E-03
3.91637E+00	5.81833E-03	4.37164E+00	6.38192E-03	1.77005E+00	5.54404E-03	3.91637E+00	7.47002E-03
4.21988E+00	5.89958E-03	4.89196E+00	6.54214E-03	2.03021E+00	5.63377E-03	4.34996E+00	7.72917E-03
4.54508E+00	6.00126E-03	5.32556E+00	6.67065E-03	2.25869E+00	5.72594E-03	4.82692E+00	7.98650E-03
4.82692E+00	6.10877E-03	5.78084E+00	6.80098E-03	2.45381E+00	5.83810E-03	4.95700E+00	8.07913E-03
5.17380E+00	6.18774E-03	6.23612E+00	6.91456E-03	2.70229E+00	5.92991E-03	5.30388E+00	8.21300E-03
5.47732E+00	6.28212E-03	6.66972E+00	7.04391E-03	2.89741E+00	6.04436E-03	5.56404E+00	8.39484E-03
5.82520E+00	6.41779E-03	7.14667E+00	7.17581E-03	3.11421E+00	6.12676E-03	5.91092E+00	8.55615E-03
5.93260E+00	6.53357E-03	7.60195E+00	7.31063E-03	3.33101E+00	6.21679E-03	6.21444E+00	8.74996E-03
5.93260E+00	6.58152E-03	8.03555E+00	7.46665E-03	3.50445E+00	6.30556E-03	6.49623E+00	8.91315E-03
6.04100E+00	6.63404E-03	8.51251E+00	7.56953E-03	3.69957E+00	6.43257E-03	6.82147E+00	9.08286E-03
6.04100E+00	6.66733E-03	8.96779E+00	7.85839E-03	4.08981E+00	6.56077E-03	7.12499E+00	9.25153E-03
6.04100E+00	6.69831E-03	9.29299E+00	7.22119E-03	4.41500E+00	6.70989E-03	7.38515E+00	9.44990E-03
6.04100E+00	6.71516E-03	9.66154E+00	5.45274E-03	4.71852E+00	6.81780E-03	7.73203E+00	9.88767E-03
6.08436E+00	6.70673E-03	9.94338E+00	4.11856E-03	4.97868E+00	6.86032E-03	8.03555E+00	9.31140E-03
6.08436E+00	6.69831E-03			5.30388E+00	6.88085E-03	8.33907E+00	9.25243E-03
6.14940E+00	6.68852E-03			5.50740E+00	6.90878E-03	8.72931E+00	9.17521E-03
6.17108E+00	6.65682E-03			5.91092E+00	7.01205E-03	9.24963E+00	9.12455E-03
6.19276E+00	6.60781E-03			6.19276E+00	7.11631E-03	9.68322E+00	9.07595E-03
6.38788E+00	6.19048E-03			6.51796E+00	7.23699E-03	1.01602E+01	7.98298E-03
6.51796E+00	5.47245E-03			6.84315E+00	7.35666E-03	1.05938E+01	7.94218E-03
6.69140E+00	4.71008E-03			7.14667E+00	7.47621E-03	1.10707E+01	7.89427E-03
6.79979E+00	4.16360E-03			7.36347E+00	7.64266E-03	1.15477E+01	7.92509E-03
6.99491E+00	3.76438E-03			7.53691E+00	7.65810E-03	1.16344E+01	7.71778E-03
7.12499E+00	3.48995E-03			7.66599E+00	7.72118E-03	1.16778E+01	7.45490E-03
7.27675E+00	3.28996E-03			7.81875E+00	7.82591E-03	1.16778E+01	7.28250E-03
7.42851E+00	3.13553E-03			7.97051E+00	7.91487E-03	1.16778E+01	7.23020E-03
7.64531E+00	3.01347E-03			8.10059E+00	7.86436E-03	1.16778E+01	7.14315E-03
7.77539E+00	2.91763E-03			8.29571E+00	7.41197E-03	1.16995E+01	7.11235E-03
7.90547E+00	2.84264E-03			8.46915E+00	6.69327E-03	1.16995E+01	7.10404E-03
8.03555E+00	2.78713E-03			8.57755E+00	5.93059E-03	1.17211E+01	5.89703E-03
8.20899E+00	2.74183E-03			8.72931E+00	5.18751E-03	1.17211E+01	4.55451E-03
				8.88107E+00	4.64201E-03	1.17211E+01	4.35044E-03
				9.01115E+00	4.13206E-03	1.17211E+01	4.11556E-03
				9.16291E+00	3.80965E-03	1.17211E+01	3.94883E-03
				9.33635E+00	3.57488E-03	1.17211E+01	3.88324E-03
				9.48810E+00	3.40090E-03		
				9.76994E+00	3.16848E-03		
				1.00518E+01	3.03553E-03		
				1.03553E+01	2.96095E-03		
				1.06371E+01	2.91185E-03		
				1.09407E+01	2.88498E-03		
				1.12442E+01	2.86809E-03		

TABLE III.- Continued

ORIFICE 5 $P_s/P_{t_\infty} = 0.001202$				ORIFICE 6 $P_s/P_{t_\infty} = 0.001006$				ORIFICE 7 $P_s/P_{t_\infty} = 0.000923$				ORIFICE 8 $P_s/P_{t_\infty} = 0.000854$					
$Z_{\infty}$	mm	$P_{t_1}/P_{t_\infty}$	$Z_{\infty}$	mm	$P_{t_1}/P_{t_\infty}$	$Z_{\infty}$	mm	$P_{t_1}/P_{t_\infty}$	$Z_{\infty}$	mm	$P_{t_1}/P_{t_\infty}$	$Z_{\infty}$	mm	$P_{t_1}/P_{t_\infty}$	$Z_{\infty}$	mm	$P_{t_1}/P_{t_\infty}$
3.17500E-01		5.03678E-03	3.17500E-01		2.10325E-03	3.17500E-01		4.45742E-03	3.17500E-01		4.45742E-03	3.17500E-01		1.76153E-03	3.17500E-01		1.76153E-03
5.12619E-01		5.18231E-03	3.60960E-01		2.14479E-03	4.69259E-01		4.67115E-03	4.69259E-01		4.67115E-03	4.69259E-01		1.77410E-03	4.69259E-01		1.77410E-03
5.48005E-01		5.80005E-03	4.90939E-01		2.27597E-03	5.55979E-01		5.03047E-03	5.55979E-01		5.03047E-03	5.55979E-01		1.83110E-03	5.55979E-01		1.83110E-03
7.25418E-01		5.82484E-03	5.77459E-01		2.45498E-03	6.86059E-01		5.71338E-03	6.86059E-01		5.71338E-03	6.86059E-01		1.91803E-03	6.86059E-01		1.91803E-03
8.58498E-01		6.13950E-03	6.64379E-01		2.74427E-03	7.72787E-01		6.10354E-03	7.72787E-01		6.10354E-03	7.72787E-01		2.11223E-03	7.72787E-01		2.11223E-03
9.23249E-01		6.37276E-03	7.51098E-01		3.15720E-03	8.68178E-01		6.57641E-03	8.68178E-01		6.57641E-03	8.68178E-01		2.35242E-03	8.68178E-01		2.35242E-03
6.51498E-03		6.51498E-03	4.37318E-01		3.65269E-03	9.67897E-01		6.82493E-03	9.67897E-01		6.82493E-03	9.67897E-01		2.57953E-03	9.67897E-01		2.57953E-03
1.14134E+00		6.63881E-03	4.24538E-01		4.19360E-03	1.05462E+00		7.01895E-03	1.05462E+00		7.01895E-03	1.05462E+00		3.07844E-03	1.05462E+00		3.07844E-03
1.35814E+00		6.90939E-03	1.01112E+00		4.69083E-03	1.14134E+00		7.15951E-03	1.14134E+00		7.15951E-03	1.05462E+00		3.58459E-03	1.05462E+00		3.58459E-03
1.57494E+00		7.13630E-03	1.09798E+00		5.13946E-03	1.20638E+00		7.25809E-03	1.20638E+00		7.25809E-03	1.14134E+00		4.09839E-03	1.14134E+00		4.09839E-03
1.81341E+00		7.35176E-03	1.31478E+00		5.74079E-03	1.29310E+00		7.33527E-03	1.29310E+00		7.33527E-03	1.27142E+00		4.62553E-03	1.27142E+00		4.62553E-03
2.03021E+00		7.50630E-03	1.37982E+00		5.93180E-03	1.37982E+00		7.46195E-03	1.37982E+00		7.46195E-03	1.33646E+00		5.07721E-03	1.33646E+00		5.07721E-03
2.16197E+00		7.65992E-03	1.46654E+00		6.07752E-03	1.46654E+00		7.54526E-03	1.46654E+00		7.54526E-03	1.50790E+00		5.60925E-03	1.50790E+00		5.60925E-03
2.39877E+00		7.76700E-03	1.57494E+00		6.18901E-03	1.57494E+00		7.67655E-03	1.57494E+00		7.67655E-03	1.61829E+00		6.05394E-03	1.61829E+00		6.05394E-03
2.57221E+00		7.88535E-03	1.66165E+00		6.28897E-03	1.79173E+00		7.80119E-03	1.79173E+00		7.80119E-03	1.79173E+00		6.19250E-03	1.79173E+00		6.19250E-03
2.76733E+00		7.96831E-03	1.74837E+00		6.38075E-03	1.96517E+00		7.88063E-03	1.96517E+00		7.88063E-03	1.79173E+00		6.34919E-03	1.79173E+00		6.34919E-03
2.91909E+00		8.05478E-03	1.85677E+00		6.44660E-03	2.16029E+00		7.96526E-03	2.16029E+00		7.96526E-03	1.62181E+00		6.28401E-03	1.62181E+00		6.28401E-03
3.11421E+00		8.15496E-03	1.96517E+00		6.55809E-03	2.33373E+00		8.05129E-03	2.33373E+00		8.05129E-03	2.05189E+00		6.36995E-03	2.05189E+00		6.36995E-03
3.35268E+00		8.27111E-03	2.09525E+00		6.64406E-03	2.48849E+00		8.13628E-03	2.48849E+00		8.13628E-03	2.09525E+00		6.46052E-03	2.09525E+00		6.46052E-03
3.62777E+00		8.35195E-03	2.13861E+00		6.70594E-03	2.65893E+00		8.19443E-03	2.65893E+00		8.19443E-03	2.25533E+00		6.54198E-03	2.25533E+00		6.54198E-03
3.87789E+00		8.44718E-03	2.31205E+00		6.74797E-03	2.85405E+00		8.27602E-03	2.85405E+00		8.27602E-03	2.29037E+00		6.60544E-03	2.29037E+00		6.60544E-03
4.08296E+00		8.54585E-03	2.50717E+00		7.00464E-03	3.02749E+00		8.32903E-03	3.02749E+00		8.32903E-03	2.42031E+00		6.68552E-03	2.42031E+00		6.68552E-03
4.36688E+00		8.61762E-03	2.70229E+00		7.14237E-03	3.20093E+00		8.33390E-03	3.20093E+00		8.33390E-03	2.46381E+00		6.75816E-03	2.46381E+00		6.75816E-03
4.63668E+00		8.68438E-03	2.91909E+00		7.27603E-03	3.39605E+00		8.34038E-03	3.39605E+00		8.34038E-03	2.57221E+00		6.81393E-03	2.57221E+00		6.81393E-03
4.71892E+00		8.74477E-03	3.09253E+00		7.40205E-03	3.59499E+00		8.35189E-03	3.59499E+00		8.35189E-03	2.87573E+00		6.94180E-03	2.87573E+00		6.94180E-03
5.00036E+00		8.76429E-03	3.26213E+00		7.51756E-03	3.72125E+00		8.35797E-03	3.72125E+00		8.35797E-03	3.15757E+00		7.14392E-03	3.15757E+00		7.14392E-03
5.25564E+00		8.83036E-03	3.49927E+00		7.63900E-03	3.89649E+00		8.36997E-03	3.89649E+00		8.36997E-03	3.46109E+00		7.31357E-03	3.46109E+00		7.31357E-03
5.41092E+00		8.88539E-03	3.61637E+00		7.79317E-03	4.06613E+00		8.37973E-03	4.06613E+00		8.37973E-03	3.80797E+00		7.49496E-03	3.80797E+00		7.49496E-03
5.69956E+00		8.89664E-03	3.91317E+00		8.03378E-03	4.21988E+00		8.28962E-03	4.21988E+00		8.28962E-03	4.11149E+00		7.61566E-03	4.11149E+00		7.61566E-03
6.84315E+00		8.78984E-03	4.24156E+00		8.10311E-03	4.48004E+00		8.21328E-03	4.48004E+00		8.21328E-03	4.39332E+00		7.71357E-03	4.39332E+00		7.71357E-03
7.27675E+00		8.65051E-03	4.43668E+00		8.14376E-03	4.80524E+00		8.12200E-03	4.80524E+00		8.12200E-03	4.71952E+00		7.73479E-03	4.71952E+00		7.73479E-03
7.77539E+00		8.56431E-03	4.63668E+00		8.18394E-03	5.23884E+00		7.96663E-03	5.23884E+00		7.96663E-03	5.05540E+00		7.82716E-03	5.05540E+00		7.82716E-03
8.18731E+00		8.45815E-03	4.82340E+00		8.21865E-03	5.69412E+00		7.83149E-03	5.69412E+00		7.83149E-03	5.32556E+00		7.85980E-03	5.32556E+00		7.85980E-03
8.64277E+00		8.34131E-03	4.61012E+00		8.25549E-03	6.13490E+00		7.67310E-03	6.13490E+00		7.67310E-03	5.52908E+00		7.83930E-03	5.52908E+00		7.83930E-03
9.09738E+00		8.16260E-03	4.69649E+00		8.27593E-03	6.62335E+00		7.51390E-03	6.62335E+00		7.51390E-03	5.95428E+00		7.82716E-03	5.95428E+00		7.82716E-03
9.42306E+00		7.99156E-03	4.82692E+00		8.31332E-03	7.08163E+00		7.39888E-03	7.08163E+00		7.39888E-03	6.25780E+00		7.30194E-03	6.25780E+00		7.30194E-03
9.68322E+00		7.90487E-03	4.95700E+00		8.35400E-03	7.55859E+00		7.24261E-03	7.55859E+00		7.24261E-03	6.58302E+00		7.6441E-03	6.58302E+00		7.6441E-03
1.00301E+01		7.85956E-03	5.06540E+00		8.37557E-03	8.01387E+00		7.08152E-03	8.01387E+00		7.08152E-03	6.8651E+00		7.72550E-03	6.8651E+00		7.72550E-03
1.01819E+01		7.63917E-03	5.21716E+00		8.37300E-03	8.46915E+00		6.84397E-03	8.46915E+00		6.84397E-03	7.19003E+00		7.67913E-03	7.19003E+00		7.67913E-03
1.03366E+01		7.13751E-03	5.39060E+00		8.37300E-03	8.62091E+00		6.76806E-03	8.62091E+00		6.76806E-03	7.51523E+00		7.51523E+00	7.51523E+00		7.51523E+00
1.05071E+01		6.48983E-03	5.52068E+00		8.40631E-03	8.90275E+00		6.65194E-03	8.90275E+00		6.65194E-03	7.81875E+00		7.53794E-03	7.81875E+00		7.53794E-03
1.06371E+01		5.65137E-03	5.82420E+00		8.40225E-03	9.27719E+00		6.60255E-03	9.27719E+00		6.60255E-03	8.51251E+00		7.46711E-03	8.51251E+00		7.46711E-03
1.09190E+01		4.34550E-03	6.17108E+00		8.37520E-03	9.72279E+00		6.61632E-03	9.72279E+00		6.61632E-03	8.79435E+00		7.40283E-03	8.79435E+00		7.40283E-03
1.10924E+01		3.93730E-03	6.7460E+00		8.32265E-03	9.35802E+00		6.60784E-03	9.35802E+00		6.60784E-03	9.15291E+00		7.28629E-03	9.15291E+00		7.28629E-03
1.12225E+01		3.82647E-03	6.77811E+00		8.26487E-03	9.50978E+00		6.61273E-03	9.50978E+00		6.61273E-03	9.46842E+00		7.18995E-03	9.46842E+00		7.18995E-03
1.13959E+01		3.40571E-03	7.08163E+00		8.26873E-03	9.66544E+00		6.63483E-03	9.66544E+00		6.63483E-03	9.74826E+00		7.09254E-03	9.74826E+00		7.09254E-03
1.15477E+01		3.24880E-03	7.42891E+00		8.23839E-03	9.81330E+00		6.64672E-03	9.81330E+00		6.64672E-03	1.00951E+01		6.92413E-03	1.00951E+01		6.92413E-03
1.16778E+01		3.11966E-03	7.68367E+00		8.19385E-03	9.96505E+00		6.64919E-03	9.96505E+00		6.64919E-03	1.03987E+01		6.82147E-03	1.03987E+01		6.82147E-03
1.18515E+01		3.03888E-03	8.03555E+00		8.17332E-03	1.01686E+01		6.71499E-03	1.01686E+01		6.71499E-03	1.07239E+01		6.69430E-03	1.07239E+01		6.69430E-03
1.19813E+01		2.96029E-03	8.33907E+00		8.13563E-03	1.02686E+01		6.77545E-03	1.02686E+01		6.77545E-03	1.10733E+01		6.61273E-03	1.10733E+01		6.61273E-03
1.21331E+01		2.92678E-03	8.64259E+00		8.10950E-03	1.05721E+01		6.85306E-03	1.05721E+01		6.85306E-03	1.13526E+01		6.57394E-03	1.13526E+01		6.57394E-03
1.22848E+01		2.87692E-03	8.94611E+00		8.04495E-03	1.08756E+01		6.91963E-03	1.08756E+01		6.91963E-03	1.16344E+01		6.50747E-03	1.16344E+01		6.50747E-03
1.24583E+01		2.86242E-03	9.24963E+00		7.98319E-03	1.11358E+01		6.97239E-03	1.11358E+01		6.97239E-03	1.19163E+01		6.48874E-03	1.19163E+01		6.48874E-03
1.26883E+01		2.83020E-03	9.59650E+00		7												

TABLE III.- Continued

ORIFICE 6 (Continued)			ORIFICE 7 (Continued)			ORIFICE 8 (Continued)		
$Z_{\infty}$ mm	$P_t/P_{t_{\infty}}$		$Z_{\infty}$ mm	$P_t/P_{t_{\infty}}$		$Z_{\infty}$ mm	$P_t/P_{t_{\infty}}$	
1.05071E+01	7.77041E-03		1.18295E+01	6.94981E-03		1.31303E+01	6.70040E-03	
1.07672E+01	7.66622E-03		1.20463E+01	6.94141E-03		1.34772E+01	6.78043E-03	
1.11141E+01	7.53296E-03		1.23063E+01	6.94503E-03		1.37590E+01	6.82038E-03	
1.14176E+01	7.40590E-03		1.26317E+01	6.96431E-03		1.42192E+01	6.85931E-03	
1.17211E+01	7.24791E-03		1.29352E+01	6.99277E-03		1.43661E+01	6.92353E-03	
1.20247E+01	7.07912E-03		1.32171E+01	7.02218E-03		1.46262E+01	6.96177E-03	
1.23282E+01	6.93019E-03		1.34622E+01	7.07852E-03		1.49298E+01	7.00473E-03	
1.24583E+01	6.87873E-03		1.36241E+01	7.14537E-03		1.52983E+01	7.08366E-03	
1.26317E+01	6.81923E-03		1.39542E+01	7.21424E-03		1.55832E+01	7.04281E-03	
1.28051E+01	6.77936E-03		1.41052E+01	7.28066E-03		1.58837E+01	7.07120E-03	
1.29786E+01	6.74675E-03		1.42577E+01	7.30213E-03		1.61655E+01	7.10180E-03	
1.31087E+01	6.70497E-03		1.44094E+01	7.19121E-03		1.64907E+01	7.15636E-03	
1.32387E+01	6.66717E-03		1.45395E+01	6.8264E-03		1.68376E+01	7.18320E-03	
1.33688E+01	6.62867E-03		1.47130E+01	6.23835E-03		1.71411E+01	7.26754E-03	
1.35422E+01	6.63419E-03		1.48647E+01	5.54142E-03		1.73766E+01	7.29289E-03	
1.43010E+01	6.60670E-03		1.51466E+01	4.39948E-03		1.77048E+01	7.33849E-03	
1.46046E+01	6.72237E-03		1.53200E+01	3.99113E-03		1.83300E+01	7.37299E-03	
1.49081E+01	6.78298E-03		1.54718E+01	3.6607E-03		1.83118E+01	7.37896E-03	
1.52116E+01	6.82536E-03		1.56018E+01	3.6607E-03		1.85370E+01	7.40846E-03	
1.55368E+01	6.89369E-03		1.57753E+01	3.30000E-03		1.89405E+01	7.47078E-03	
1.57970E+01	6.94302E-03		1.59270E+01	3.17549E-03		1.92244E+01	7.45642E-03	
1.61438E+01	6.97243E-03		1.60788E+01	3.08039E-03		1.95042E+01	7.47155E-03	
1.63823E+01	7.01163E-03		1.62305E+01	3.00999E-03		1.97644E+01	7.46702E-03	
1.65558E+01	7.04312E-03		1.63609E+01	2.95752E-03		2.01329E+01	7.52053E-03	
1.67292E+01	7.08894E-03		1.65341E+01	2.91448E-03		2.04148E+01	7.52939E-03	
1.68593E+01	7.09670E-03		1.66642E+01	2.87898E-03		2.07400E+01	7.56207E-03	
1.70110E+01	7.01254E-03		1.68159E+01	2.85683E-03		2.10218E+01	7.62716E-03	
1.71845E+01	6.76170E-03		1.69672E+01	2.83900E-03		2.11736E+01	7.64258E-03	
1.73362E+01	6.20972E-03		1.71628E+01	2.82817E-03		2.13253E+01	7.66552E-03	
1.75097E+01	5.59478E-03		1.73146E+01	2.81196E-03		2.14555E+01	7.67054E-03	
1.78132E+01	4.41100E-03		1.74663E+01	2.80432E-03		2.16072E+01	7.70499E-03	
1.79866E+01	3.96055E-03					2.17589E+01	7.73174E-03	
1.81167E+01	3.62619E-03					2.19107E+01	7.76051E-03	
1.82902E+01	3.38803E-03					2.20841E+01	7.72023E-03	
1.84636E+01	3.21183E-03					2.22575E+01	7.58212E-03	
1.85937E+01	3.08569E-03					2.23877E+01	7.25214E-03	
1.87237E+01	2.93366E-03					2.25611E+01	6.74945E-03	
1.88972E+01	2.92235E-03					2.26912E+01	5.97349E-03	
1.90706E+01	2.87505E-03					2.28646E+01	5.28945E-03	
1.92007E+01	2.83641E-03					2.29947E+01	4.76657E-03	
1.93741E+01	2.80962E-03					2.31681E+01	4.21937E-03	
1.95042E+01	2.78696E-03					2.33199E+01	3.84315E-03	
1.95042E+01	2.77326E-03					2.34717E+01	3.55129E-03	
1.95042E+01	2.76396E-03					2.36234E+01	3.34357E-03	
1.95259E+01	2.75797E-03					2.37752E+01	3.53639E-03	
1.95476E+01	2.75032E-03					2.39269E+01	3.06785E-03	
1.95259E+01	2.74534E-03					2.39920E+01	2.65911E-03	
1.95476E+01	2.74497E-03							



TABLE III.- Continued

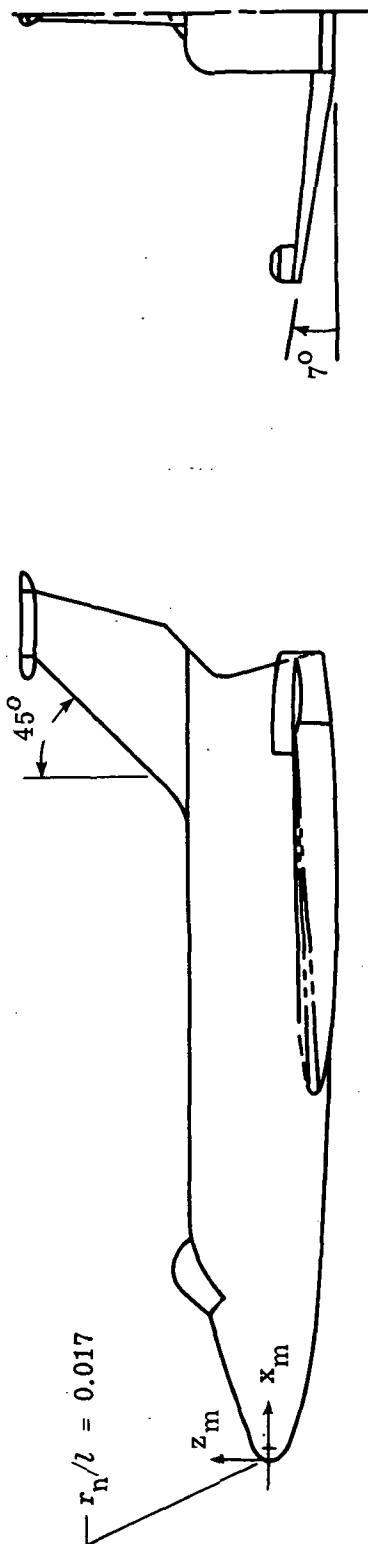
ORIFICE 9				ORIFICE 10				ORIFICE 11				ORIFICE 12			
$P_S/P_{t_\infty} = 0.000878$				$P_S/P_{t_\infty} = 0.001082$				$P_S/P_{t_\infty} = 0.000730$				$P_S/P_{t_\infty} = 0.000941$			
$Z_\infty$ mm	$P_{t_3}/P_{t_\infty}$	$Z_\infty$ mm	$P_{t_3}/P_{t_\infty}$	$Z_\infty$ mm	$P_{t_3}/P_{t_\infty}$	$Z_\infty$ mm	$P_{t_3}/P_{t_\infty}$	$Z_\infty$ mm	$P_{t_3}/P_{t_\infty}$	$Z_\infty$ mm	$P_{t_3}/P_{t_\infty}$	$Z_\infty$ mm	$P_{t_3}/P_{t_\infty}$	$Z_\infty$ mm	$P_{t_3}/P_{t_\infty}$
3.17500E-01	2.62185E-03	3.17500E-01	7.16782E-03	3.17500E-01	7.16782E-03	3.17500E-01	1.22433E-03	3.17500E-01	1.22433E-03	3.17500E-01	1.22433E-03	3.17500E-01	1.22433E-03	3.17500E-01	1.22433E-03
3.39180E-01	2.66336E-03	3.39180E-01	7.16692E-03	3.39180E-01	7.16692E-03	4.04223E-01	1.22353E-03	4.04223E-01	1.22353E-03	4.04223E-01	1.22353E-03	4.04223E-01	1.22353E-03	4.04223E-01	1.22353E-03
4.47599E-01	2.90296E-03	4.47599E-01	7.46702E-03	4.47599E-01	7.46702E-03	4.47599E-01	1.24178E-03	4.47599E-01	1.24178E-03	4.47599E-01	1.24178E-03	4.47599E-01	1.24178E-03	4.47599E-01	1.24178E-03
5.99339E-01	3.44466E-03	5.99339E-01	7.63123E-03	5.77659E-01	7.63123E-03	5.77659E-01	1.28121E-03	5.77659E-01	1.28121E-03	5.77659E-01	1.28121E-03	5.77659E-01	1.28121E-03	5.77659E-01	1.28121E-03
7.29418E-01	4.26644E-03	4.25900E-01	7.85020E-03	7.85020E-03	7.85020E-03	6.86059E-01	1.36511E-03	6.86059E-01	1.36511E-03	6.86059E-01	1.36511E-03	6.86059E-01	1.36511E-03	6.86059E-01	1.36511E-03
9.02485E-01	5.87014E-03	4.57579E-01	7.79194E-03	7.9194E-03	7.79194E-03	7.51008E-01	1.46418E-03	7.51008E-01	1.46418E-03	7.51008E-01	1.46418E-03	7.51008E-01	1.46418E-03	7.51008E-01	1.46418E-03
1.18470E+00	6.37934E-03	5.59199E-01	8.34142E-03	8.34142E-03	8.34142E-03	8.37818E-01	1.58832E-03	8.37818E-01	1.58832E-03	8.37818E-01	1.58832E-03	8.37818E-01	1.58832E-03	8.37818E-01	1.58832E-03
1.35816E+00	6.74548E-03	6.42699E-01	8.71758E-03	8.71758E-03	8.71758E-03	9.10112E+00	1.80112E+00	9.10112E+00	1.80112E+00	9.10112E+00	1.80112E+00	9.10112E+00	1.80112E+00	9.10112E+00	1.80112E+00
1.48822E+00	7.03924E-03	7.51098E-01	9.43244E-03	9.43244E-03	9.43244E-03	1.01125E+00	2.03591E-03	1.01125E+00	2.03591E-03	1.01125E+00	2.03591E-03	1.01125E+00	2.03591E-03	1.01125E+00	2.03591E-03
1.61829E+00	7.23767E-03	7.94458E-01	9.64010E-03	9.64010E-03	9.64010E-03	1.07630E+00	2.24930E-03	1.07630E+00	2.24930E-03	1.07630E+00	2.24930E-03	1.07630E+00	2.24930E-03	1.07630E+00	2.24930E-03
1.79117E+00	7.39913E-03	7.72778E-01	9.74905E-03	9.74905E-03	9.74905E-03	1.16302E+00	2.37258E-03	1.16302E+00	2.37258E-03	1.16302E+00	2.37258E-03	1.16302E+00	2.37258E-03	1.16302E+00	2.37258E-03
2.09525E+00	7.55028E-03	8.37818E-01	9.59070E-03	9.59070E-03	9.59070E-03	1.27142E+00	2.61687E-03	1.27142E+00	2.61687E-03	1.27142E+00	2.61687E-03	1.27142E+00	2.61687E-03	1.27142E+00	2.61687E-03
2.31205E+00	7.74234E-03	8.81178E-01	9.76828E-03	9.76828E-03	9.76828E-03	1.35816E+00	2.81591E-03	1.35816E+00	2.81591E-03	1.35816E+00	2.81591E-03	1.35816E+00	2.81591E-03	1.35816E+00	2.81591E-03
2.55033E+00	7.89150E-03	8.59498E-01	9.87794E-03	9.87794E-03	9.87794E-03	1.44486E+00	3.03267E-03	1.44486E+00	3.03267E-03	1.44486E+00	3.03267E-03	1.44486E+00	3.03267E-03	1.44486E+00	3.03267E-03
2.74565E+00	7.99242E-03	8.59498E-01	9.77534E-03	9.77534E-03	9.77534E-03	1.53326E+00	3.26364E-03	1.53326E+00	3.26364E-03	1.53326E+00	3.26364E-03	1.53326E+00	3.26364E-03	1.53326E+00	3.26364E-03
2.94077E+00	8.06420E-03	9.02858E-01	9.86255E-03	9.86255E-03	9.86255E-03	1.63979E+00	3.51481E-03	1.63979E+00	3.51481E-03	1.63979E+00	3.51481E-03	1.63979E+00	3.51481E-03	1.63979E+00	3.51481E-03
3.13589E+00	8.11302E-03	8.81178E-01	9.81190E-03	9.81190E-03	9.81190E-03	1.72669E+00	3.77269E-03	1.72669E+00	3.77269E-03	1.72669E+00	3.77269E-03	1.72669E+00	3.77269E-03	1.72669E+00	3.77269E-03
3.32619E+00	8.13184E-03	9.46218E-01	9.84716E-03	9.84716E-03	9.84716E-03	1.90013E+00	4.05038E-03	1.90013E+00	4.05038E-03	1.90013E+00	4.05038E-03	1.90013E+00	4.05038E-03	1.90013E+00	4.05038E-03
3.52613E+00	8.13459E-03	9.24538E-01	9.87409E-03	9.87409E-03	9.87409E-03	2.07357E+00	4.34731E-03	2.07357E+00	4.34731E-03	2.07357E+00	4.34731E-03	2.07357E+00	4.34731E-03	2.07357E+00	4.34731E-03
3.74293E+00	8.13014E-03	9.66218E-01	9.83116E-03	9.83116E-03	9.83116E-03	2.25561E+00	4.64965E-03	2.25561E+00	4.64965E-03	2.25561E+00	4.64965E-03	2.25561E+00	4.64965E-03	2.25561E+00	4.64965E-03
3.89449E+00	8.10728E-03	1.05442E+00	9.85038E-03	9.85038E-03	9.85038E-03	2.35541E+00	4.94305E-03	2.35541E+00	4.94305E-03	2.35541E+00	4.94305E-03	2.35541E+00	4.94305E-03	2.35541E+00	4.94305E-03
4.06813E+00	8.06434E-03	1.27142E+00	9.70288E-03	9.70288E-03	9.70288E-03	2.45488E+00	5.23999E-03	2.45488E+00	5.23999E-03	2.45488E+00	5.23999E-03	2.45488E+00	5.23999E-03	2.45488E+00	5.23999E-03
4.24136E+00	8.07843E-03	1.53158E+00	9.33649E-03	9.33649E-03	9.33649E-03	2.67333E+00	5.54266E-03	2.67333E+00	5.54266E-03	2.67333E+00	5.54266E-03	2.67333E+00	5.54266E-03	2.67333E+00	5.54266E-03
4.43668E+00	8.02521E-03	1.85616E+00	9.39461E-03	9.39461E-03	9.39461E-03	2.87513E+00	5.84716E-03	2.87513E+00	5.84716E-03	2.87513E+00	5.84716E-03	2.87513E+00	5.84716E-03	2.87513E+00	5.84716E-03
4.63668E+00	7.90688E-03	2.13861E+00	8.61616E-03	8.61616E-03	8.61616E-03	3.06109E+00	6.15352E-03	3.06109E+00	6.15352E-03	3.06109E+00	6.15352E-03	3.06109E+00	6.15352E-03	3.06109E+00	6.15352E-03
4.83044E+00	7.82445E-03	2.46381E+00	8.36364E-03	8.36364E-03	8.36364E-03	3.26364E+00	6.46335E-03	3.26364E+00	6.46335E-03	3.26364E+00	6.46335E-03	3.26364E+00	6.46335E-03	3.26364E+00	6.46335E-03
5.03044E+00	7.76702E-03	2.76733E+00	8.17329E-03	8.17329E-03	8.17329E-03	3.46109E+00	6.77269E-03	3.46109E+00	6.77269E-03	3.46109E+00	6.77269E-03	3.46109E+00	6.77269E-03	3.46109E+00	6.77269E-03
5.22908E+00	7.69317E-03	3.07085E+00	8.03042E-03	8.03042E-03	8.03042E-03	3.67348E+00	7.07269E-03	3.67348E+00	7.07269E-03	3.67348E+00	7.07269E-03	3.67348E+00	7.07269E-03	3.67348E+00	7.07269E-03
5.42934E+00	7.50302E-03	3.39605E+00	7.96637E-03	7.96637E-03	7.96637E-03	3.86136E+00	7.35974E-03	3.86136E+00	7.35974E-03	3.86136E+00	7.35974E-03	3.86136E+00	7.35974E-03	3.86136E+00	7.35974E-03
5.63494E+00	7.35974E-03	3.67789E+00	7.95299E-03	7.95299E-03	7.95299E-03	4.05038E+00	7.65949E+00	4.05038E+00	7.65949E+00	4.05038E+00	7.65949E+00	4.05038E+00	7.65949E+00	4.05038E+00	7.65949E+00
5.84919E+00	7.20937E-03	3.98141E+00	7.96989E-03	7.96989E-03	7.96989E-03	4.26364E+00	7.96989E-03	4.26364E+00	7.96989E-03	4.26364E+00	7.96989E-03	4.26364E+00	7.96989E-03	4.26364E+00	7.96989E-03
6.06436E+00	7.05347E-03	4.28492E+00	8.08345E-03	8.08345E-03	8.08345E-03	4.47329E+00	8.26364E-03	4.47329E+00	8.26364E-03	4.47329E+00	8.26364E-03	4.47329E+00	8.26364E-03	4.47329E+00	8.26364E-03
6.28436E+00	6.90374E-03	4.57200E+00	8.23406E-03	8.23406E-03	8.23406E-03	4.67516E+00	8.56850E-03	4.67516E+00	8.56850E-03	4.67516E+00	8.56850E-03	4.67516E+00	8.56850E-03	4.67516E+00	8.56850E-03
6.50436E+00	6.74815E-03	4.86136E+00	8.38785E-03	8.38785E-03	8.38785E-03	4.86166E+00	8.86166E-03	4.86166E+00	8.86166E-03	4.86166E+00	8.86166E-03	4.86166E+00	8.86166E-03	4.86166E+00	8.86166E-03
6.72436E+00	6.60204E-03	5.15352E+00	8.56850E-03	8.56850E-03	8.56850E-03	5.05252E+00	9.15352E-03	5.05252E+00	9.15352E-03	5.05252E+00	9.15352E-03	5.05252E+00	9.15352E-03	5.05252E+00	9.15352E-03
6.94436E+00	6.46335E-03	5.45725E+00	8.73444E-03	8.73444E-03	8.73444E-03	5.23999E+00	9.45038E-03	5.23999E+00	9.45038E-03	5.23999E+00	9.45038E-03	5.23999E+00	9.45038E-03	5.23999E+00	9.45038E-03
7.16436E+00	6.31953E-03	5.74269E+00	8.90814E-03	8.90814E-03	8.90814E-03	5.42849E+00	9.74269E-03	5.42849E+00	9.74269E-03	5.42849E+00	9.74269E-03	5.42849E+00	9.74269E-03	5.42849E+00	9.74269E-03
7.38436E+00	6.17444E-03	6.02144E+00	9.08345E-03	9.08345E-03	9.08345E-03	5.61266E+00	1.00208E-03	5.61266E+00	1.00208E-03	5.61266E+00	1.00208E-03	5.61266E+00	1.00208E-03	5.61266E+00	1.00208E-03
7.60436E+00	6.02937E-03	6.29333E+00	9.22414E-03	9.22414E-03	9.22414E-03	5.80342E+00	1.03042E-03	5.80342E+00	1.03042E-03	5.80342E+00	1.03042E-03	5.80342E+00	1.03042E-03	5.80342E+00	1.03042E-03
7.82436E+00	5.88244E-03	6.57269E+00	9.38785E-03	9.38785E-03	9.38785E-03	6.00827E+00	1.05849E-03	6.00827E+00	1.05849E-03	6.00827E+00	1.05849E-03	6.00827E+00	1.05849E-03	6.00827E+00	1.05849E-03
8.04436E+00	5														

TABLE III.- Continued

ORIFICE 9 (Continued)			ORIFICE 10 (Continued)			ORIFICE 11 (Continued)			ORIFICE 12 (Continued)		
$Z_{\infty}$ , mm	$p_{t,3}/p_{t,\infty}$	$Z_{\infty}$ , mm	$p_{t,3}/p_{t,\infty}$	$Z_{\infty}$ , mm	$p_{t,3}/p_{t,\infty}$	$Z_{\infty}$ , mm	$p_{t,3}/p_{t,\infty}$	$Z_{\infty}$ , mm	$p_{t,3}/p_{t,\infty}$	$Z_{\infty}$ , mm	$p_{t,3}/p_{t,\infty}$
1.87654E+01	7.87824E-03	1.23282E+01	7.33761E-03	1.81384E+01	7.10802E-03	2.03084E+01	7.46239E-03	2.03084E+01	7.46239E-03	2.03084E+01	7.46239E-03
1.89189E+01	7.83646E-03	1.27401E+01	7.30679E-03	1.85937E+01	7.21632E-03	1.85937E+01	7.21632E-03	2.07183E+01	7.46315E-03	2.07183E+01	7.46315E-03
1.90489E+01	7.79126E-03	1.31954E+01	7.27971E-03	1.90273E+01	7.28689E-03	1.90273E+01	7.28689E-03	2.12169E+01	7.52068E-03	2.12169E+01	7.52068E-03
1.92020E+01	7.60218E-03	1.36506E+01	7.24982E-03	1.95047E+01	7.33852E-03	1.95047E+01	7.33852E-03	2.16722E+01	7.53912E-03	2.16722E+01	7.53912E-03
1.93741E+01	7.20183E-03	1.41493E+01	7.22179E-03	2.00029E+01	7.37468E-03	2.00029E+01	7.37468E-03	2.21682E+01	7.70953E-03	2.21682E+01	7.70953E-03
1.94609E+01	6.65752E-03	1.45829E+01	7.21215E-03	2.04581E+01	7.39192E-03	2.04581E+01	7.39192E-03	2.25828E+01	7.77406E-03	2.25828E+01	7.77406E-03
1.96012E-03	6.26012E-03	1.50165E+01	7.22658E-03	2.09134E+01	7.38619E-03	2.09134E+01	7.38619E-03	2.30597E+01	7.86218E-03	2.30597E+01	7.86218E-03
6.00063E-03	5.83259E-03	1.54501E+01	7.10489E-03	2.13904E+01	7.37950E-03	2.13904E+01	7.37950E-03	2.34933E+01	7.86218E-03	2.34933E+01	7.86218E-03
1.94609E+01	5.83259E-03	1.56018E+01	6.84725E-03	2.18457E+01	7.38043E-03	2.18457E+01	7.38043E-03	2.39703E+01	7.83457E-03	2.39703E+01	7.83457E-03
1.94609E+01	5.72230E-03	1.57536E+01	6.54394E-03	2.23009E+01	7.40166E-03	2.23009E+01	7.40166E-03	2.44728E+01	7.80489E-03	2.44728E+01	7.80489E-03
5.60170E-03	5.72230E-03	1.59270E+01	6.12537E-03	2.27562E+01	7.43980E-03	2.27562E+01	7.43980E-03	2.49025E+01	7.77269E-03	2.49025E+01	7.77269E-03
1.94609E+01	5.6443E-03	1.60571E+01	5.55619E-03	2.32332E+01	7.46457E-03	2.32332E+01	7.46457E-03	2.50543E+01	7.68297E-03	2.50543E+01	7.68297E-03
1.61872E+01	5.6443E-03	1.61872E+01	5.55619E-03	2.37101E+01	7.50580E-03	2.37101E+01	7.50580E-03	2.52227E+01	7.46879E-03	2.52227E+01	7.46879E-03
5.0399E-03	5.0399E-03	1.63990E+01	4.57150E-03	2.41437E+01	7.55466E-03	2.41437E+01	7.55466E-03	2.54012E+01	7.06070E-03	2.54012E+01	7.06070E-03
1.94392E+01	5.36524E-03	1.65124E+01	4.14779E-03	2.45990E+01	7.61680E-03	2.45990E+01	7.61680E-03	2.55746E+01	6.43946E-03	2.55746E+01	6.43946E-03
5.51100E-03	5.51100E-03	1.66423E+01	3.81283E-03	2.50740E+01	7.68495E-03	2.50740E+01	7.68495E-03	2.57709E+01	5.80360E-03	2.57709E+01	5.80360E-03
5.52111E-03	5.52111E-03	1.67726E+01	3.50181E-03	2.55746E+01	7.73732E-03	2.55746E+01	7.73732E-03	2.58544E+01	5.21859E-03	2.58544E+01	5.21859E-03
5.48882E-03	5.48882E-03	1.69460E+01	3.37946E-03	2.60299E+01	7.76792E-03	2.60299E+01	7.76792E-03	2.60299E+01	4.53639E-03	2.60299E+01	4.53639E-03
1.71194E+01	3.37946E-03	1.71194E+01	3.23773E-03	2.64852E+01	7.74947E-03	2.64852E+01	7.74947E-03	2.61600E+01	4.51000E-03	2.61600E+01	4.51000E-03
1.72712E+01	3.12877E+01	1.72712E+01	3.06441E-03	2.69621E+01	7.77737E-03	2.69621E+01	7.77737E-03	2.63334E+01	3.78471E-03	2.63334E+01	3.78471E-03
1.74230E+01	2.98482E-03	1.74230E+01	2.98482E-03	2.70922E+01	7.77580E-03	2.70922E+01	7.77580E-03	2.64334E+01	3.51897E-03	2.64334E+01	3.51897E-03
1.77482E+01	2.94121E-03	1.77482E+01	2.94121E-03	2.72656E+01	7.57412E-03	2.72656E+01	7.57412E-03	2.66349E+01	3.32843E-03	2.66349E+01	3.32843E-03
1.78999E+01	2.90207E-03	1.78999E+01	2.90207E-03	2.73740E+01	7.21416E-03	2.73740E+01	7.21416E-03	2.67887E+01	3.17354E-03	2.67887E+01	3.17354E-03
1.80517E+01	2.87470E-03	1.80517E+01	2.87470E-03	2.75475E+01	6.74314E-03	2.75475E+01	6.74314E-03	2.69188E+01	3.07425E-03	2.69188E+01	3.07425E-03
1.81818E+01	2.82846E-03	1.81818E+01	2.82846E-03	2.78293E+01	5.51565E-03	2.78293E+01	5.51565E-03	2.70705E+01	2.98479E-03	2.70705E+01	2.98479E-03
1.83335E+01	2.83265E-03	1.83335E+01	2.83265E-03	2.81328E+01	4.31605E-03	2.81328E+01	4.31605E-03	2.72223E+01	2.92849E-03	2.72223E+01	2.92849E-03
1.85063E+01	2.82651E-03	1.85063E+01	2.82651E-03	2.82846E+01	3.91918E-03	2.82846E+01	3.91918E-03	2.73050E+01	2.88248E-03	2.73050E+01	2.88248E-03
1.86153E+01	2.81007E-03	1.86153E+01	2.81007E-03	2.84147E+01	3.61179E-03	2.84147E+01	3.61179E-03	2.74787E+01	2.88248E-03	2.74787E+01	2.88248E-03
1.87888E+01	2.80845E-03	1.87888E+01	2.80845E-03	2.85646E+01	3.40005E-03	2.85646E+01	3.40005E-03	2.75959E+01	2.88248E-03	2.75959E+01	2.88248E-03
1.89839E+01	2.80456E-03	1.89839E+01	2.80456E-03	2.87182E+01	3.22552E-03	2.87182E+01	3.22552E-03	2.76915E+01	2.88248E-03	2.76915E+01	2.88248E-03
1.91357E+01	2.79882E-03	1.91357E+01	2.79882E-03	2.88699E+01	3.10916E-03	2.88699E+01	3.10916E-03	2.77844E+01	2.88248E-03	2.77844E+01	2.88248E-03
1.92224E+01	2.79349E-03	1.92224E+01	2.79349E-03	2.90671E+01	2.94809E-03	2.90671E+01	2.94809E-03	2.78441E+01	2.88248E-03	2.78441E+01	2.88248E-03
1.94609E+01	2.79349E-03	1.94609E+01	2.79349E-03	2.92651E+01	2.89815E-03	2.92651E+01	2.89815E-03	2.79590E+01	2.88248E-03	2.79590E+01	2.88248E-03
1.96012E-03	2.79349E-03	1.96012E-03	2.79349E-03	2.94609E+01	2.84813E-03	2.94609E+01	2.84813E-03	2.80867E+01	2.88248E-03	2.80867E+01	2.88248E-03
1.94609E+01	2.79349E-03	1.94609E+01	2.79349E-03	2.96867E+01	2.83118E-03	2.96867E+01	2.83118E-03	2.82846E+01	2.88248E-03	2.82846E+01	2.88248E-03
1.94609E+01	2.79349E-03	1.94609E+01	2.79349E-03	2.98867E+01	2.81815E-03	2.98867E+01	2.81815E-03	2.84813E+01	2.88248E-03	2.84813E+01	2.88248E-03
1.94609E+01	2.79349E-03	1.94609E+01	2.79349E-03	3.00867E+01	2.80671E-03	3.00867E+01	2.80671E-03	2.86867E+01	2.88248E-03	2.86867E+01	2.88248E-03
1.94609E+01	2.79349E-03	1.94609E+01	2.79349E-03	3.02867E+01	2.79590E-03	3.02867E+01	2.79590E-03	2.88867E+01	2.88248E-03	2.88867E+01	2.88248E-03
1.94609E+01	2.79349E-03	1.94609E+01	2.79349E-03	3.04867E+01	2.78441E-03	3.04867E+01	2.78441E-03	2.90867E+01	2.88248E-03	2.90867E+01	2.88248E-03
1.94609E+01	2.79349E-03	1.94609E+01	2.79349E-03	3.06867E+01	2.77288E-03	3.06867E+01	2.77288E-03	2.92867E+01	2.88248E-03	2.92867E+01	2.88248E-03

TABLE III.- Concluded

ORIFICE 13 $P_s/P_{t,\infty} = 0.000814$				ORIFICE 14 $P_s/P_{t,\infty} = 0.000977$				ORIFICE 13 (Continued)				ORIFICE 14 (Continued)			
$Z_{\infty}, \text{mm}$	$P_t/P_{t,\infty}$	$P_t/P_{t,\infty}$	$P_t/P_{t,\infty}$	$Z_{\infty}, \text{mm}$	$P_t/P_{t,\infty}$	$P_t/P_{t,\infty}$	$P_t/P_{t,\infty}$	$Z_{\infty}, \text{mm}$	$P_t/P_{t,\infty}$	$P_t/P_{t,\infty}$	$P_t/P_{t,\infty}$	$Z_{\infty}, \text{mm}$	$P_t/P_{t,\infty}$	$P_t/P_{t,\infty}$	$P_t/P_{t,\infty}$
3.17500E-01	3.30719E-03	3.30719E-03	3.30719E-03	3.60860E-01	6.56637E-03	6.56637E-03	6.56637E-03	1.78566E+01	7.24242E-03	7.24242E-03	7.24242E-03	1.88538E+01	7.08138E-03	7.08138E-03	7.08138E-03
4.69259E-01	3.99854E-03	3.99854E-03	3.99854E-03	3.39180E-01	6.66433E-03	6.66433E-03	6.66433E-03	1.83118E+01	7.26836E-03	7.26836E-03	7.26836E-03	1.90273E+01	7.05649E-03	7.05649E-03	7.05649E-03
5.99339E-01	4.93890E-03	4.93890E-03	4.93890E-03	3.39180E-01	6.66433E-03	6.66433E-03	6.66433E-03	1.87888E+01	7.30295E-03	7.30295E-03	7.30295E-03	1.91790E+01	6.85102E-03	6.85102E-03	6.85102E-03
7.72778E-01	5.84006E-03	5.84006E-03	5.84006E-03	3.39180E-01	6.66433E-03	6.66433E-03	6.66433E-03	1.92224E+01	7.30295E-03	7.30295E-03	7.30295E-03	1.93091E+01	6.57602E-03	6.57602E-03	6.57602E-03
9.24538E-01	6.87550E-03	6.87550E-03	6.87550E-03	3.60860E-01	6.56637E-03	6.56637E-03	6.56637E-03	1.97210E+01	7.30295E-03	7.30295E-03	7.30295E-03	1.94825E+01	6.17699E-03	6.17699E-03	6.17699E-03
1.05462E+00	7.51212E-03	7.51212E-03	7.51212E-03	3.60860E-01	6.56637E-03	6.56637E-03	6.56637E-03	2.01763E+01	7.28076E-03	7.28076E-03	7.28076E-03	1.96126E+01	5.64843E-03	5.64843E-03	5.64843E-03
1.20638E+00	7.86068E-03	7.86068E-03	7.86068E-03	3.60860E-01	6.56637E-03	6.56637E-03	6.56637E-03	2.06316E+01	7.24805E-03	7.24805E-03	7.24805E-03	1.97644E+01	5.09980E-03	5.09980E-03	5.09980E-03
1.37982E+00	8.00857E-03	8.00857E-03	8.00857E-03	4.69259E-01	6.95102E-03	6.95102E-03	6.95102E-03	2.10869E+01	7.23645E-03	7.23645E-03	7.23645E-03	1.98945E+01	4.64894E-03	4.64894E-03	4.64894E-03
1.53158E+00	8.04714E-03	8.04714E-03	8.04714E-03	5.55979E-01	7.51040E-03	7.51040E-03	7.51040E-03	2.15638E+01	7.24076E-03	7.24076E-03	7.24076E-03	2.00679E+01	4.19200E-03	4.19200E-03	4.19200E-03
1.68333E+00	8.02612E-03	8.02612E-03	8.02612E-03	6.21019E-01	8.08318E-03	8.08318E-03	8.08318E-03	2.20191E+01	7.29136E-03	7.29136E-03	7.29136E-03	2.02197E+01	3.84955E-03	3.84955E-03	3.84955E-03
1.83509E+00	7.98809E-03	7.98809E-03	7.98809E-03	7.51098E-01	8.58688E-03	8.58688E-03	8.58688E-03	2.25276E+01	7.31642E-03	7.31642E-03	7.31642E-03	2.03714E+01	3.58382E-03	3.58382E-03	3.58382E-03
1.98685E+00	7.93977E-03	7.93977E-03	7.93977E-03	9.16138E-01	8.93471E-03	8.93471E-03	8.93471E-03	2.29297E+01	7.34725E-03	7.34725E-03	7.34725E-03	2.05212E+01	3.38072E-03	3.38072E-03	3.38072E-03
2.13861E+00	7.88918E-03	7.88918E-03	7.88918E-03	9.24538E-01	9.06190E-03	9.06190E-03	9.06190E-03	2.34066E+01	7.35975E-03	7.35975E-03	7.35975E-03	2.06966E+01	3.23051E-03	3.23051E-03	3.23051E-03
2.44213E+00	7.78897E-03	7.78897E-03	7.78897E-03	9.67897E-01	9.23034E-03	9.23034E-03	9.23034E-03	2.39000E+01	7.37609E-03	7.37609E-03	7.37609E-03	2.08484E+01	3.11902E-03	3.11902E-03	3.11902E-03
2.81069E+00	7.60271E-03	7.60271E-03	7.60271E-03	1.05462E+00	9.29259E-03	9.29259E-03	9.29259E-03	2.37318E+01	7.42438E-03	7.42438E-03	7.42438E-03	2.09785E+01	3.02777E-03	3.02777E-03	3.02777E-03
3.04317E+00	7.49178E-03	7.49178E-03	7.49178E-03	1.19666E+00	9.29836E-03	9.29836E-03	9.29836E-03	2.39052E+01	7.45237E-03	7.45237E-03	7.45237E-03	2.11519E+01	2.96227E-03	2.96227E-03	2.96227E-03
3.28745E+00	7.39406E-03	7.39406E-03	7.39406E-03	1.18470E+00	9.30884E-03	9.30884E-03	9.30884E-03	2.40570E+01	7.38287E-03	7.38287E-03	7.38287E-03	2.12820E+01	2.91116E-03	2.91116E-03	2.91116E-03
3.50445E+00	7.31932E-03	7.31932E-03	7.31932E-03	1.31478E+00	9.29170E-03	9.29170E-03	9.29170E-03	2.42088E+01	7.25089E-03	7.25089E-03	7.25089E-03	2.14337E+01	2.87749E-03	2.87749E-03	2.87749E-03
3.74293E+00	7.24168E-03	7.24168E-03	7.24168E-03	1.40150E+00	9.29152E-03	9.29152E-03	9.29152E-03	2.43605E+01	6.94123E-03	6.94123E-03	6.94123E-03	2.16072E+01	2.84688E-03	2.84688E-03	2.84688E-03
3.98141E+00	7.18026E-03	7.18026E-03	7.18026E-03	1.46054E+00	9.27349E-03	9.27349E-03	9.27349E-03	2.45123E+01	6.49140E-03	6.49140E-03	6.49140E-03	2.17589E+01	2.81939E-03	2.81939E-03	2.81939E-03
4.17653E+00	7.11593E-03	7.11593E-03	7.11593E-03	1.53158E+00	9.25636E-03	9.25636E-03	9.25636E-03	2.46640E+01	5.92424E-03	5.92424E-03	5.92424E-03	2.19541E+01	2.80213E-03	2.80213E-03	2.80213E-03
4.36688E+00	7.07544E-03	7.07544E-03	7.07544E-03	1.66165E+00	9.25109E-03	9.25109E-03	9.25109E-03	2.48375E+01	5.27141E-03	5.27141E-03	5.27141E-03				
4.63180E+00	7.05915E-03	7.05915E-03	7.05915E-03	1.70501E+00	9.23619E-03	9.23619E-03	9.23619E-03	2.49892E+01	4.75779E-03	4.75779E-03	4.75779E-03				
4.82692E+00	7.08864E-03	7.08864E-03	7.08864E-03	1.92181E+00	9.20324E-03	9.20324E-03	9.20324E-03	2.51193E+01	4.22565E-03	4.22565E-03	4.22565E-03				
5.06540E+00	7.08864E-03	7.08864E-03	7.08864E-03	2.03021E+00	9.16322E-03	9.16322E-03	9.16322E-03	2.52928E+01	3.86064E-03	3.86064E-03	3.86064E-03				
5.28220E+00	7.09504E-03	7.09504E-03	7.09504E-03	2.09525E+00	9.11488E-03	9.11488E-03	9.11488E-03	2.54445E+01	3.57845E-03	3.57845E-03	3.57845E-03				
5.45564E+00	7.14791E-03	7.14791E-03	7.14791E-03	2.29037E+00	9.01061E-03	9.01061E-03	9.01061E-03	2.55746E+01	3.38082E-03	3.38082E-03	3.38082E-03				
5.75313E+00	7.16827E-03	7.16827E-03	7.16827E-03	2.65993E+00	8.70541E-03	8.70541E-03	8.70541E-03	2.57480E+01	3.21813E-03	3.21813E-03	3.21813E-03				
6.23612E+00	7.27027E-03	7.27027E-03	7.27027E-03	3.00581E+00	8.31766E-03	8.31766E-03	8.31766E-03	2.58781E+01	3.01420E-03	3.01420E-03	3.01420E-03				
6.44804E+00	7.43083E-03	7.43083E-03	7.43083E-03	3.37437E+00	7.89765E-03	7.89765E-03	7.89765E-03	2.60082E+01	2.95513E-03	2.95513E-03	2.95513E-03				
7.14667E+00	7.56238E-03	7.56238E-03	7.56238E-03	3.76461E+00	7.51307E-03	7.51307E-03	7.51307E-03	2.61600E+01	2.90543E-03	2.90543E-03	2.90543E-03				
7.64531E+00	7.72886E-03	7.72886E-03	7.72886E-03	4.34996E+00	7.14575E-03	7.14575E-03	7.14575E-03	2.63334E+01	2.86447E-03	2.86447E-03	2.86447E-03				
8.05723E+00	7.86882E-03	7.86882E-03	7.86882E-03	4.97868E+00	6.91922E-03	6.91922E-03	6.91922E-03	2.64852E+01	2.83448E-03	2.83448E-03	2.83448E-03				
8.53131E+00	7.35881E-03	7.35881E-03	7.35881E-03	5.56404E+00	6.79926E-03	6.79926E-03	6.79926E-03	2.66152E+01	2.80516E-03	2.80516E-03	2.80516E-03				
9.01115E+00	8.08756E-03	8.08756E-03	8.08756E-03	6.21444E+00	6.75206E-03	6.75206E-03	6.75206E-03	2.67453E+01	2.79434E-03	2.79434E-03	2.79434E-03				
9.44474E+00	8.08245E-03	8.08245E-03	8.08245E-03	6.82147E+00	6.71277E-03	6.71277E-03	6.71277E-03	2.68971E+01	2.77660E-03	2.77660E-03	2.77660E-03				
9.87834E+00	8.04910E-03	8.04910E-03	8.04910E-03	7.45019E+00	6.71524E-03	6.71524E-03	6.71524E-03	2.70488E+01	2.76812E-03	2.76812E-03	2.76812E-03				
1.03119E+01	7.97934E-03	7.97934E-03	7.97934E-03	8.07891E+00	6.72489E-03	6.72489E-03	6.72489E-03	2.72006E+01	2.76684E-03	2.76684E-03	2.76684E-03				
1.07889E+01	7.88741E-03	7.88741E-03	7.88741E-03	8.66427E+00	6.73825E-03	6.73825E-03	6.73825E-03	2.73524E+01	2.75574E-03	2.75574E-03	2.75574E-03				
1.12442E+01	7.78650E-03	7.78650E-03	7.78650E-03	9.31467E+00	6.70962E-03	6.70962E-03	6.70962E-03	2.75041E+01							
1.17428E+01	7.71774E-03	7.71774E-03	7.71774E-03	9.92170E+00	6.70348E-03	6.70348E-03	6.70348E-03								
1.21981E+01	7.62779E-03	7.62779E-03	7.62779E-03	1.05071E+01	6.73230E-03	6.73230E-03	6.73230E-03								
1.26317E+01	7.58194E-03	7.58194E-03	7.58194E-03	1.10924E+01	6.74018E-03	6.74018E-03	6.74018E-03								
1.30653E+01	7.51465E-03	7.51465E-03	7.51465E-03	1.16995E+01	6.76112E-03	6.76112E-03	6.76112E-03								
1.35422E+01	7.44252E-03	7.44252E-03	7.44252E-03	1.23282E+01	6.77358E-03	6.77358E-03	6.77358E-03								
1.37590E+01	7.31741E-03	7.31741E-03	7.31741E-03	1.29135E+01	6.80250E-03	6.80250E-03	6.80250E-03								
1.37807E+01	7.33942E-03	7.33942E-03	7.33942E-03	1.32604E+01	6.78529E-03	6.78529E-03	6.78529E-03								
1.38241E+01	7.33847E-03	7.33847E-03	7.33847E-03	1.33254E+01	6.76578E-03	6.76578E-03	6.76578E-03								
1.39342E+01	7.32411E-03	7.32411E-03	7.32411E-03	1.39542E+01	6.80365E-03	6.80365E-03	6.80365E-03								
1.42360E+01	7.28489E-03	7.28489E-03	7.28489E-03	1.45395E+01	6.81833E-03	6.81833E-03	6.81833E-03								
1.47130E+01	7.23134E-03	7.23134E-03	7.23134E-03	1.51466E+01	6.79542E-03	6.79542E-03	6.79542E-03								
1.51466E+01	7.19020E-03	7.19020E-03	7.19020E-03	1.57753E+01	6.86097E-03	6.86097E-03	6.86097E-03								
1.55802E+01	7.18443E-03	7.18443E-03	7.18443E-03	1.63823E+01	6.89816E-03	6.89816E-03	6.89816E-03								
1.60255E+01	7.17478E-03	7.17478E-03	7.17478E-03	1.70110E+01	6.91036E-03	6.91036E-03	6.91036E-03								
1															



$A = 1.712 \text{ mm}^2$   
 $S = 114.5 \text{ mm}$   
 $b = 168.02 \text{ mm}$   
 $l = 250.14 \text{ mm}$

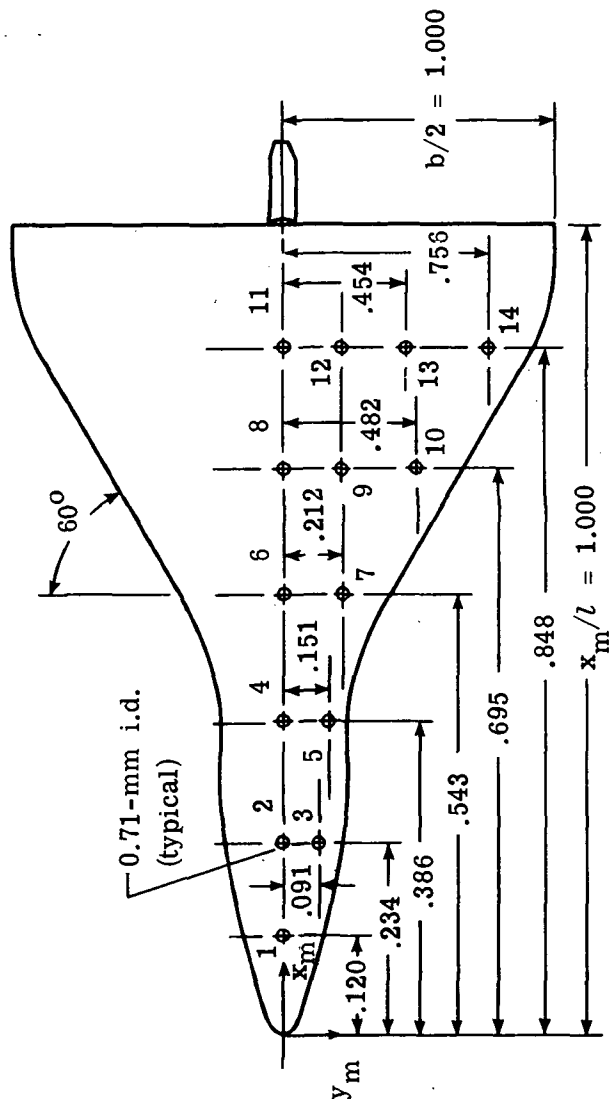
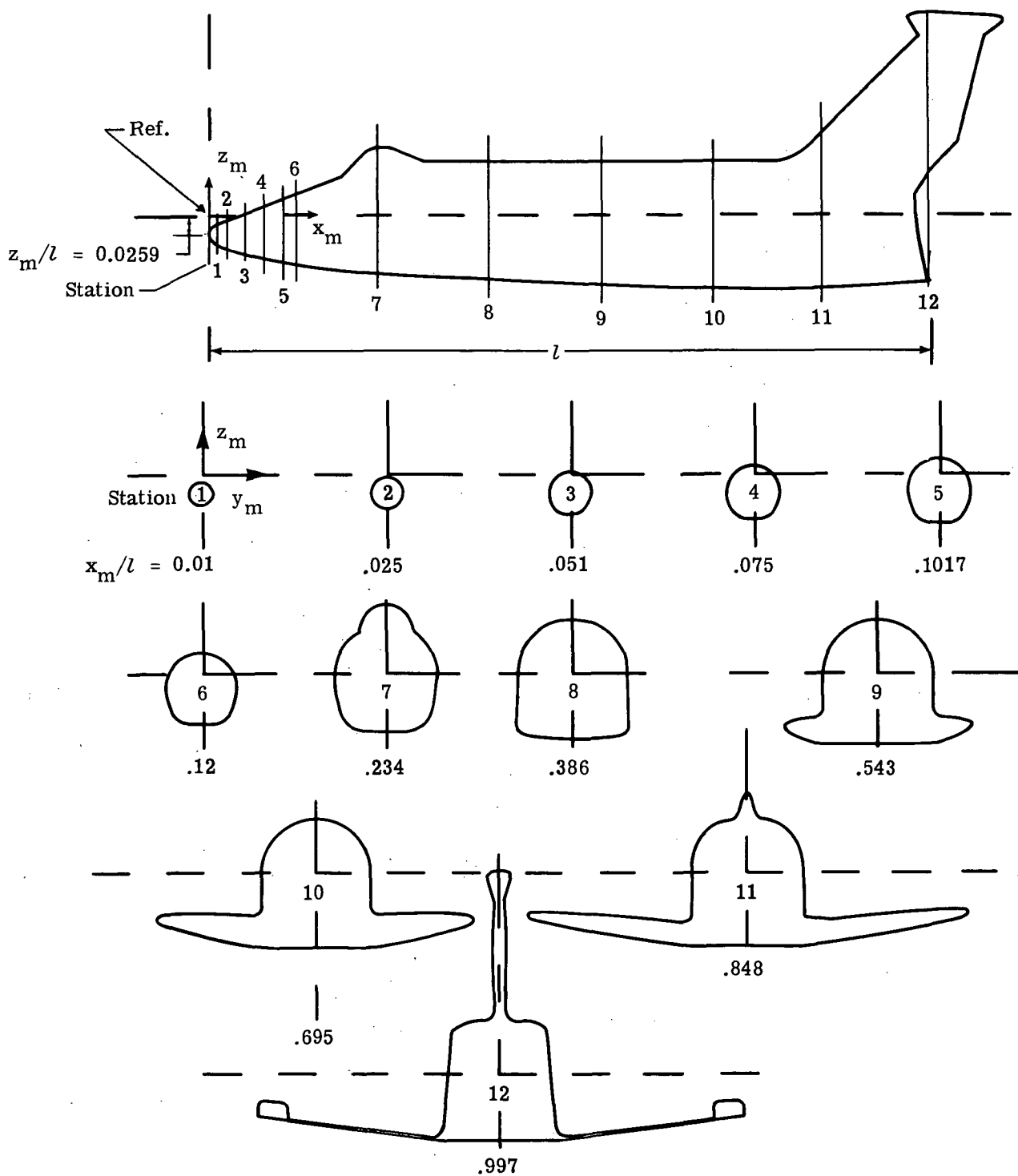
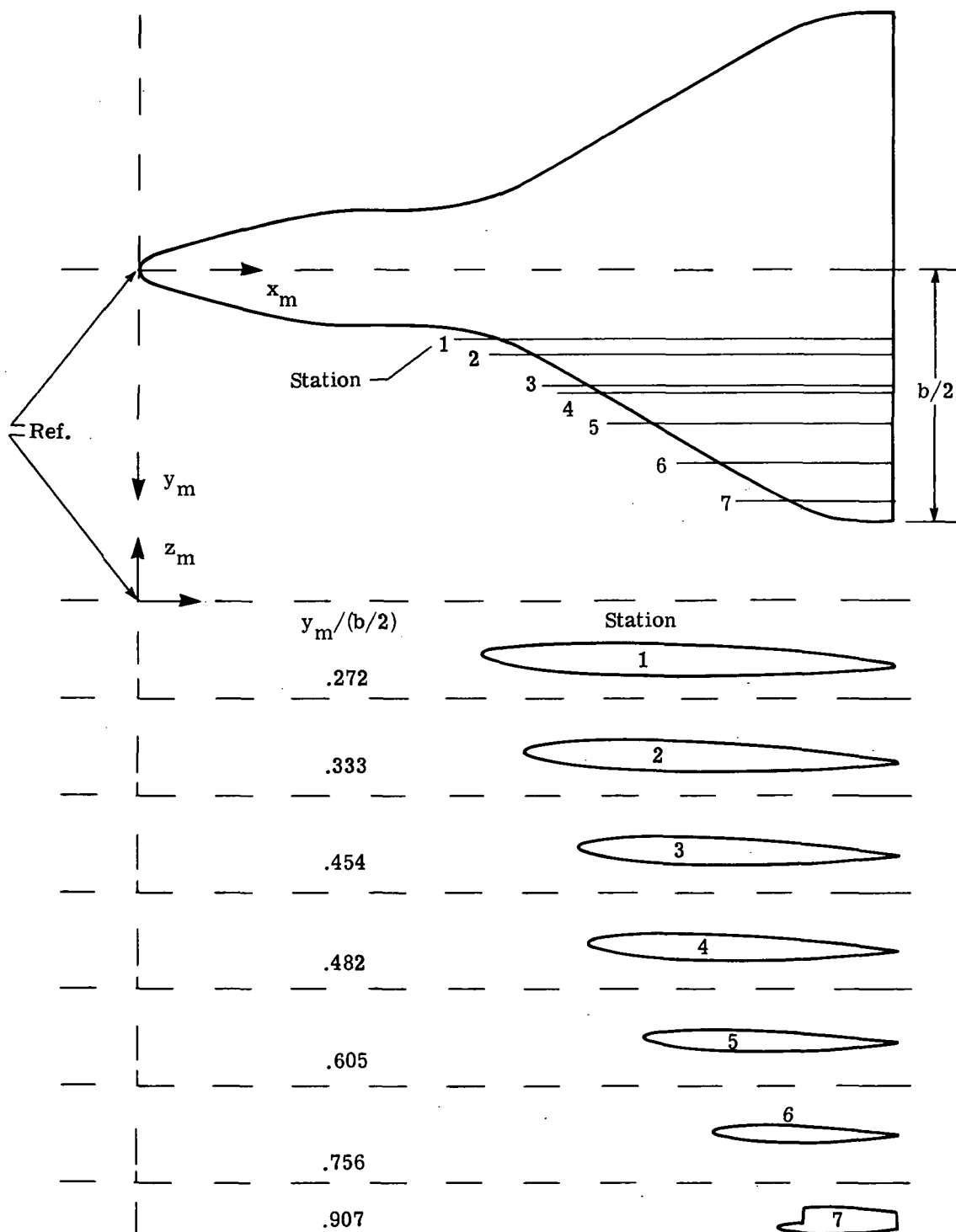


Figure 1.- NASA 040A space shuttle orbiter configuration showing pressure orifice locations. All axial and spanwise dimensions are in terms of body length and semispan, respectively.



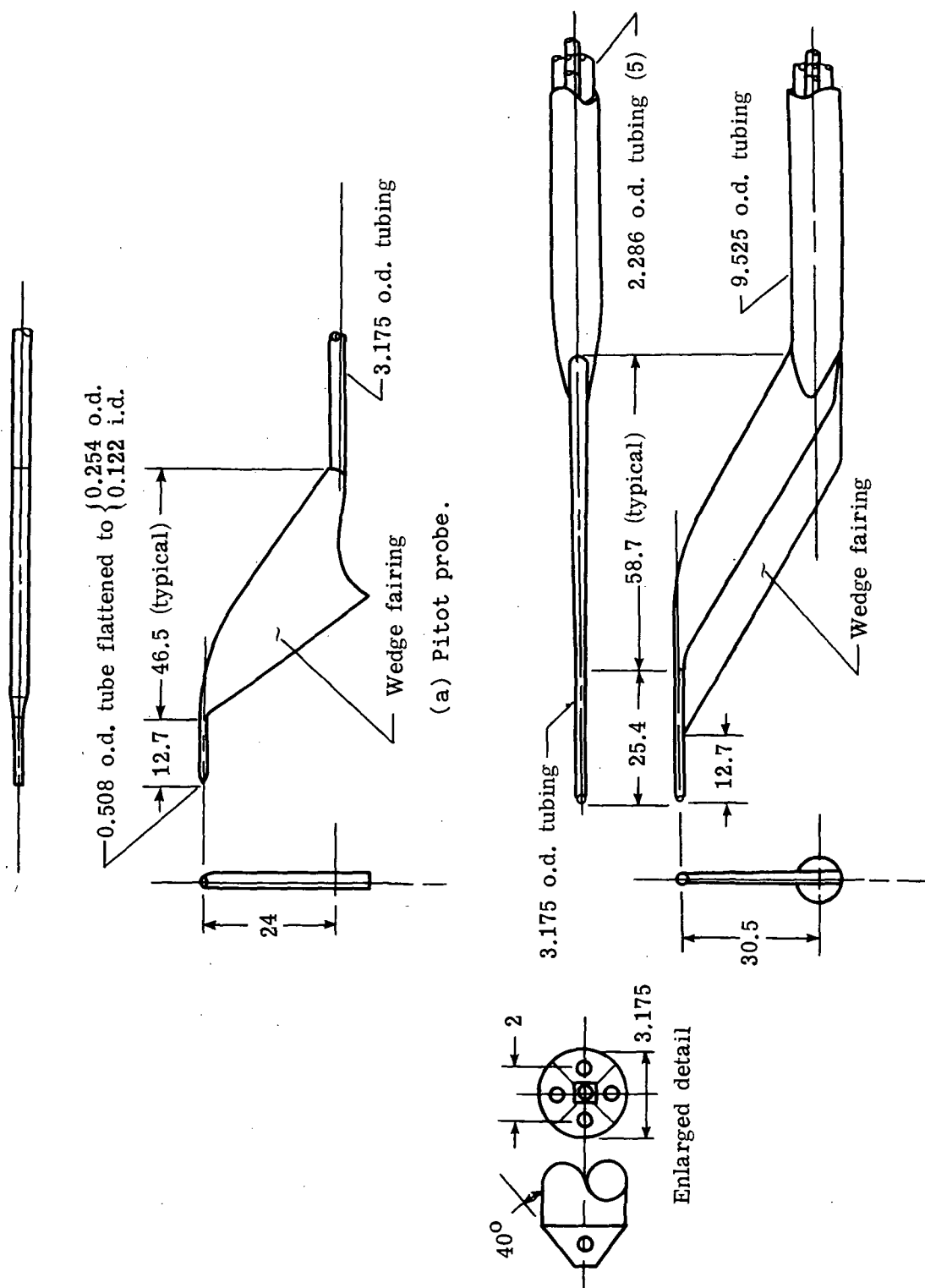
(a) Cross sections.

Figure 2.- Measured shapes of NASA 040A space shuttle orbiter configuration.



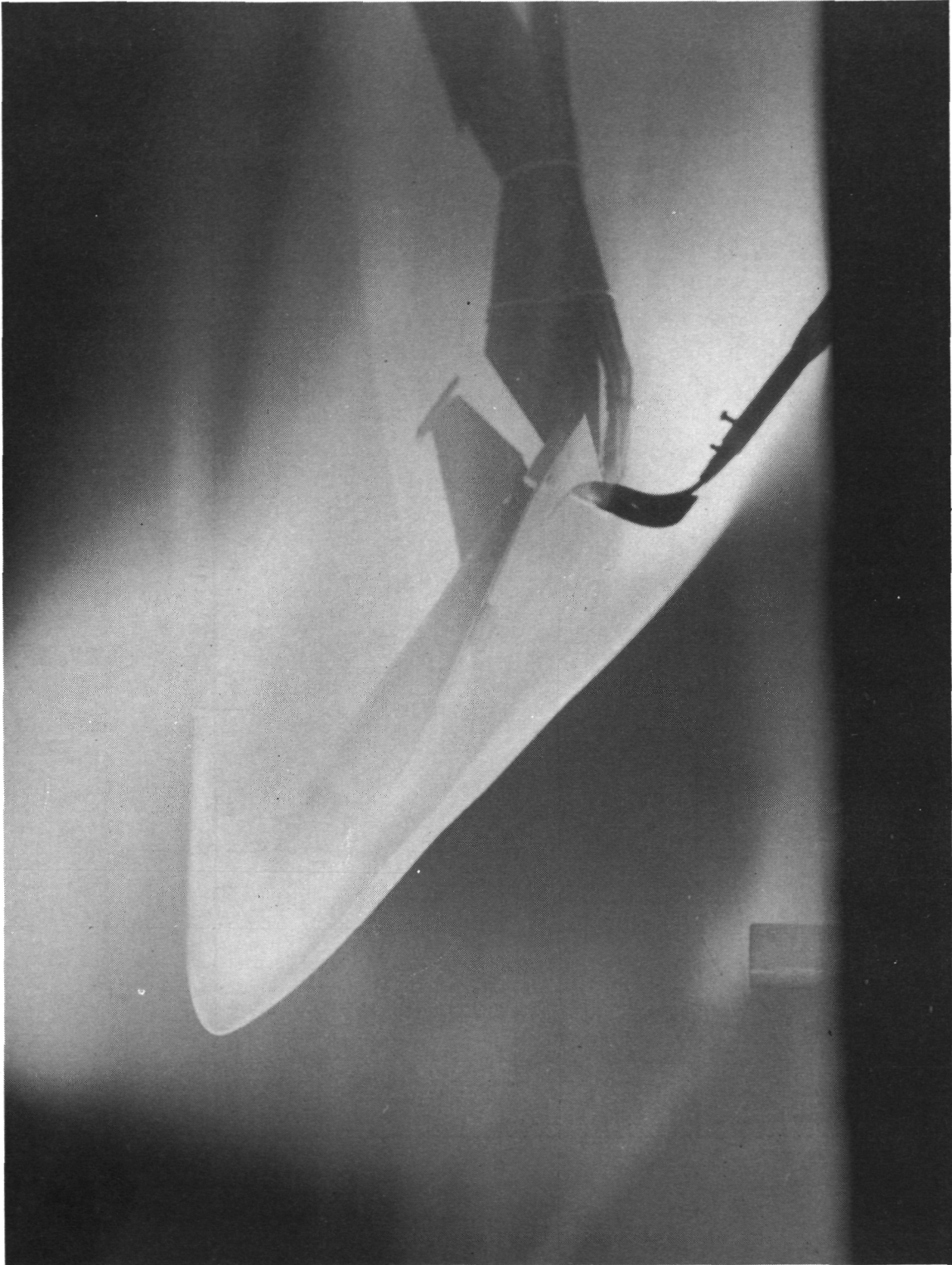
(b) Wing profiles.

Figure 2.- Concluded.



(b) Flow-direction probe.

Figure 3.- Survey probes. All dimensions are in mm.



L-73-7120

Figure 4.- Electron-beam illumination of flow field during typical probe traverse.



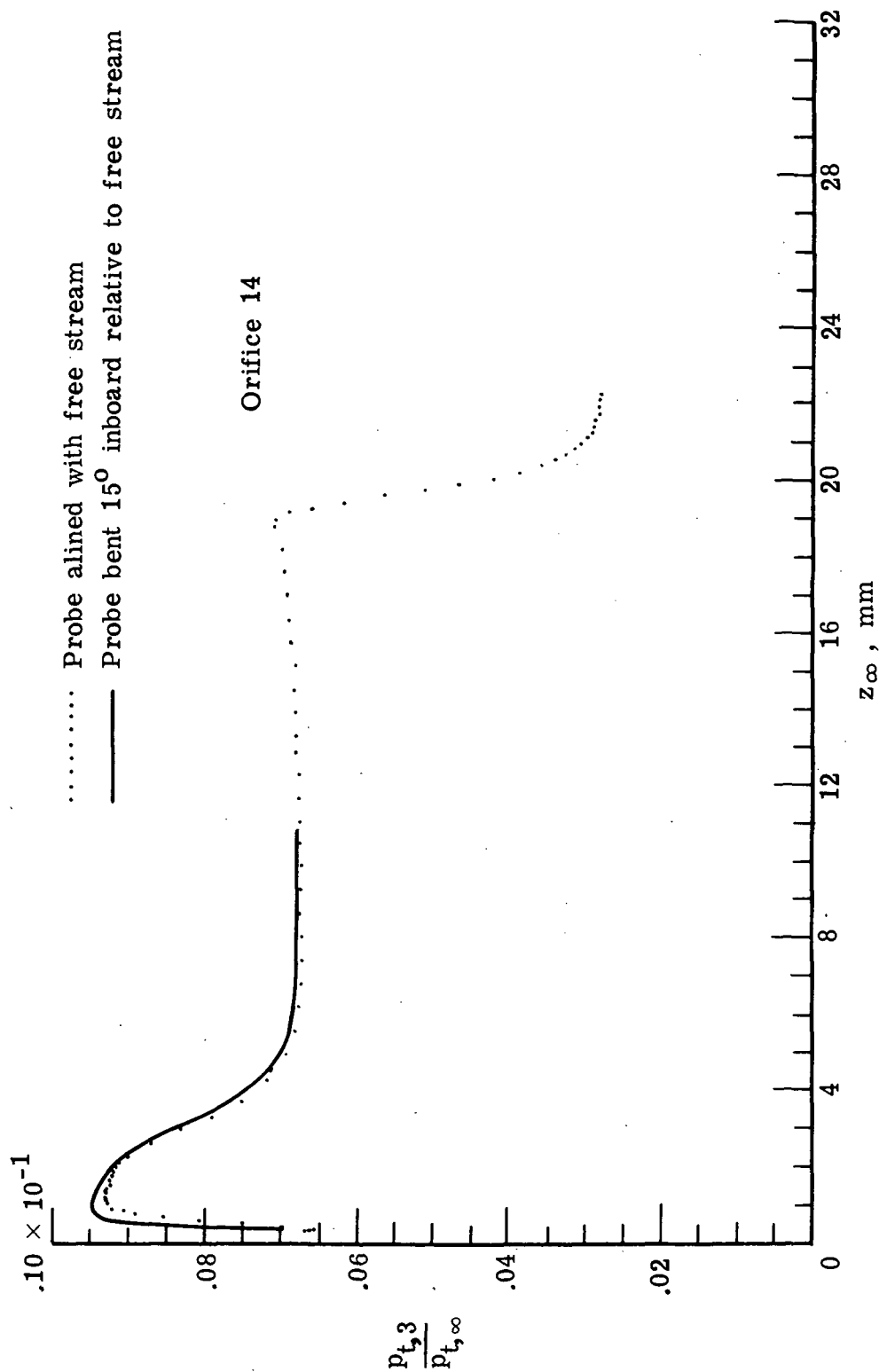


Figure 5.- Comparison of pitot profiles with probe at two angles to free stream.

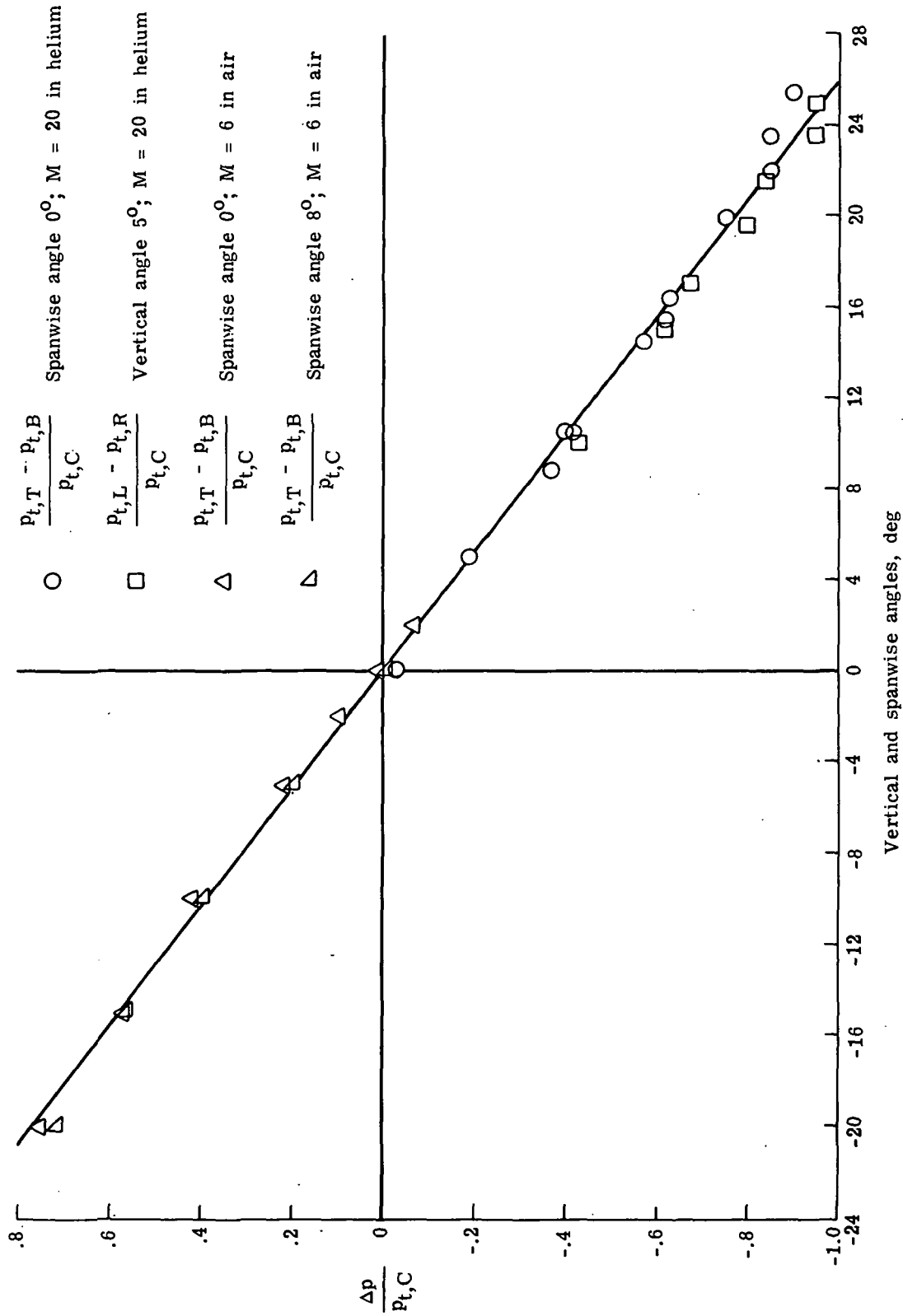


Figure 6.- Typical calibration of five-tube flow-direction probe.

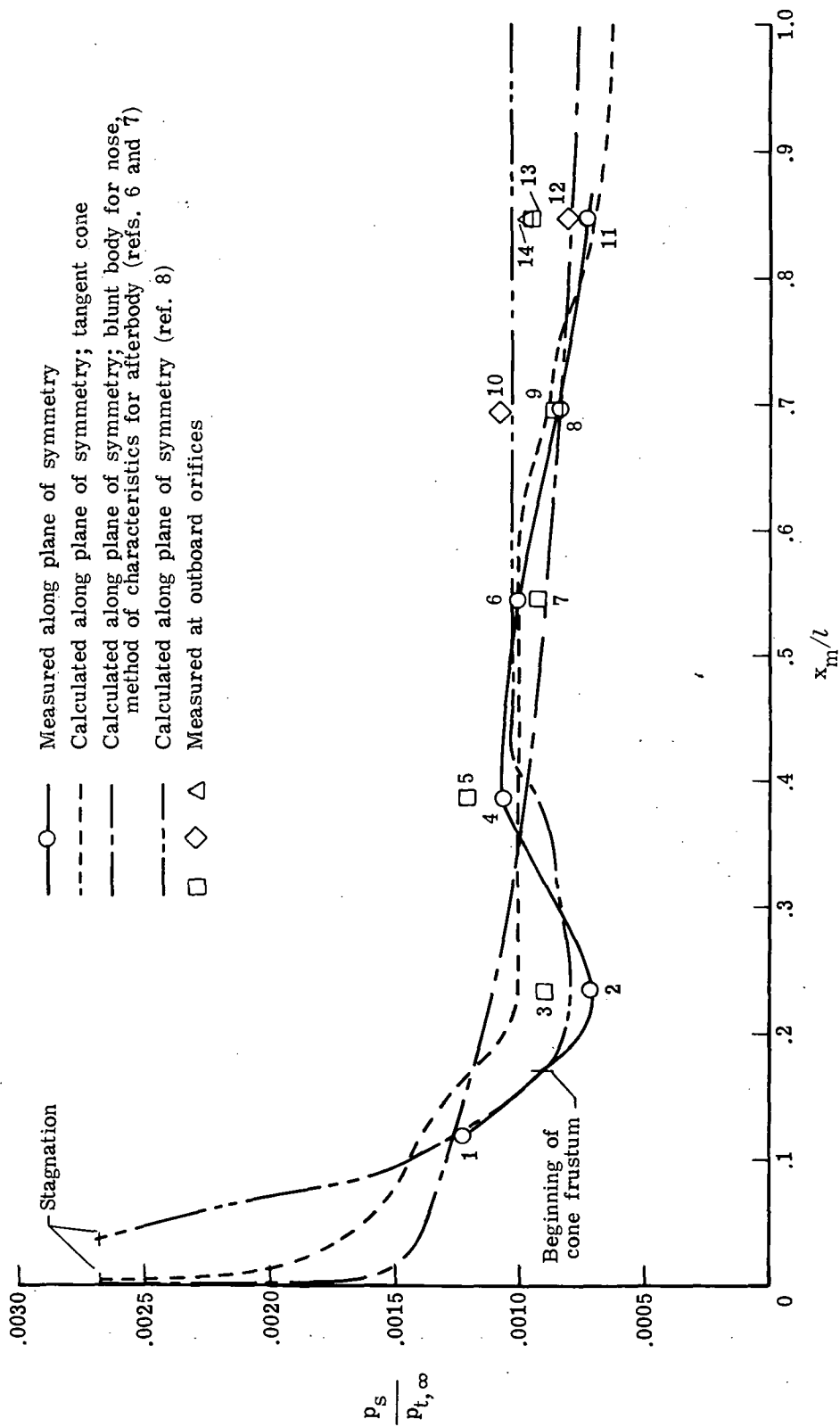
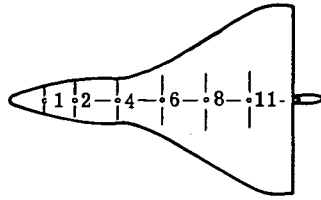
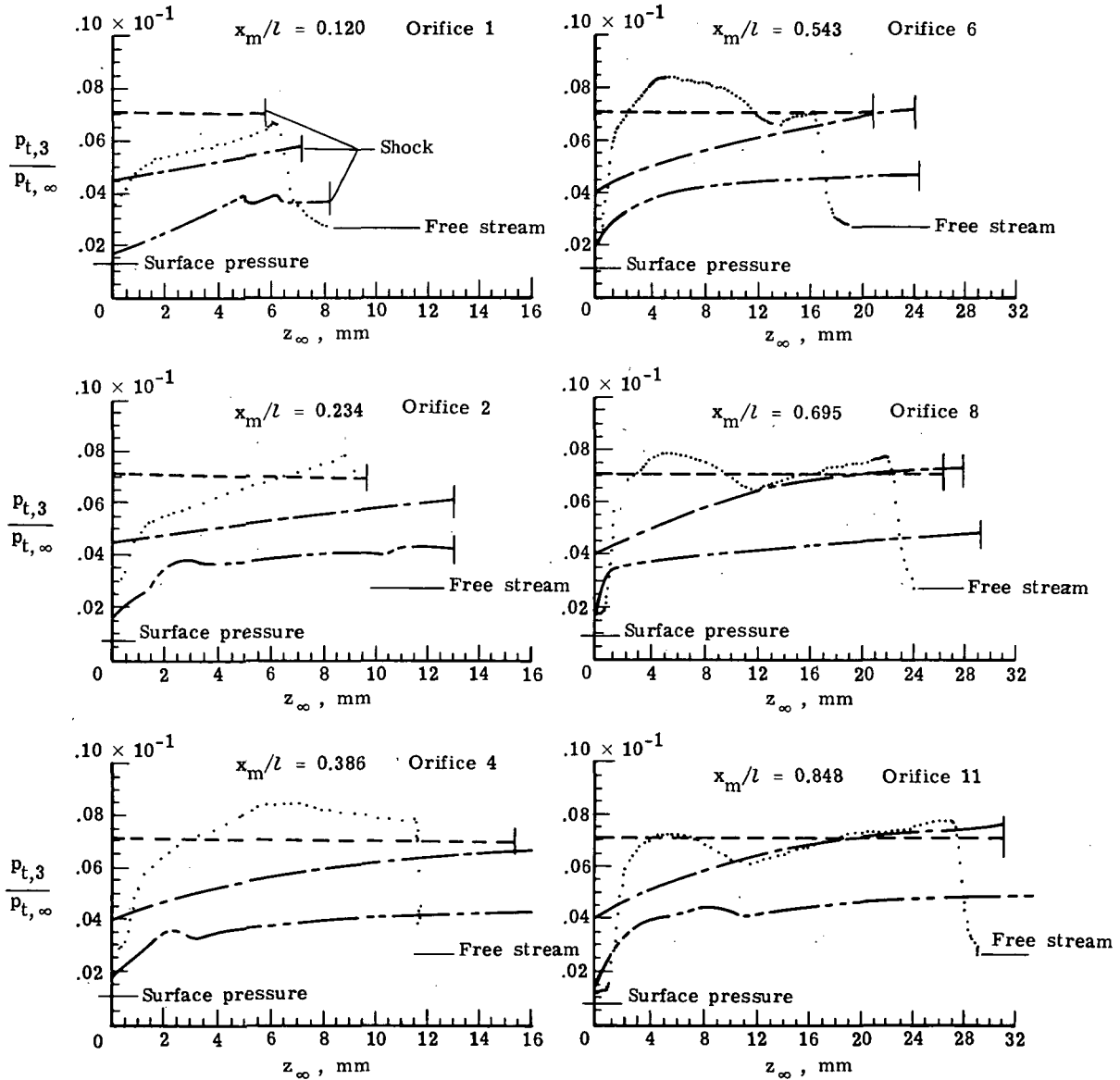


Figure 7.- Surface pressures on lower surface of NASA 040A space shuttle orbiter at Mach 20 and  $\alpha = 31^\circ$  in helium. Numbers by symbols are orifice numbers (see fig. 1).

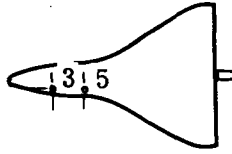


- ..... Measured
- Plane of symmetry surface represented by  $33.75^\circ$  cone
- Plane of symmetry surface represented by  $45^\circ$  conical nose and power-law body
- Plane of symmetry surface represented by ellipsoid nose and power-law body



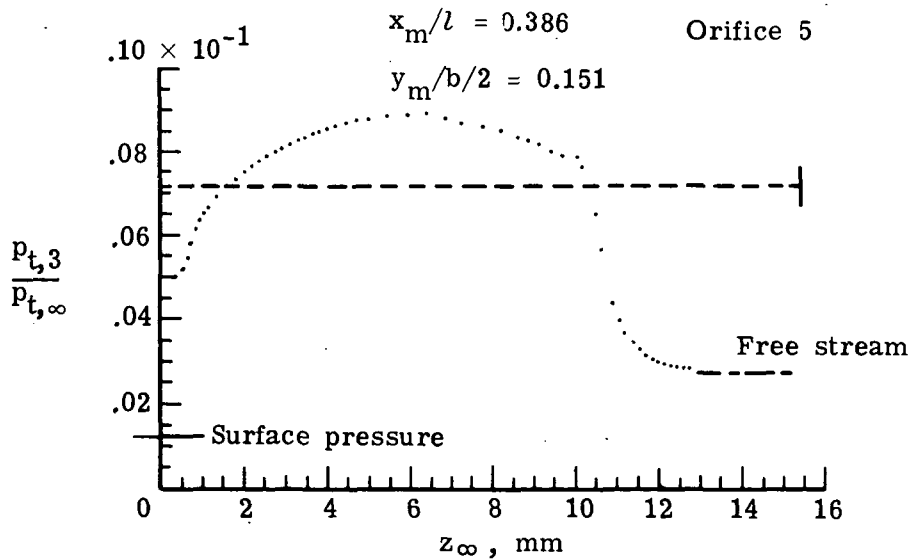
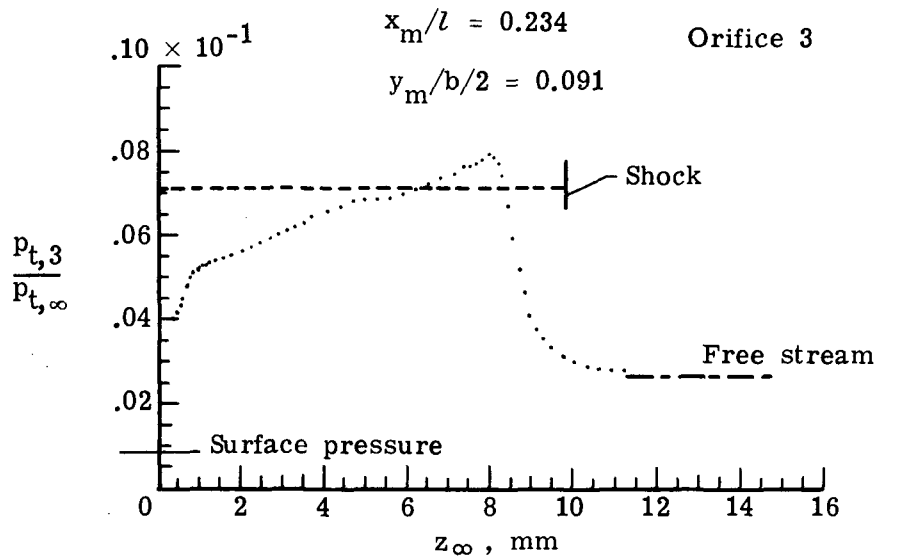
(a) Along plane of symmetry.

Figure 8.- Comparison of calculated pitot profiles with measured profiles.



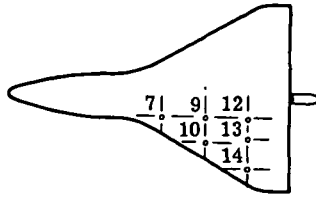
..... Measured

----- Plane of symmetry surface represented by  $33.75^\circ$  cone



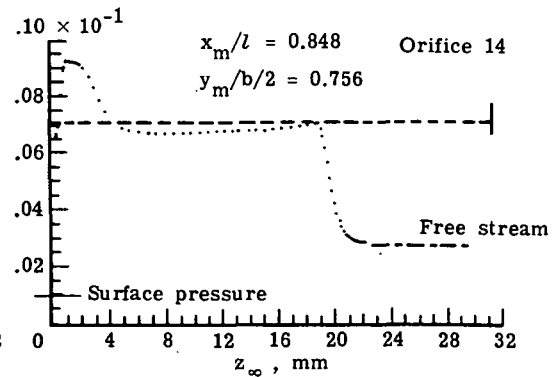
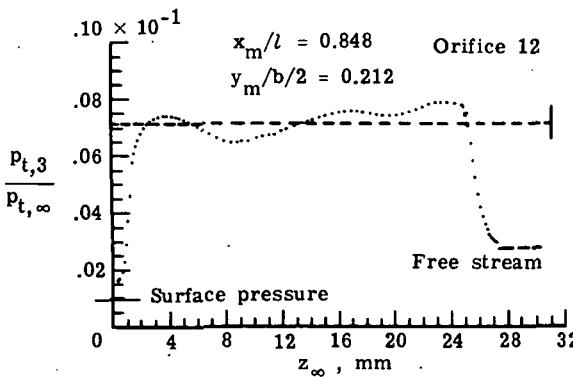
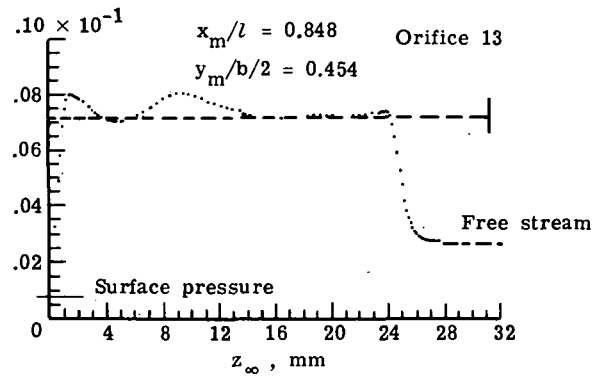
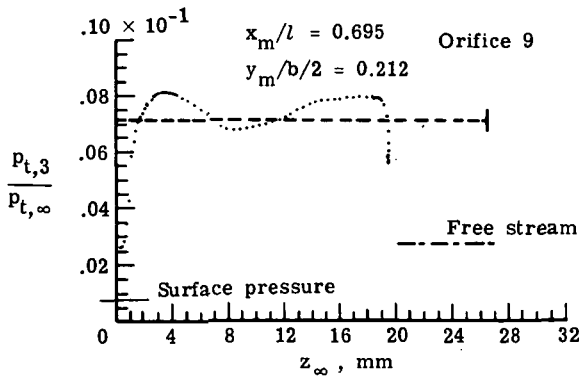
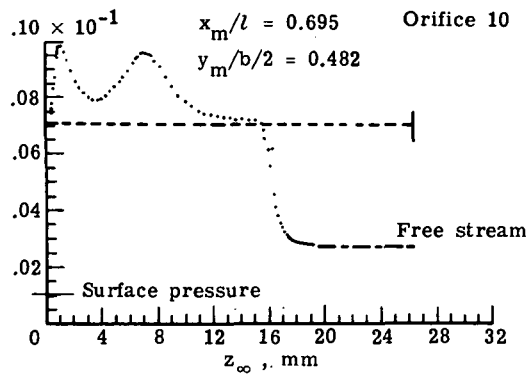
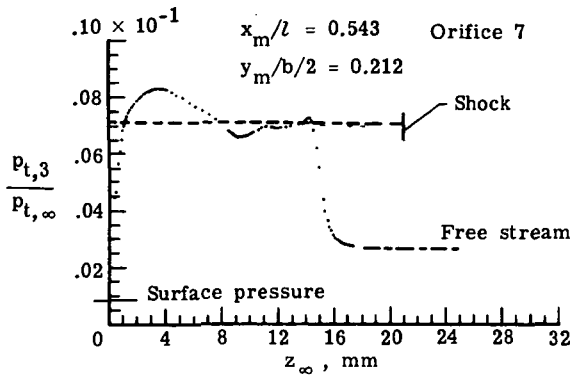
(b) Outboard on body.

Figure 8.- Continued.



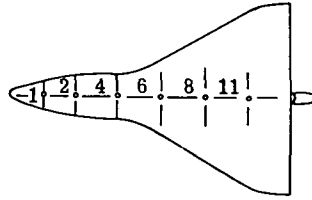
..... Measured

----- Plane of symmetry surface represented by  $33.75^\circ$  cone



(c) Outboard on wing.

Figure 8.- Concluded.



- ..... Measured
- Calculated using ellipsoid nose and power-law body for plane of symmetry surface (inviscid)
- Calculated in boundary layer using computed shock shape and pressure (body of revolution)

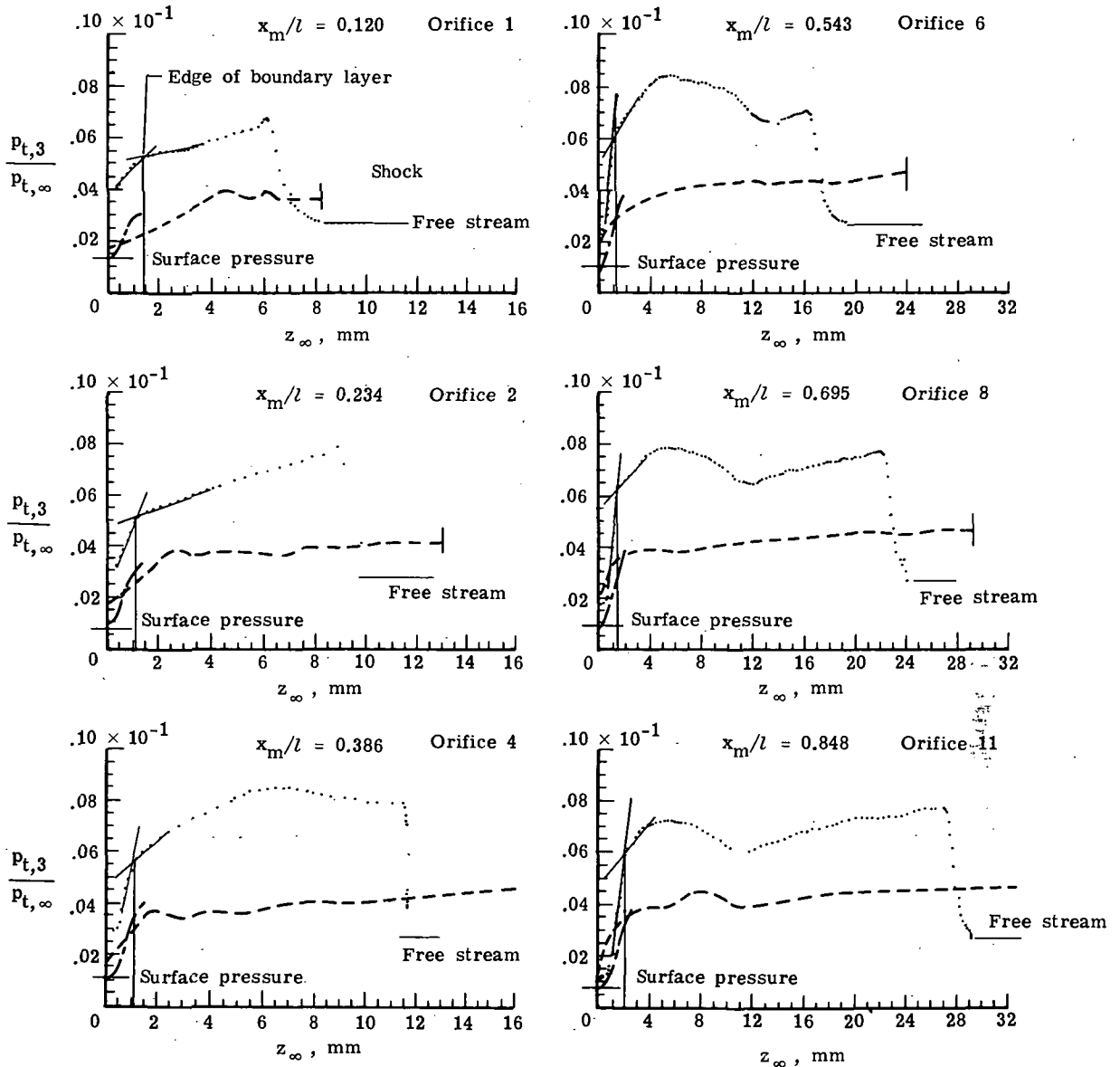
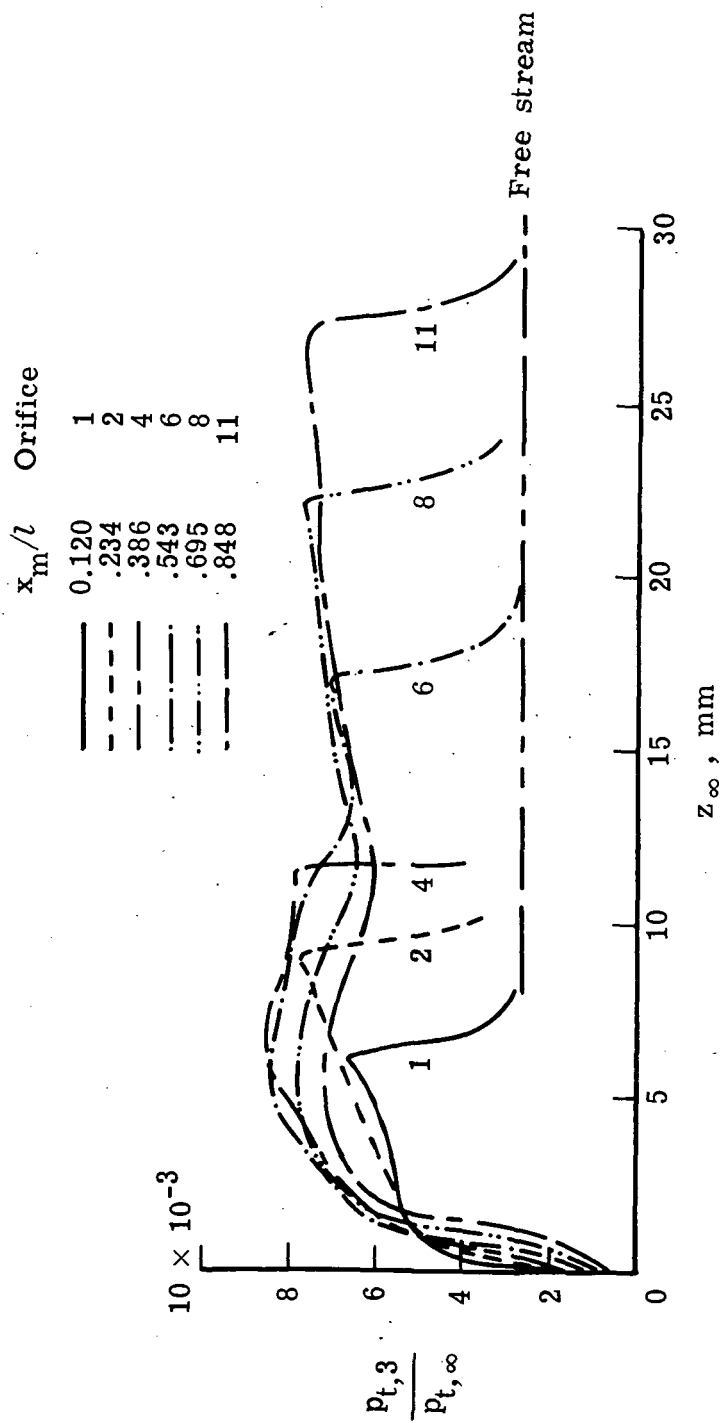
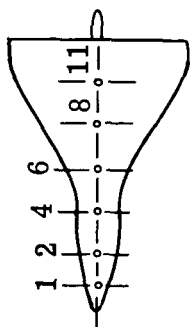


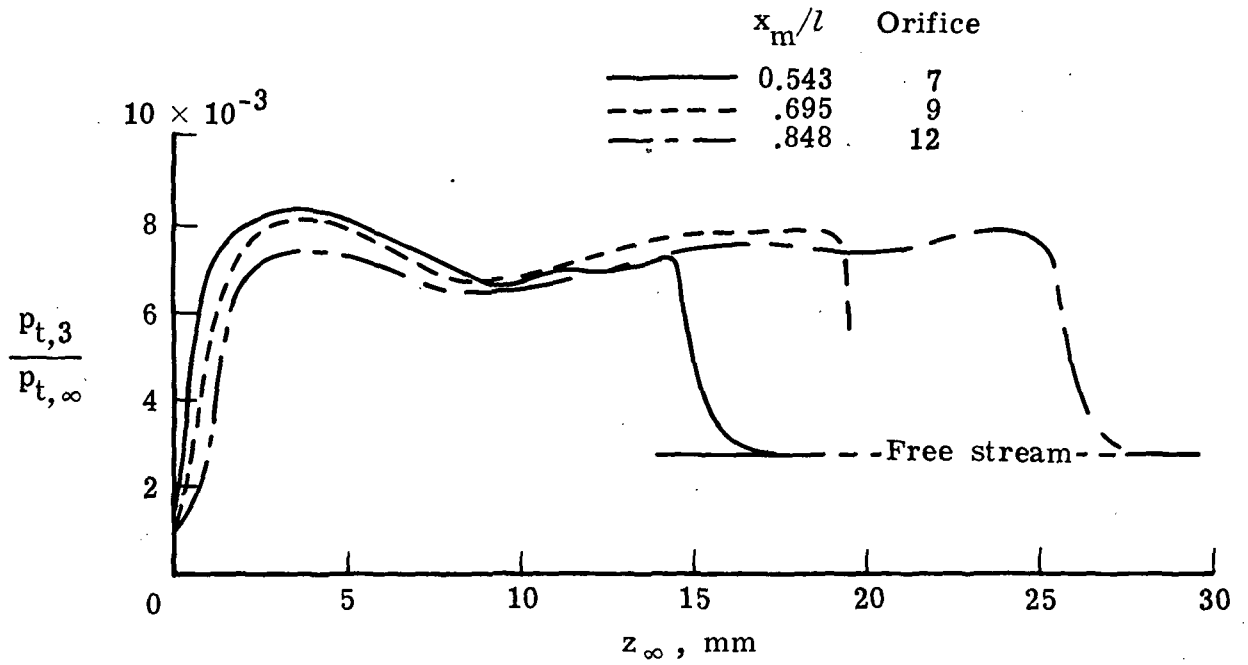
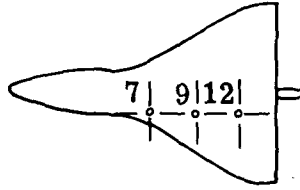
Figure 9.- Comparison of calculated pitot profiles in boundary layer with measured and inviscid profiles along body plane of symmetry.



$$(a) \quad \frac{y_m}{b/2} = 0.$$

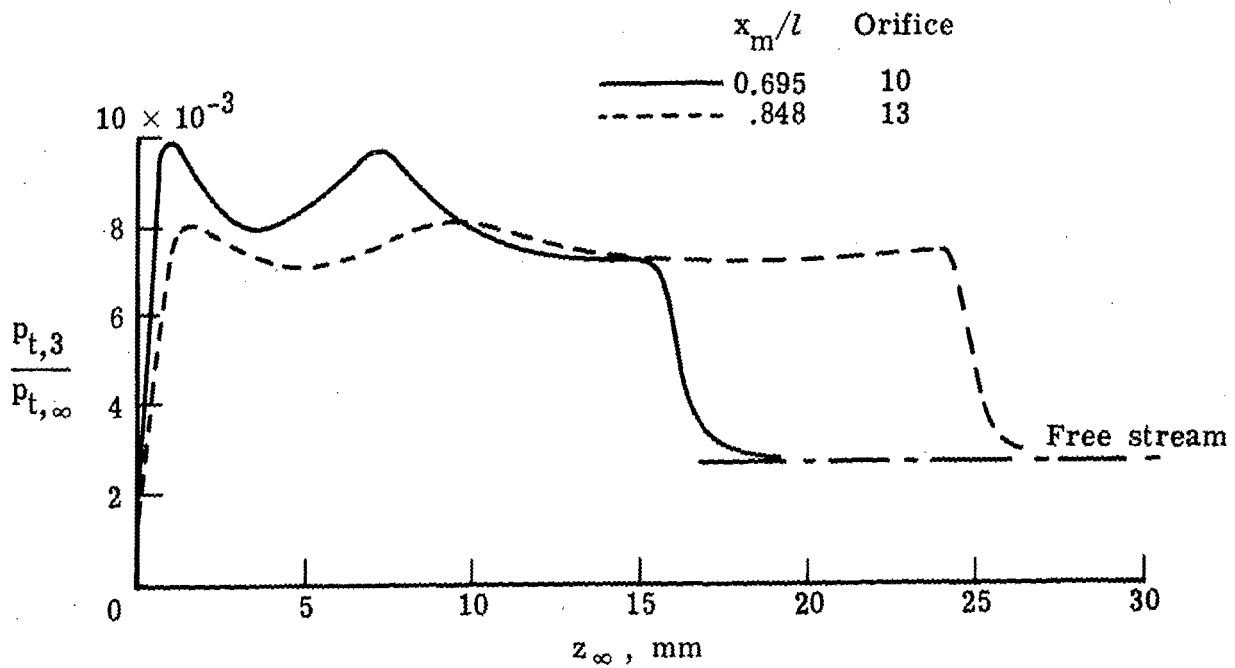
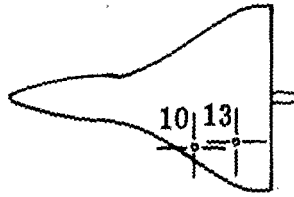
Figure 10.- Comparison of pitot profiles at several spanwise stations.





(b)  $\frac{y_m}{b/2} = 0.212.$

Figure 10.- Continued.



(c)  $\frac{y_m}{b/2} = 0.482$  and  $0.454$ .

Figure 10.- Concluded.

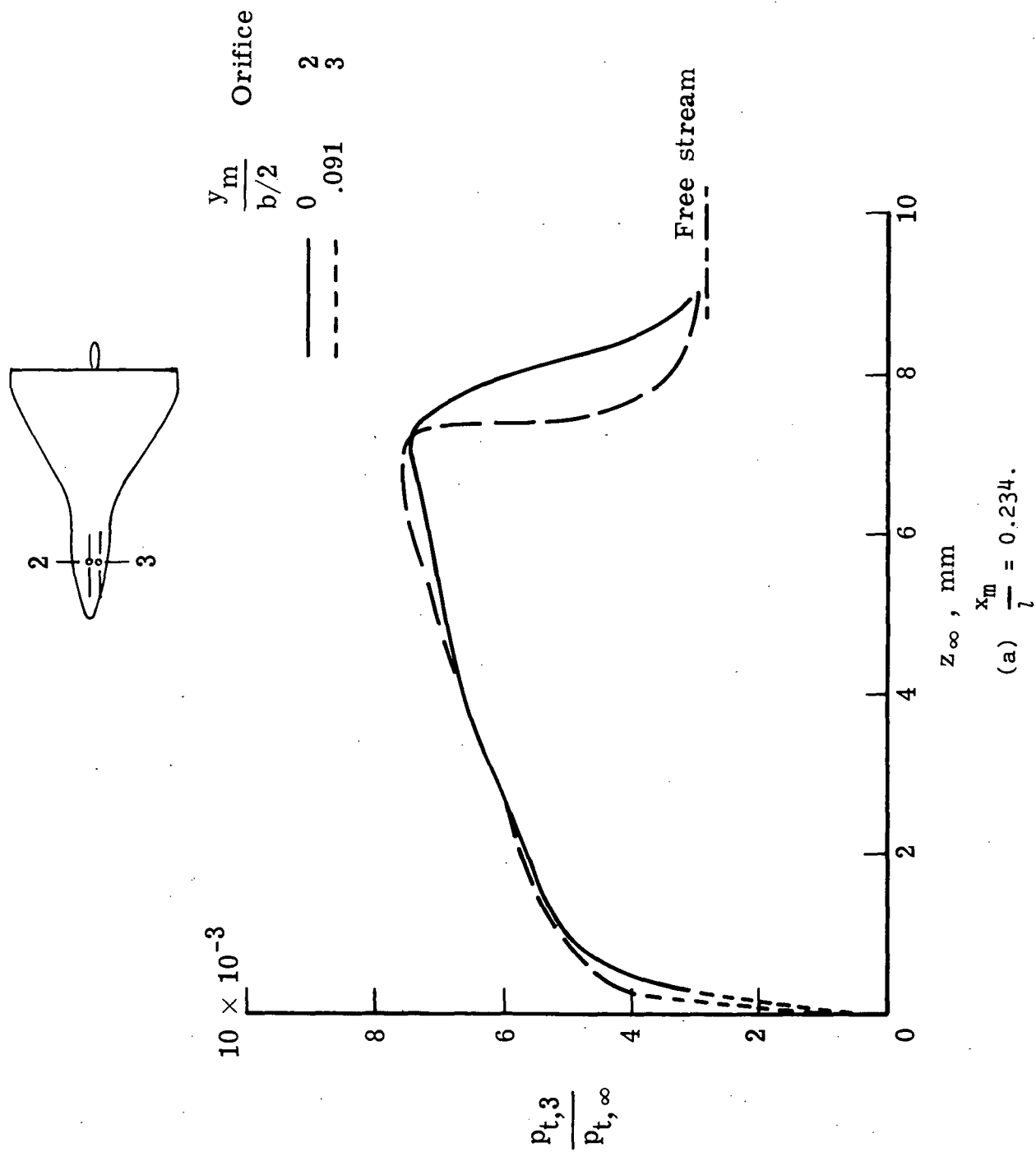
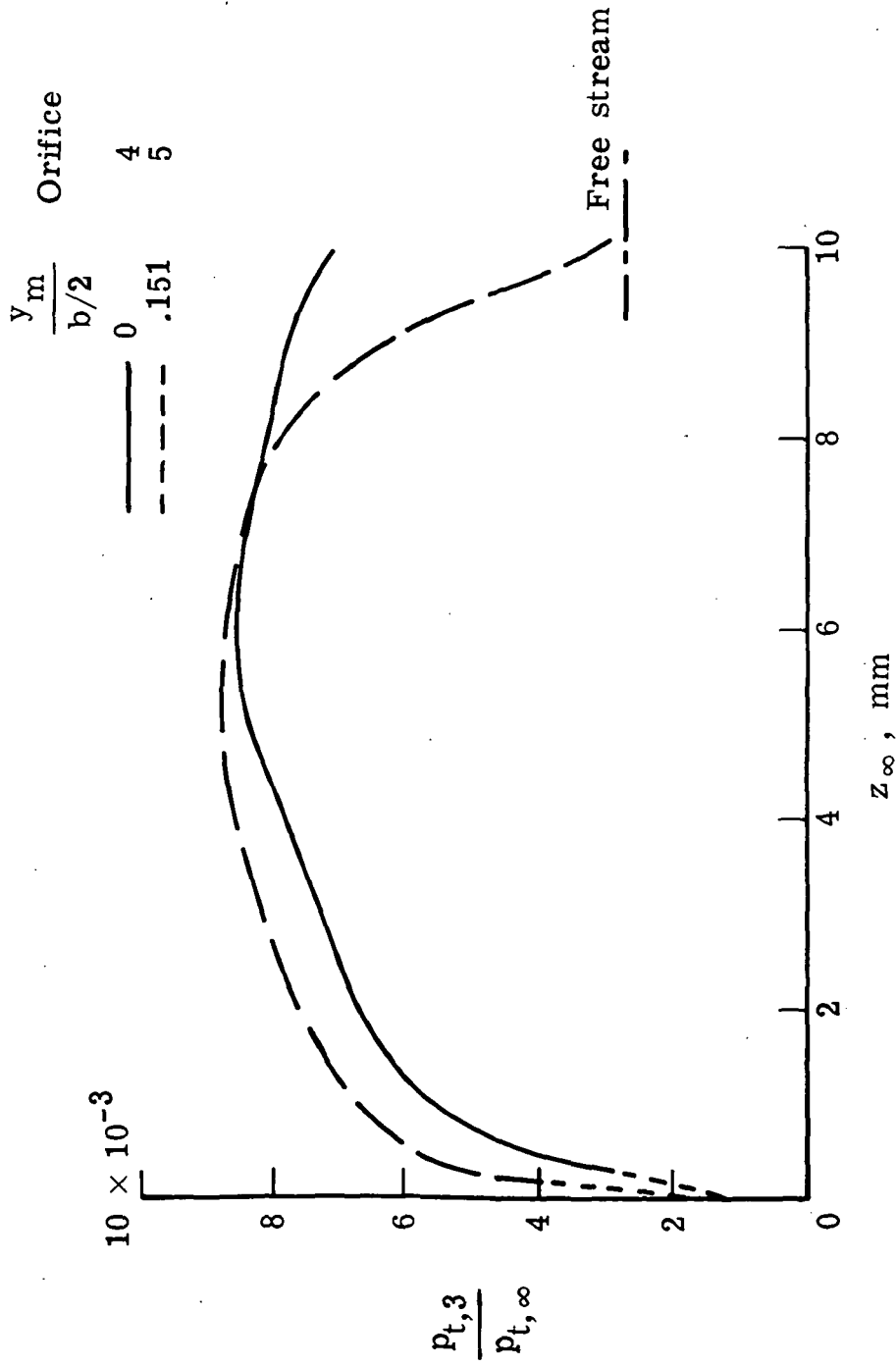
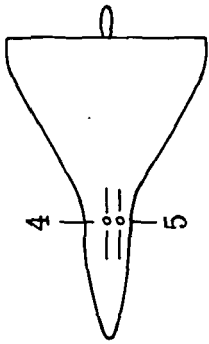


Figure 11.- Comparison of pitot profiles at several longitudinal stations.



(b)  $\frac{x_m}{l} = 0.386$ .

Figure 11.- Continued.

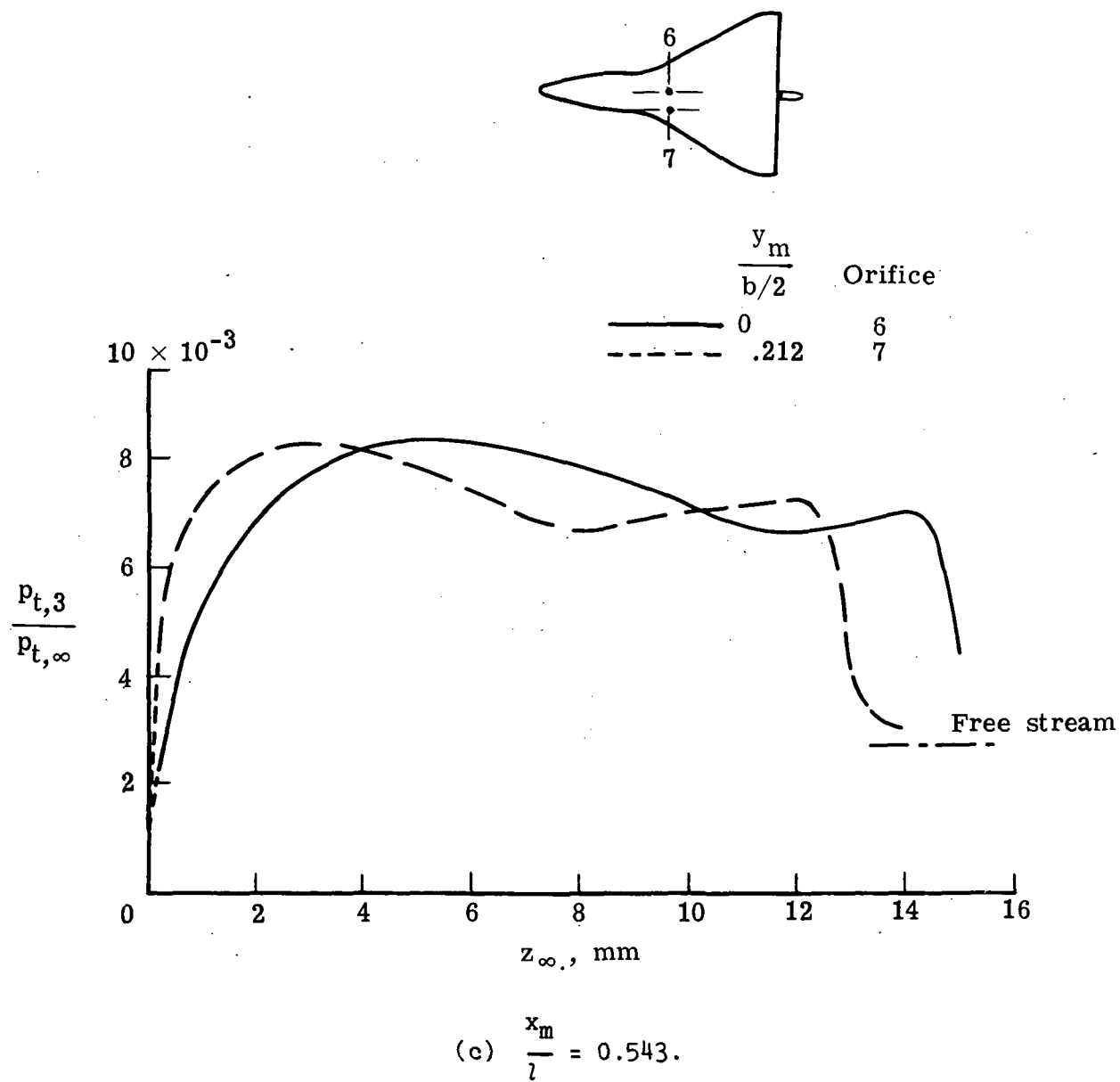
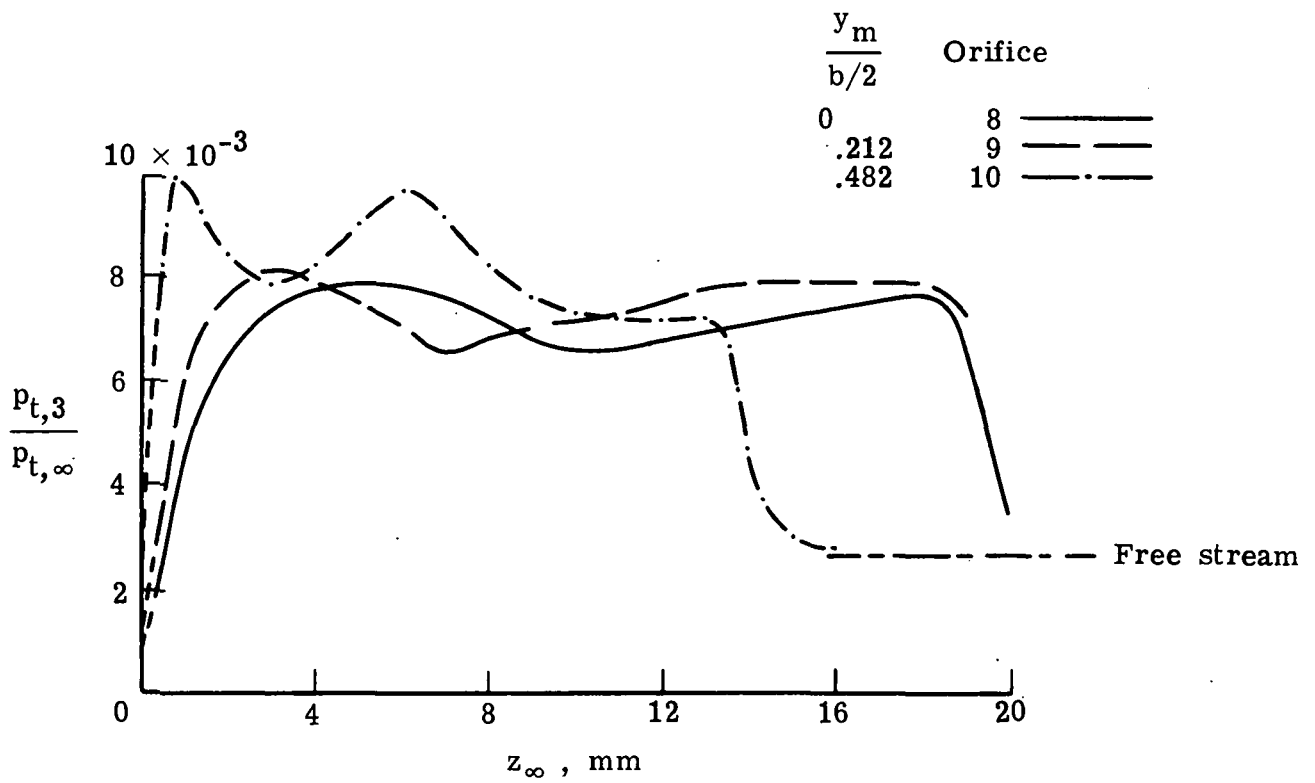
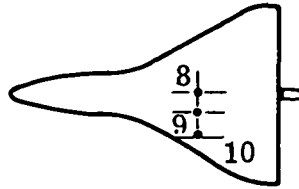
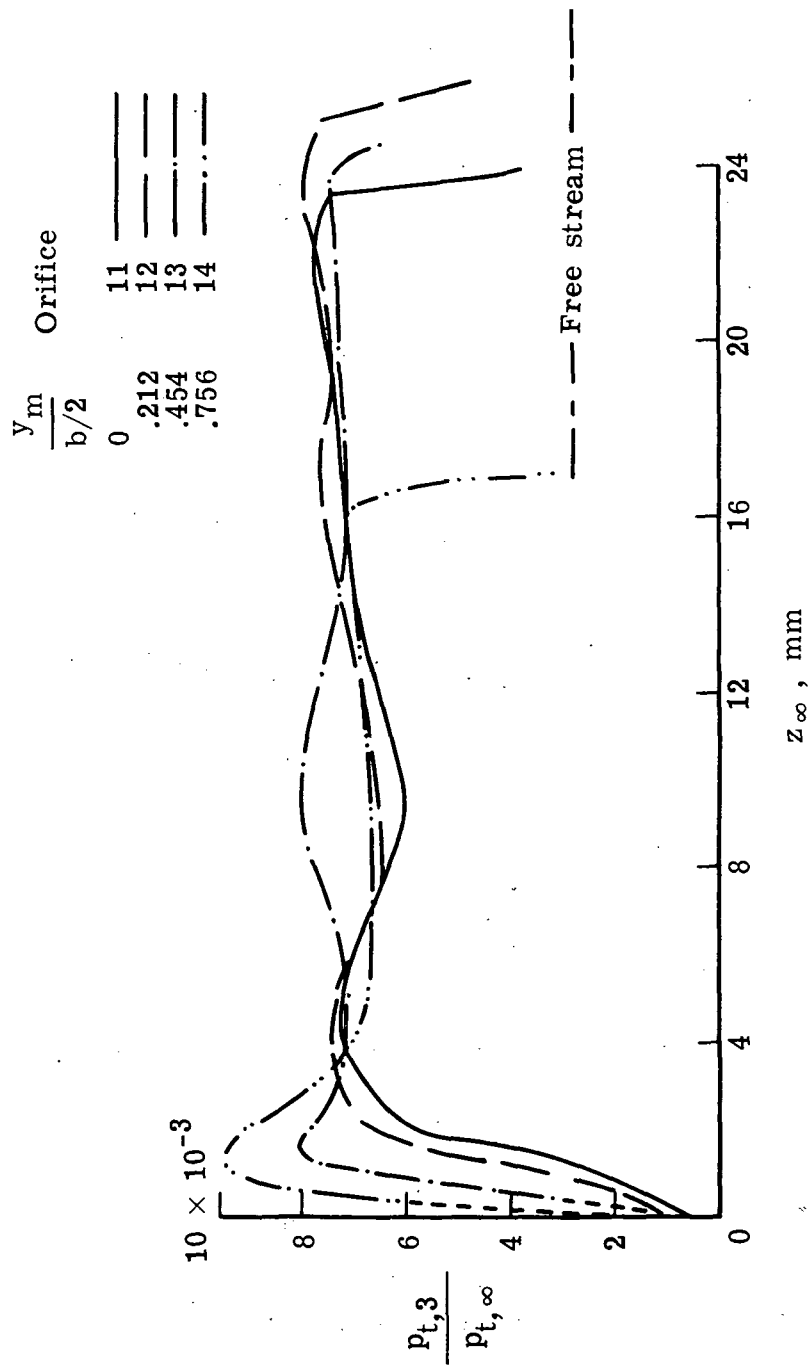
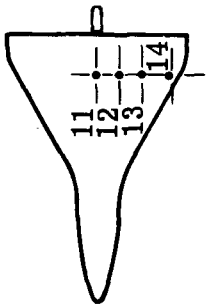


Figure 11.- Continued.



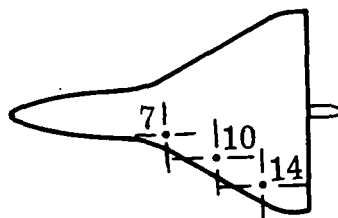
(d)  $\frac{x_m}{l} = 0.695.$

Figure 11.- Continued.



(e)  $\frac{x_m}{l} = 0.848.$

Figure 11.- Concluded.



	$x_m/l$	Orifice
—————	0.543	7
- - - - -	.695	10
- - - - -	.848	14

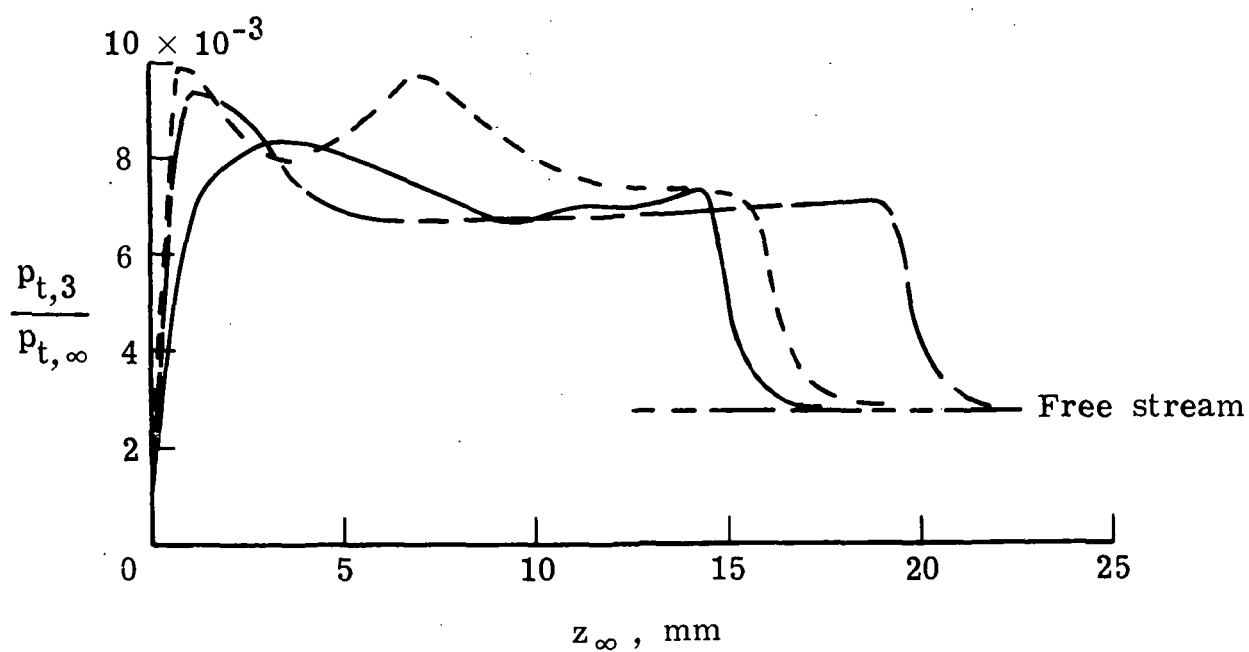
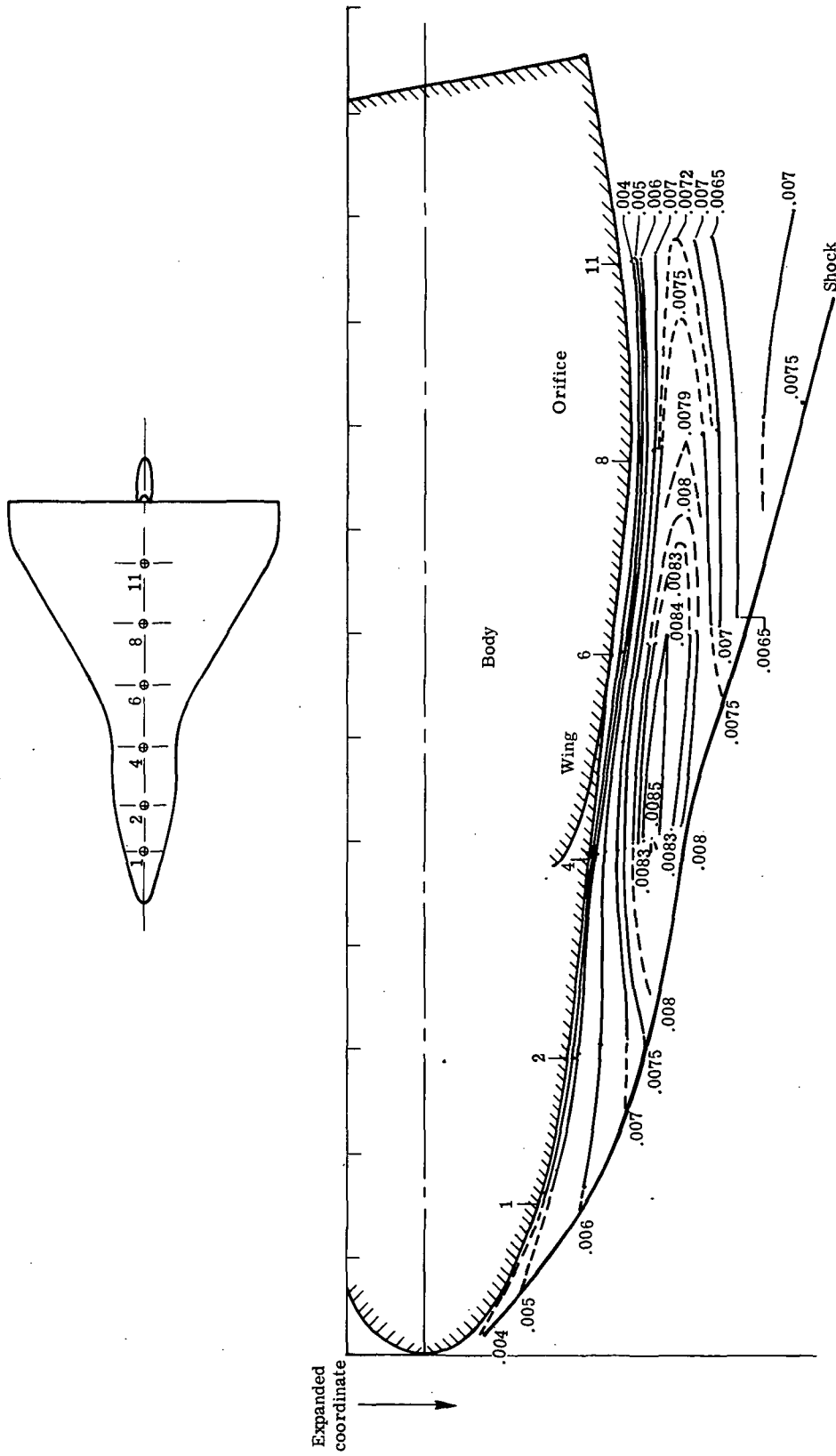


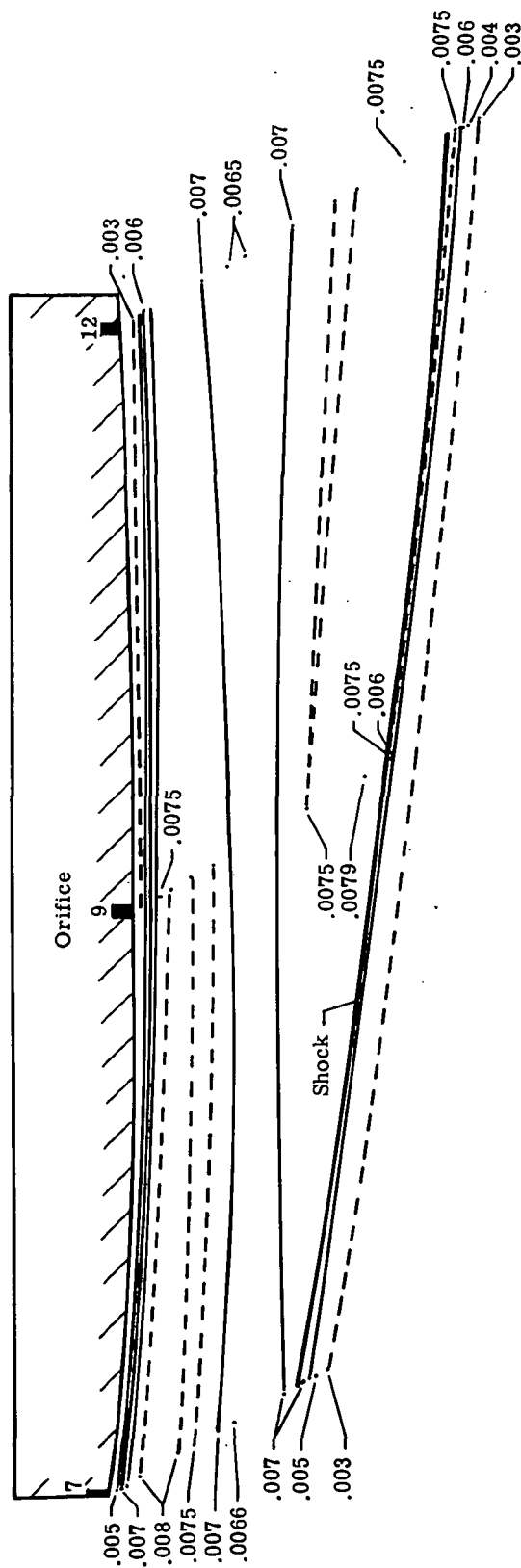
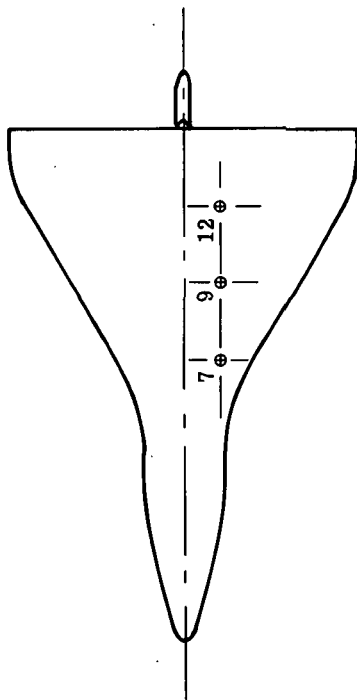
Figure 12.- Comparison of pitot profiles at orifices nearest wing leading edge.





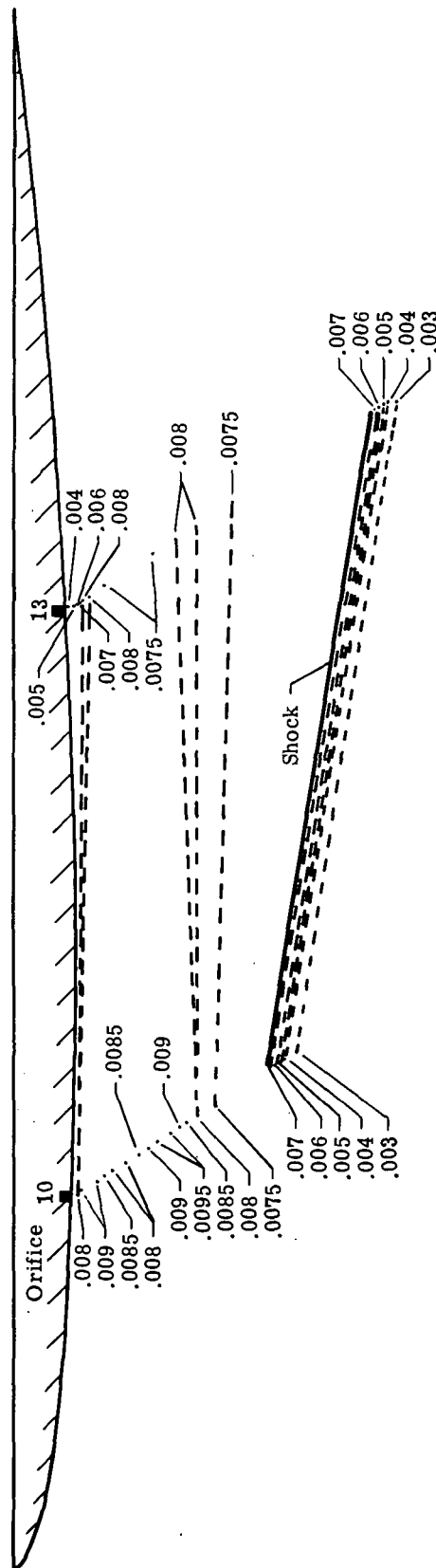
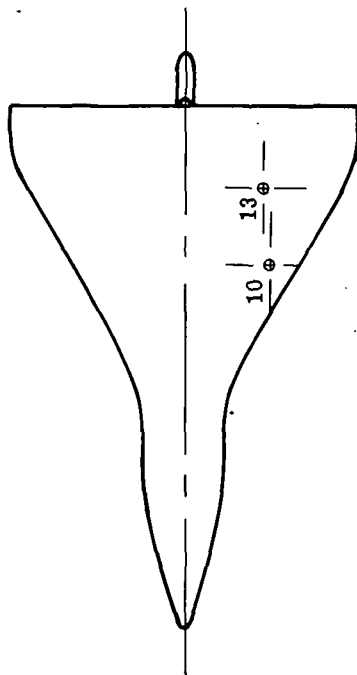
(a) Plane of symmetry.

Figure 13.- Pitot-pressure  $p_{t,3/pt,\infty}$  contours between various groups of orifices. Vertical scale enlarged to show details between shock and body in figure 13(a) only.



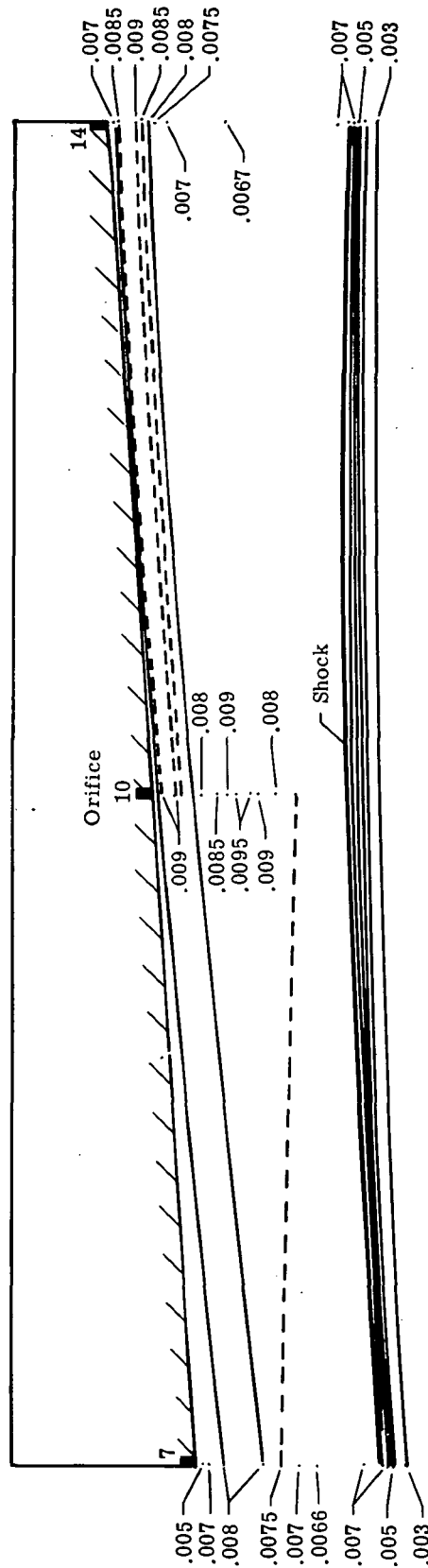
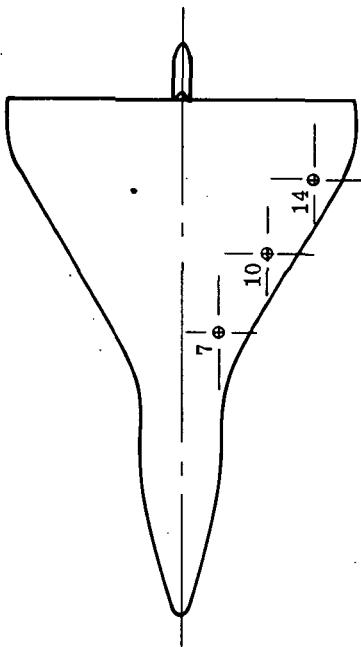
(b) Wing profile between orifices 7 and 12;  $\frac{y_m}{b/2} = 0.212$ .

Figure 13.- Continued.



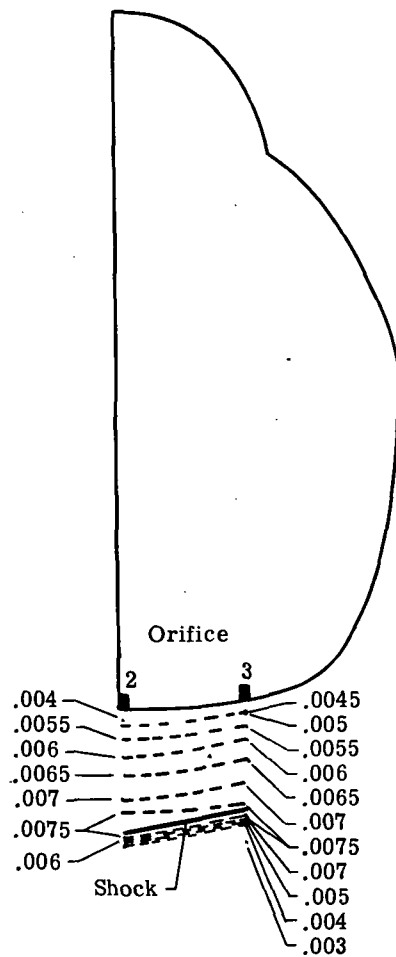
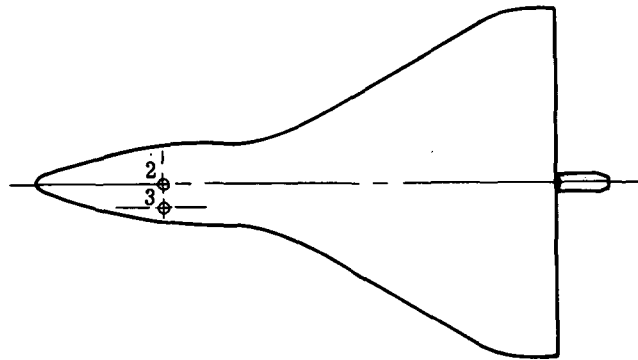
(c) Wing profile through orifices 10 and 13;  $\frac{y_m}{b/2} = 0.482$  and  $0.454$ .

Figure 13.- Continued.



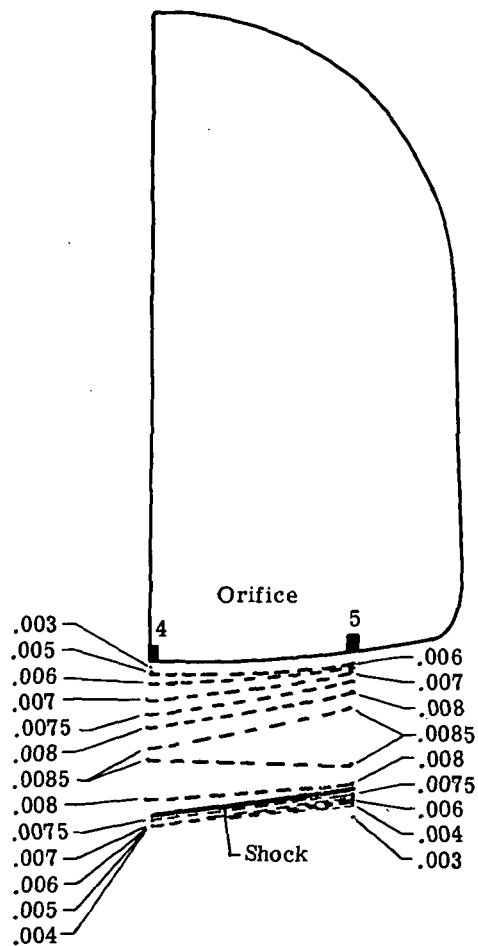
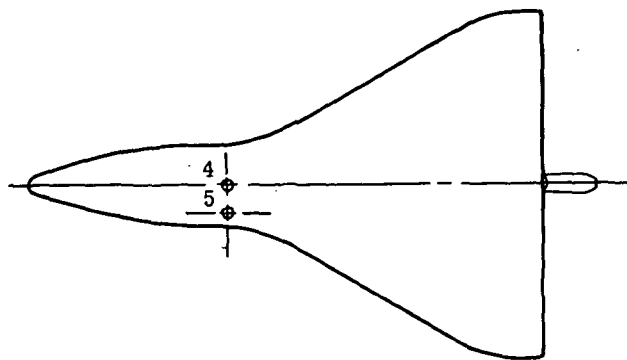
(d) Section through orifices 7, 10, and 14 parallel to wing leading edge.

Figure 13.- Continued.



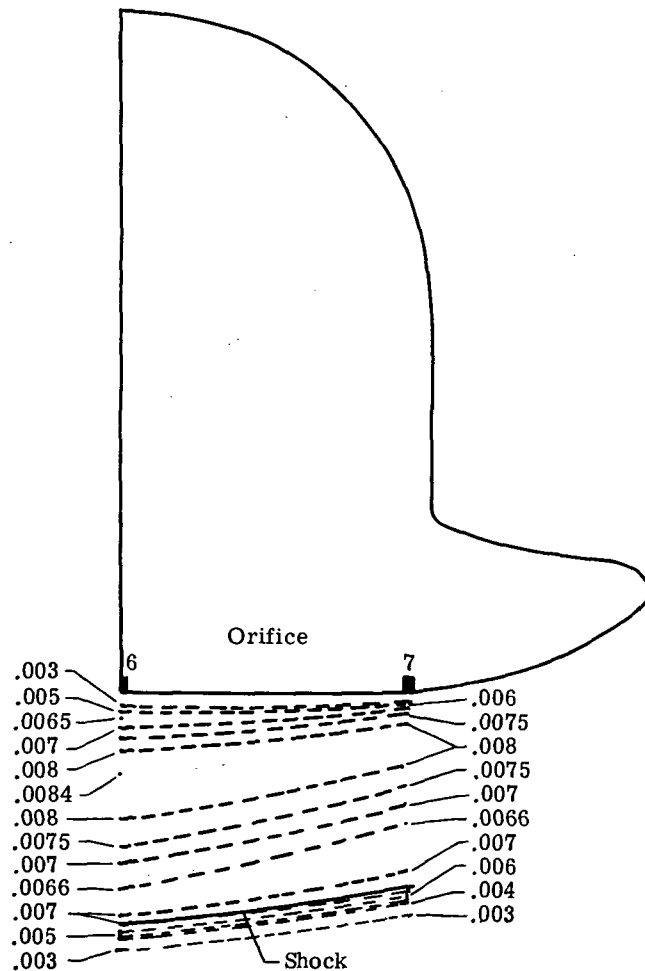
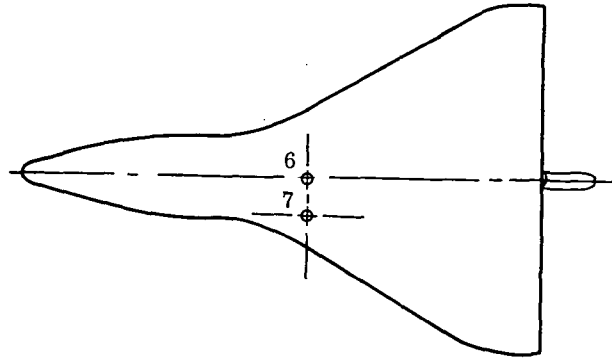
(e) Cross section through orifices 2 and 3;  $\frac{x_m}{l} = 0.234$ .

Figure 13.- Continued.



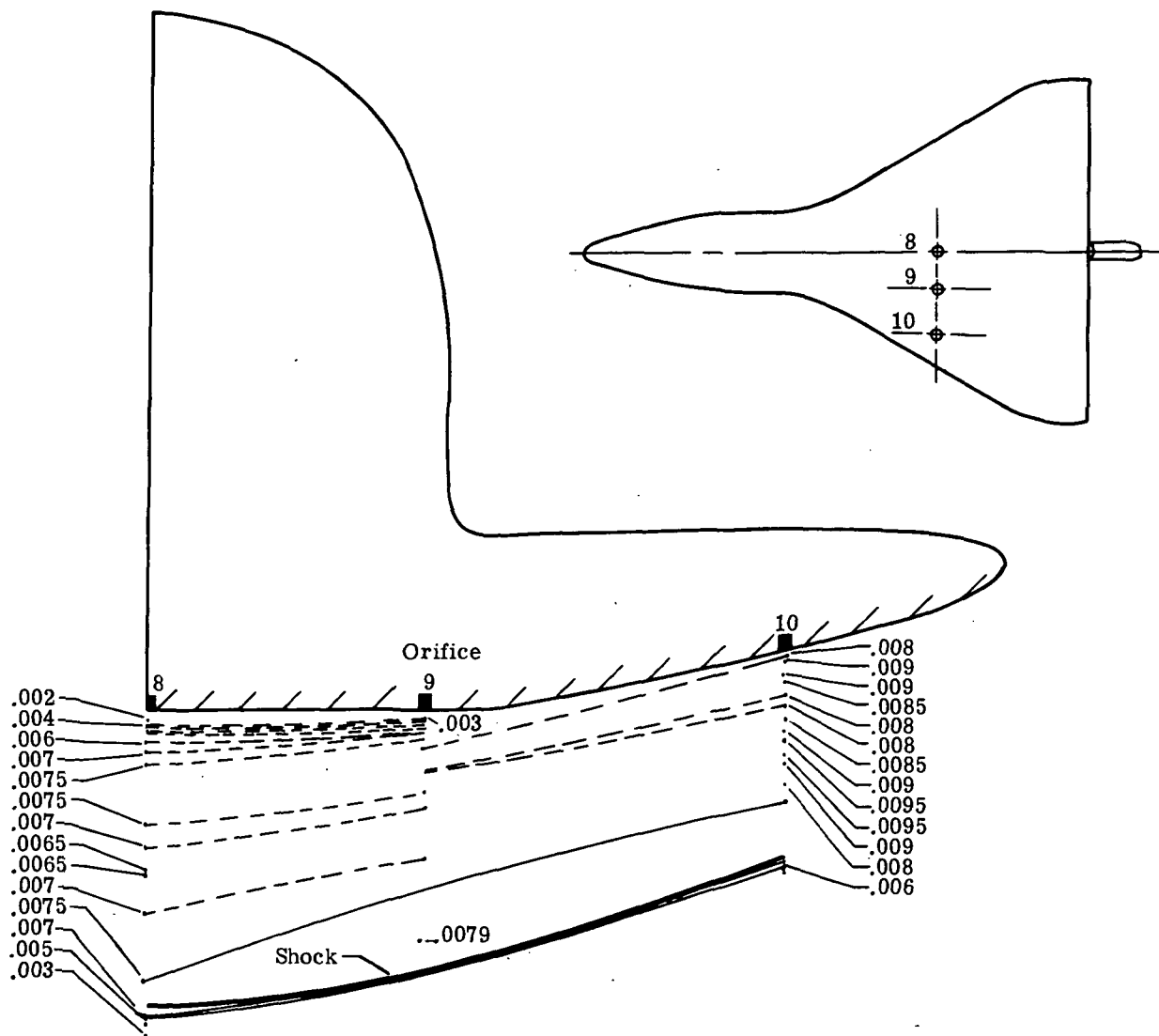
(f) Cross section through orifices 4 and 5;  $\frac{x_m}{l} = 0.386$ .

Figure 13.- Continued.



(g) Cross section through orifices 6 and 7;  $\frac{x_m}{l} = 0.543$ .

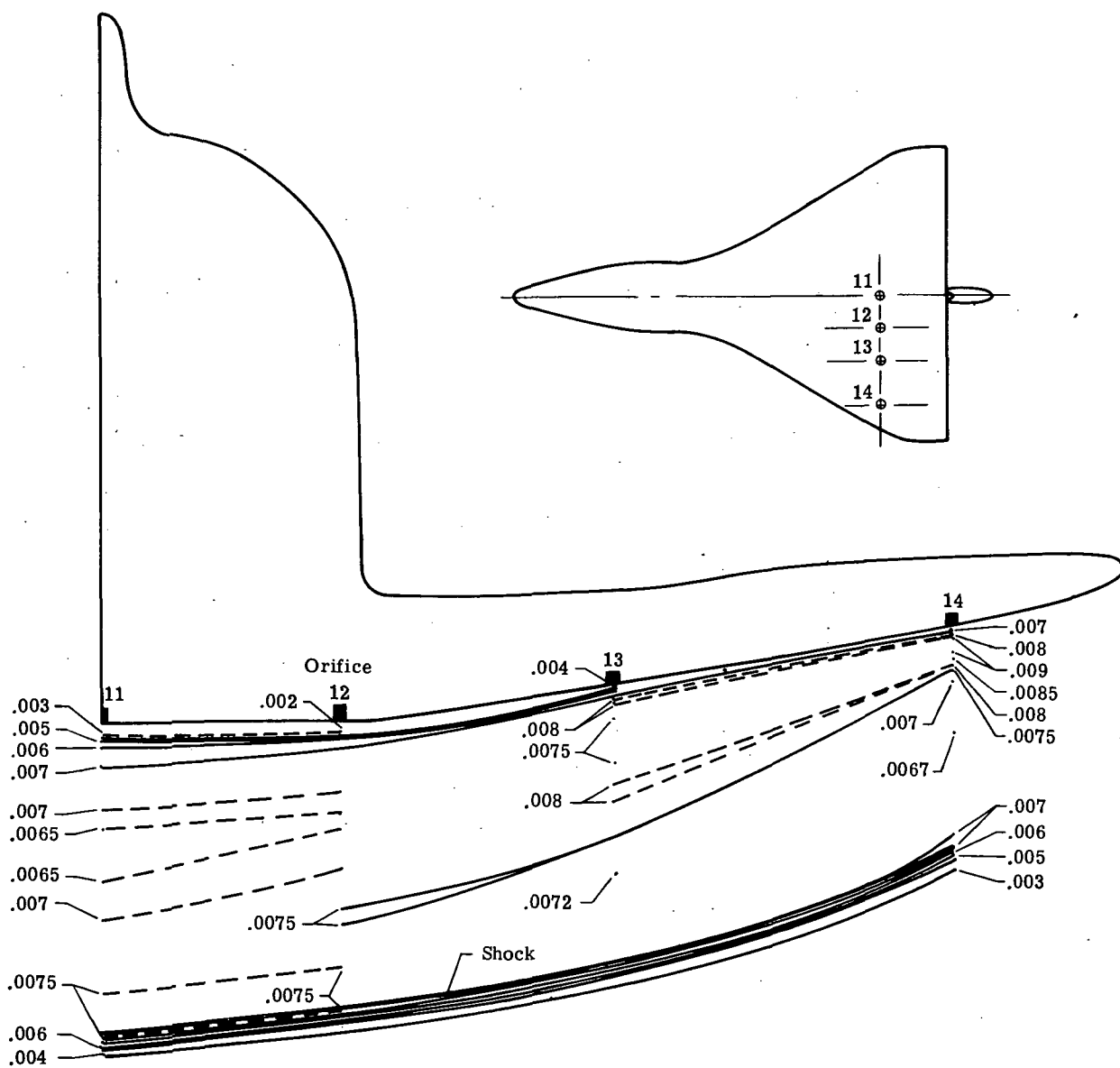
Figure 13.- Continued.



(h) Cross section through orifices 8, 9, and 10;  $\frac{x_m}{l} = 0.695$ .

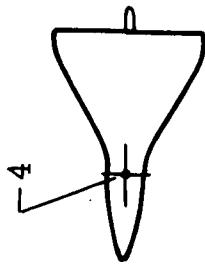
Figure 13.- Continued.



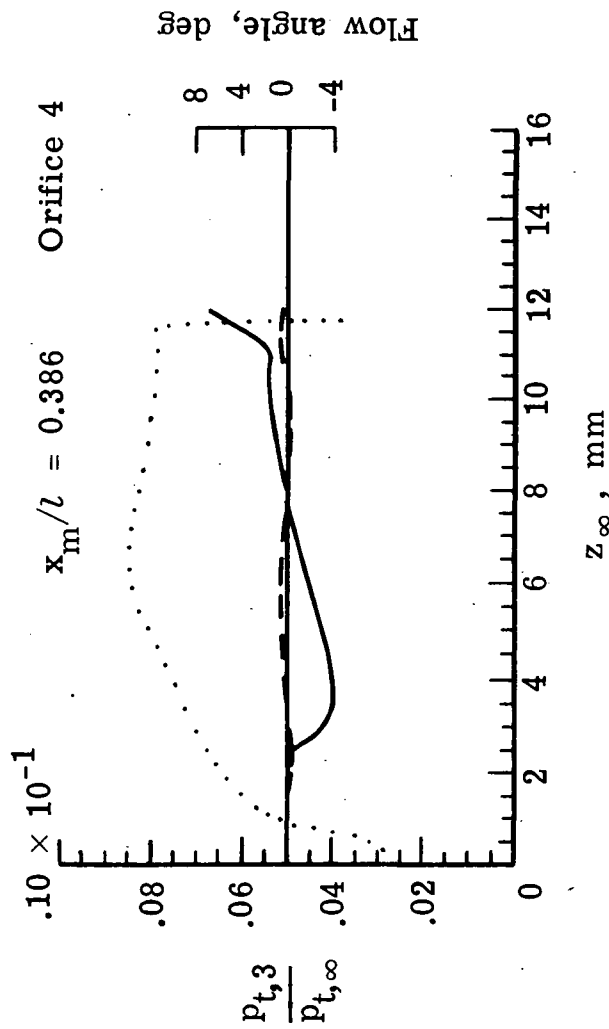


(i) Cross section through orifices 11, 12, 13, and 14;  $\frac{x_m}{l} = 0.848$ .

Figure. 13.- Concluded.

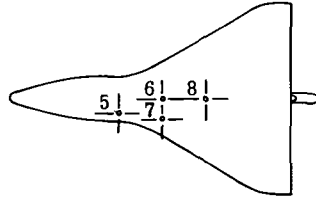


- ..... Measured pitot profiles
- Measured vertical flow angle, positive is toward surface
- - - - - Measured spanwise flow angle, positive is outboard

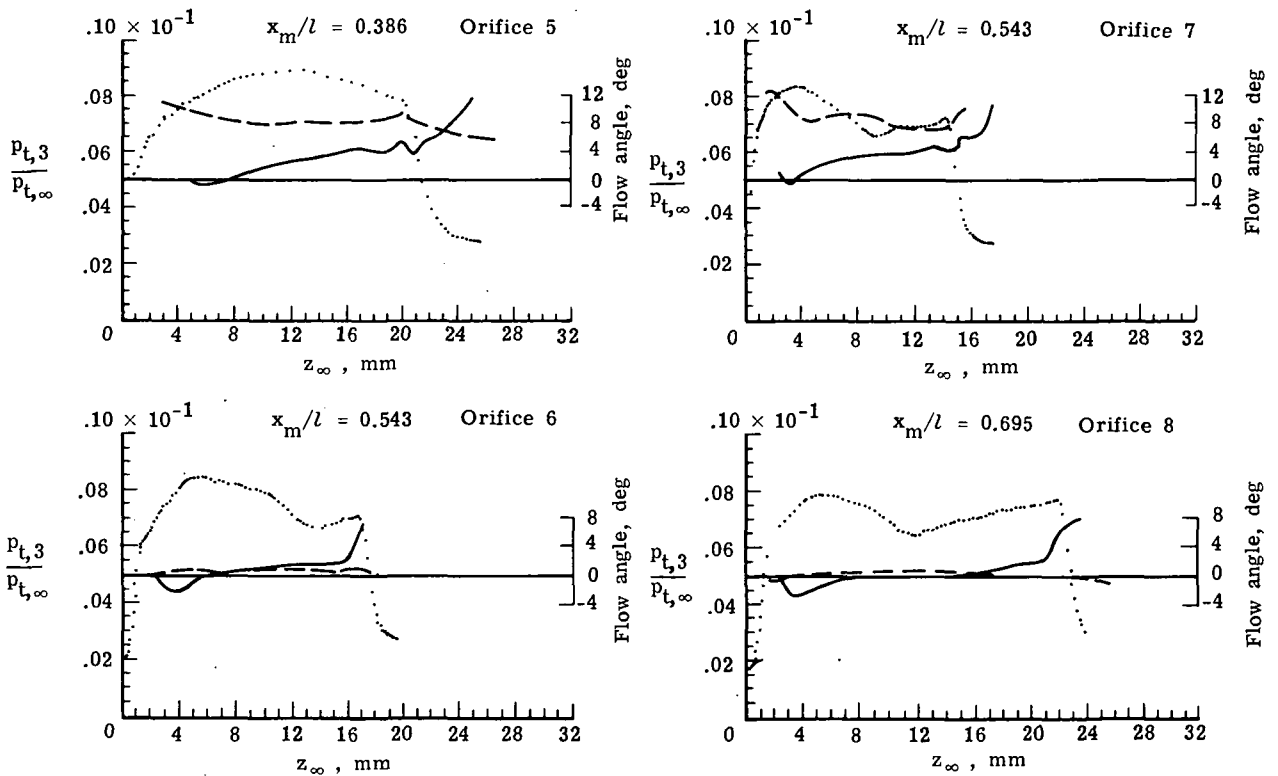


(a) Orifice 4.

Figure 14.- Measured flow angles between body and shock at several orifices.

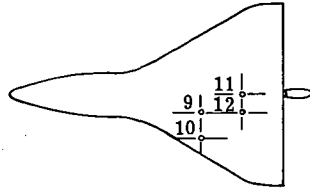


- ..... Measured pitot profile
- Measured vertical flow angle, positive is towards surface
- Measured spanwise flow angle, positive is outboard

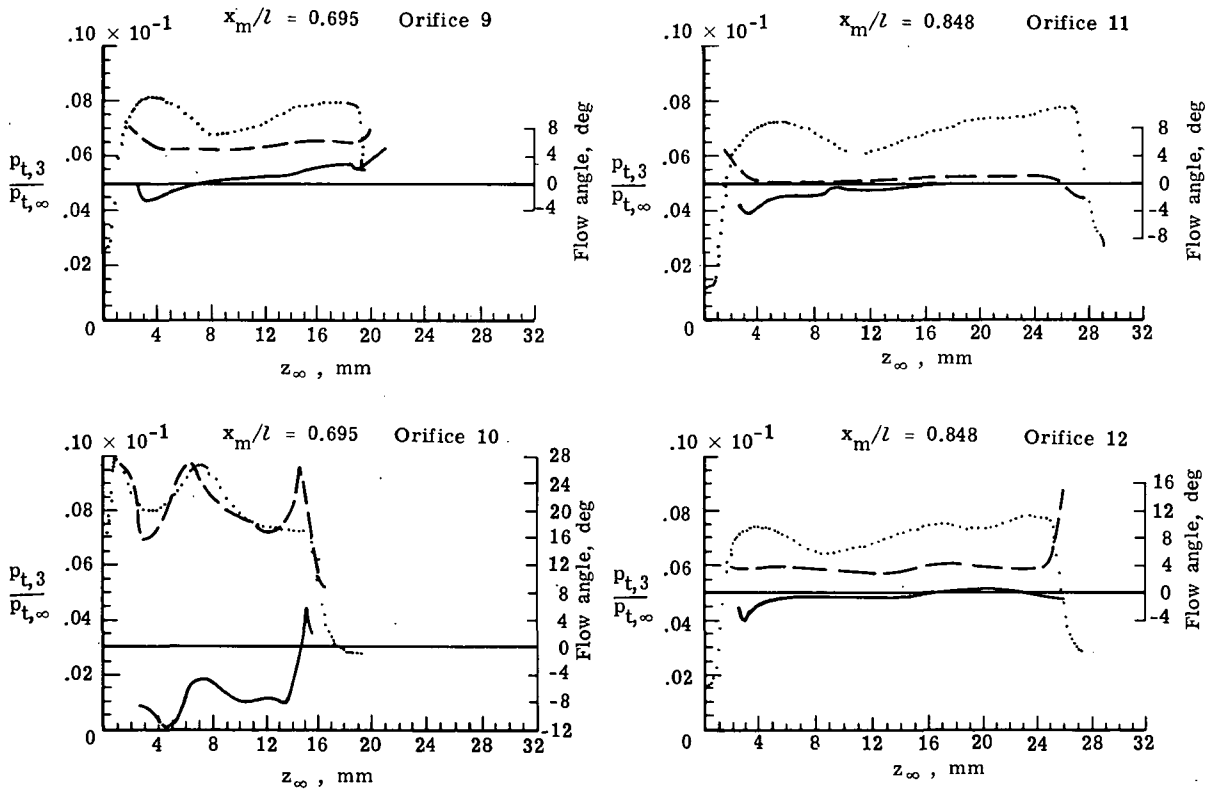


(b) Orifices 5 through 8.

Figure 14.- Continued.

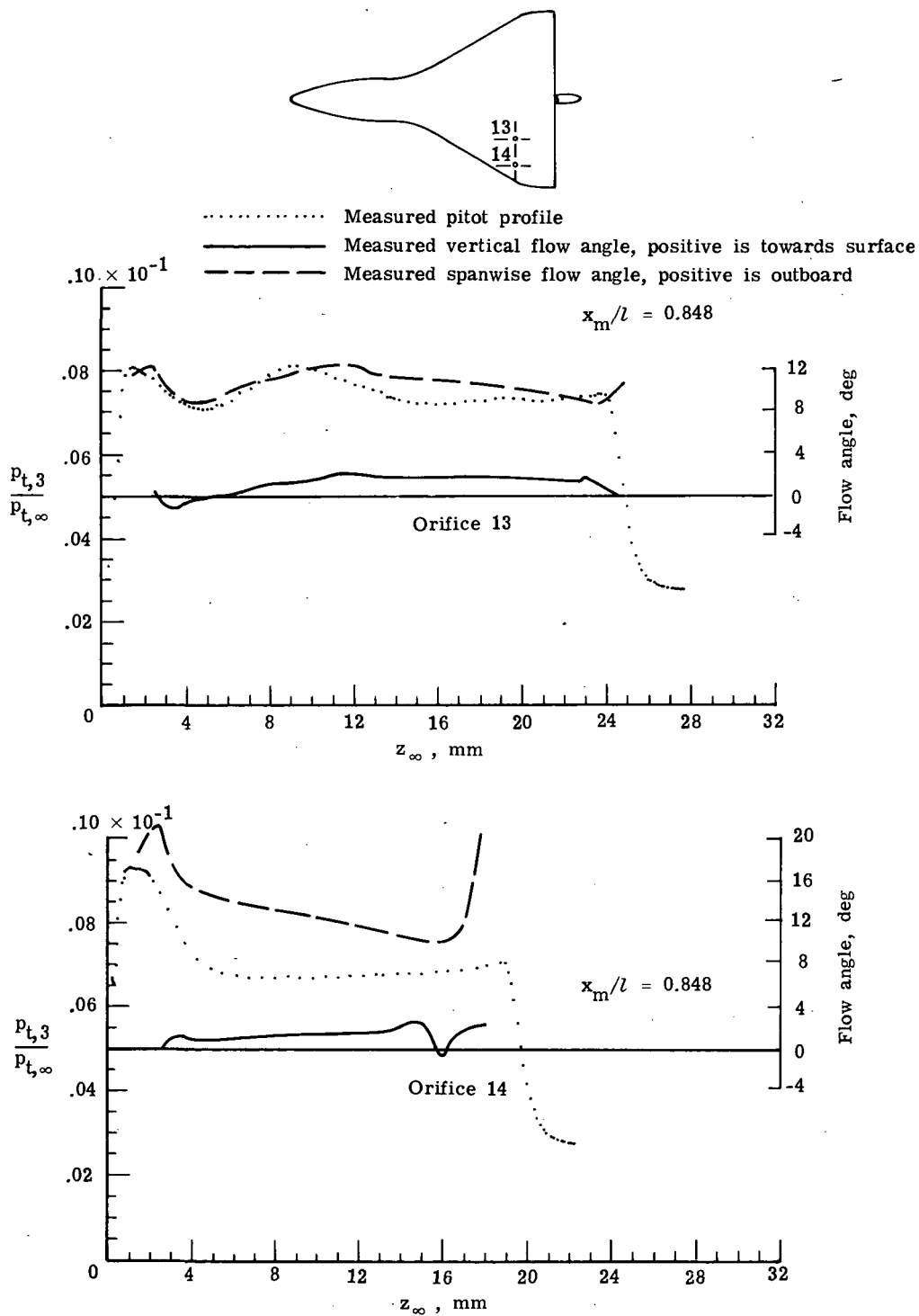


- ..... Measured pitot profile
- Measured vertical flow angle, positive is towards surface
- - - - Measured spanwise flow angle, positive is outboard



(c) Orifices 9 through 12.

Figure 14.- Continued.



(d) Orifices 13 through 14.

Figure 14.- Concluded.



THIRD-CLASS BULK RATE

POSTMASTER : If Undeliverable (Section 158  
Postal Manual) Do Not Return

*"The aeronautical and space activities of the United States shall be conducted so as to contribute . . . to the expansion of human knowledge of phenomena in the atmosphere and space. The Administration shall provide for the widest practicable and appropriate dissemination of information concerning its activities and the results thereof."*

—NATIONAL AERONAUTICS AND SPACE ACT OF 1958

## NASA SCIENTIFIC AND TECHNICAL PUBLICATIONS

**TECHNICAL REPORTS:** Scientific and technical information considered important, complete, and a lasting contribution to existing knowledge.

**TECHNICAL NOTES:** Information less broad in scope but nevertheless of importance as a contribution to existing knowledge.

**TECHNICAL MEMORANDUMS:** Information receiving limited distribution because of preliminary data, security classification, or other reasons. Also includes conference proceedings with either limited or unlimited distribution.

**CONTRACTOR REPORTS:** Scientific and technical information generated under a NASA contract or grant and considered an important contribution to existing knowledge.

**TECHNICAL TRANSLATIONS:** Information published in a foreign language considered to merit NASA distribution in English.

**SPECIAL PUBLICATIONS:** Information derived from or of value to NASA activities. Publications include final reports of major projects, monographs, data compilations, handbooks, sourcebooks, and special bibliographies.

**TECHNOLOGY UTILIZATION PUBLICATIONS:** Information on technology used by NASA that may be of particular interest in commercial and other non-aerospace applications. Publications include Tech Briefs, Technology Utilization Reports and Technology Surveys.

*Details on the availability of these publications may be obtained from:*

**SCIENTIFIC AND TECHNICAL INFORMATION OFFICE  
NATIONAL AERONAUTICS AND SPACE ADMINISTRATION  
Washington, D.C. 20546**